THE UNIVERSITY OF MICHIGAN
COLLEGE OF ENGINEERING
Department of Electrical Engineering
Space Physics Research Laboratory

Final Report

STUDIES TOWARD THE DEVELOPMENT OF A D-REGION PROBE

J. C. Pearl

ORA Project 05235

under contract with:

DEPARTMENT OF THE ARMY
DETROIT ORDNANCE DISTRICT
CONTRACT NO. DA-20-018-ORD-24992
DETROIT, MICHIGAN

administered through:

OFFICE OF RESEARCH ADMINISTRATION ANN ARBOR

April 1965

ACKNOWLEDGMENTS

The author wishes to express his appreciation to Professor A. F. Nagy for his constant and willing advice and guidance throughout the period during which this work was performed. Further thanks go to Gary Poole and James Nichols for carrying out the extensive programming which the problem necessitated.

For the design and construction of the electronics for the prototype probe assembly thanks are due to Tuck Bin Lee; the cooperation of the staff of the BRL Wind Tunnel during the actual testing of this probe is thankfully acknowledged.

TABLE OF CONTENTS

LIST OF FIGURES

LIST OF FIGURES (Concluded)

Figure		Page

NOMENCLATURE

Alphabetic

A	surface area
A_i	see Eqn. (5.4-10)
a	probe radius $(= \frac{a'}{\lambda})$
B_i	see Eqn. (5.4-10)
D	coefficient of diffusion
e	electronic charge
f	function representing r_o (Eqn. (5.3-5));
	function used in sheath cutoff (Eqn. (6.4-24))
g	function used in sheath cutoff (Eqn. (6.4-29))
H	parameter for finite difference calculations (Eqn. (5.2-8))
h	function used in sheath cutoff (Eqn. (6.4-30))
I	current
J	current density (positive species)
K	mobility constant $(= \frac{eD}{kT})$
k	index for solutions of cubic equation (Eqn. (6.4-14));
	Boltzmann constant
L	current density (negative species)
ℓ	displacement
n	number of incremented steps in a calculation;
	number of particles in a Debye cube

Alphabetic

P	arbitrary field point
p	parameter used in flow line computation (Eqn. (5.2-12))
Q	charge;
	point on central axis of torus (Fig. 11)
q	charge
R	distance from coordinate origin
$R_1, R_2, R(P)$	distances identified in Fig. 9.
r	radial cylindrical coordinate;
	minor radius of torus (Eqn. (5.4-18))
S	point in charge density field (Fig. 11)
s	distance normal to flow lines
T	point on torus (Fig. 11);
	temperature
t	time ($= \frac{t'V'}{\lambda}$);
	variable used in sheath cutoff (Eqn. (6.4-27))
V	neutral gas flow velocity ($= \frac{\lambda V}{D}$)
v	composite velocity term (Eqn. (5.2-2))
x	variable used in sheath cutoff (Eqn. (6.4-23))
y	see Eqn. (6.4-6)
z	axial cylindrical coordinate
α_i	dimensionless ratio (Eqn. (5.4-13))

Alphabetic

β	dimensionless parameter (Eqn. (6.2-5))
γ	parameter used in sheath cutoff (Eqn. (6.4-27))
Δ	parameter in difference formula (Fig. 7)
δ	indicator of finite increment
ϵ	dielectric constant; error due to approximations
ζ	negative charge density ($= \frac{\zeta'}{\zeta'_\infty}$)
η	parameter used in sheath cutoff (Eqn. (6.4-33))
κ	complete elliptic integral of the first kind
λ	Debye length ($= \sqrt{\frac{\epsilon kT}{e\sigma'_\infty}}$)
μ	see Eqn. (6.4-12)
ρ	charge density (Eqn. (5.4-9))
Σ', Σ''	see Eqn. (5.4-26)
σ	positive charge density ($= \frac{\sigma'}{\sigma'_\infty}$)
τ	volume
Φ	electrical potential ($= \frac{e\Phi'}{kT}$)
ϕ	azimuthal cylindrical coordinate

Subscripts

i	counting or identifying index
n	evaluation after n increments; summation index

Subscripts

o	identifies flow line (see Section 5.3, p. 16).
	evaluation for sphere in torus routine (Eqn. (5.4-24))
p	condition at probe
r	radial component
z	axial component
∞	condition at infinity

Superscripts and Miscellaneous

'	quantity before being nondimensionalized;
	image (Eqn. (5.4-5));
	evaluation for flow line tangent to probe (Eqn. 6.4-3))
"	evaluation for flow line target to probe (see p.30)
$\hat{}$	unit vector
∇	gradient operator ($= \lambda \vec{\nabla}'$)
$\|a\|$	absolute value of a
[a]	greatest integer in a.

1. INTRODUCTION

Since 1946, when University of Michigan investigators first proposed such experiments, Langmuir probes have been widely used to study the E and F regions of the ionosphere. The theory of operation of Langmuir probes, for these regions, where the mean free path of the particles is large, is well understood and therefore their volt-ampere characteristics can be accurately interpreted in terms of ambient charged particle parameters.

The growing interest in the physical properties of the lower parts of the ionosphere has provided impetus to study the feasibility of the use of such current collecting probes for the D region. Recently a number of Langmuir probe measurements have been made at these low altitudes. It is, however, difficult to interpret the data from such measurements, since to date no relevant theoretical work has been published dealing with the current collection characteristics of such probes in regions of high neutral gas density.

This report deals with the development of a probe for D region charged particle density measurements and the work done to enable the interpretation of the current measured by such a probe in terms of the ambient density. A test model of the probe was constructed and placed in the wind tunnel of the Aberdeen Proving Grounds. The results of these tests are also discussed.

2. SELECTION OF THE PROBE CONFIGURATION

A probe configuration enabling measurements to be made in the E as well as the D region was the aim of this study, since the sounding rockets which are likely to carry these experiments will pass through both of these regions. Because there is a great deal of confidence in E region Langmuir probe measurements, these results could also be used to provide some degree of calibration for the interpretation of the D region data.

First the question of the probe position received a great deal of consideration. The velocity of the vehicle is expected to be supersonic, resulting in the formation of a bow shock wave. As even the neutral gas flow well behind the shock is not understood it is considered imperative that the probe be located on the tip of the nose cone or on a boom of sufficient length to place it outside the shock cone of the vehicle. In either case the probe itself will create its own shock disturbance. A nose cone probe was chosen since the technical problems involved in its construction are considerably less than those for a boom supported probe. Because the tip of the nose cone is preferred for a number of other experiments it is felt that if the results from the nose cone probe experiments are encouraging work should be initiated towards the design of boom mounted probes.

Having established the nose tip as the preferred position of the probe, a configuration using a hemispherical tip was chosen. The main advantages of such a probe over a conical one, are:

(a) the collector area projected in the direction perpendicular to the velocity vector is not very sensitive to small changes in angle of attack as would be the case for example with the usual conical nose tip;

(b) the current collection theory for spherical collector has been worked out for the long mean free path operation to be encountered in the E region.

The principal disadvantage of the spherical over the sharp conical arrangement is the increased aerodynamic drag, but this increase is not expected to be significant for most applications. For both D and E region application it is considered important to minimize the effects of the distortion in the sheath about the probe, caused by the rest of the nose cone. All these considerations led to the choice of probe configuration indicated in Fig. 1.

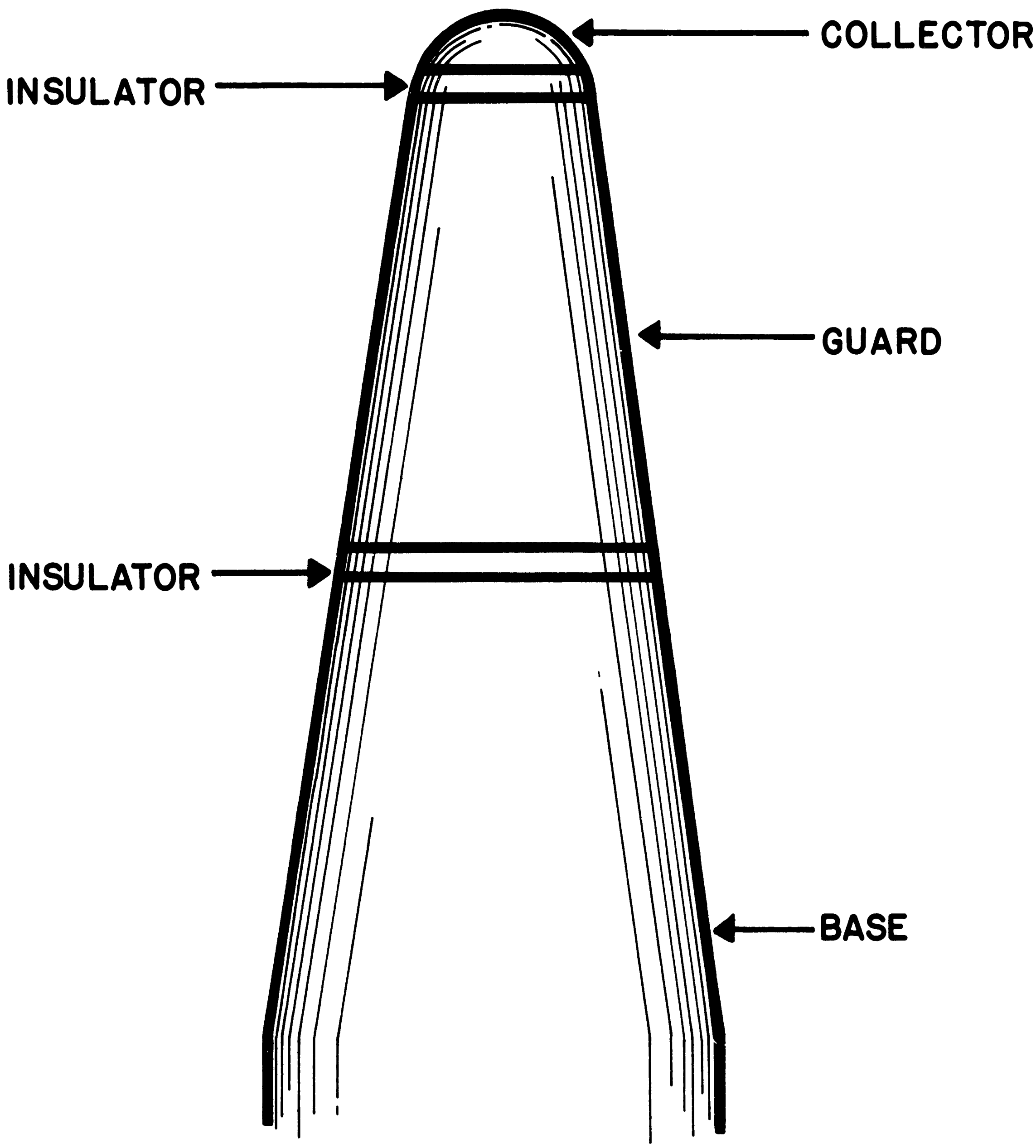

Fig. 1. Configuration of probe assembly.

3. WIND TUNNEL TESTS

A decision was made at the beginning of the contract period to observe the behavior of the probe in the wind tunnel at the Aberdeen Proving Grounds. The relatively high operating pressure of this wind tunnel (total pressure 100 torr) clearly does not permit the simultion of conditions typical of the D region but still tests were carried out in the hope of obtaining certain information about the behavior of the probe (e.g., saturation, etc.). A radioactive source was employed to achieve partial ionization in the tunnel, but since there was no way of knowing the degree of ionization, the percentage of electrons and negative ions and what the recombination rates were along the flow, no real interpretation of the experimental results was possible.

A photograph of the probe constructed for these tests shown in Fig. 2. The electrometer amplifier used in this test fixture was capable of measuring currents from 10^{-13} to 10^{-7} amperes in seven linear ranges. A remote controlled voltage stepping circuit allowed the application of eleven different voltages from -15 to +15 volts to the collector and guard.

Current versus voltage readings were taken for a number of Mach numbers and source strength values. Figure 3 shows the current versus voltage characteristics for M=3.02. These data indicate a strong relation between the current collected and the radioactive source strength. These tests gave no indication of current saturation, so the test setup was changed to permit the application of potentials up to 200V. The results of such a test are shown in Fig. 4; even here there is no clear indication of saturation. The current detector and the voltage source for these runs had to be situated outside the tunnel and connected to the probe via shielded cable and therefore considerable noise voltage may have been present. This noise however is not believed to have been of sufficient magnitude to mask the real results.

Numerous Schlieren photographs were taken during the test (Fig. 5). These show that the shock separation as expected, was very small. It was possible to vary the angle of attack in the wind tunnel from 0° to 15°. Changes in the angle of attack over this range resulted in no detectable change in the current collected. However, since these tests were also run with the electronics outside the tunnel the results have to be treated with caution.

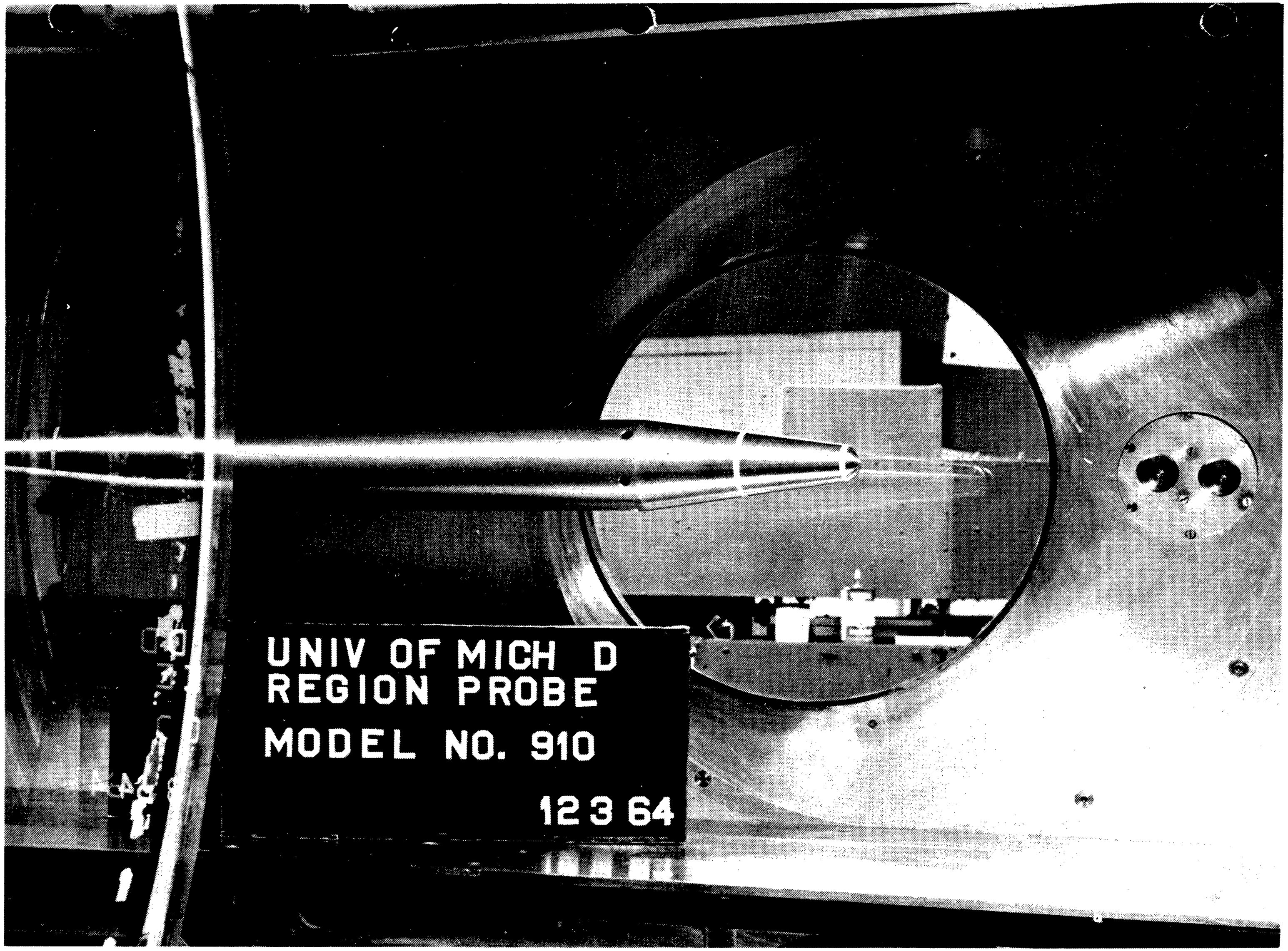

Fig. 2. Probe installed for wind tunnel test.

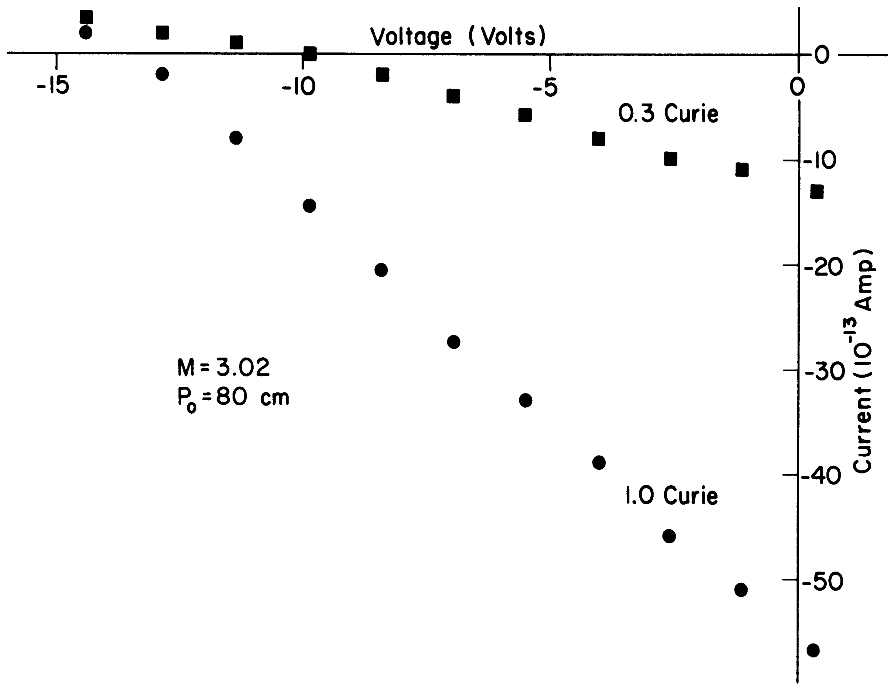

Fig. 3. Measured voltage-current characteristic at M=3.02 for low range of applied voltages.

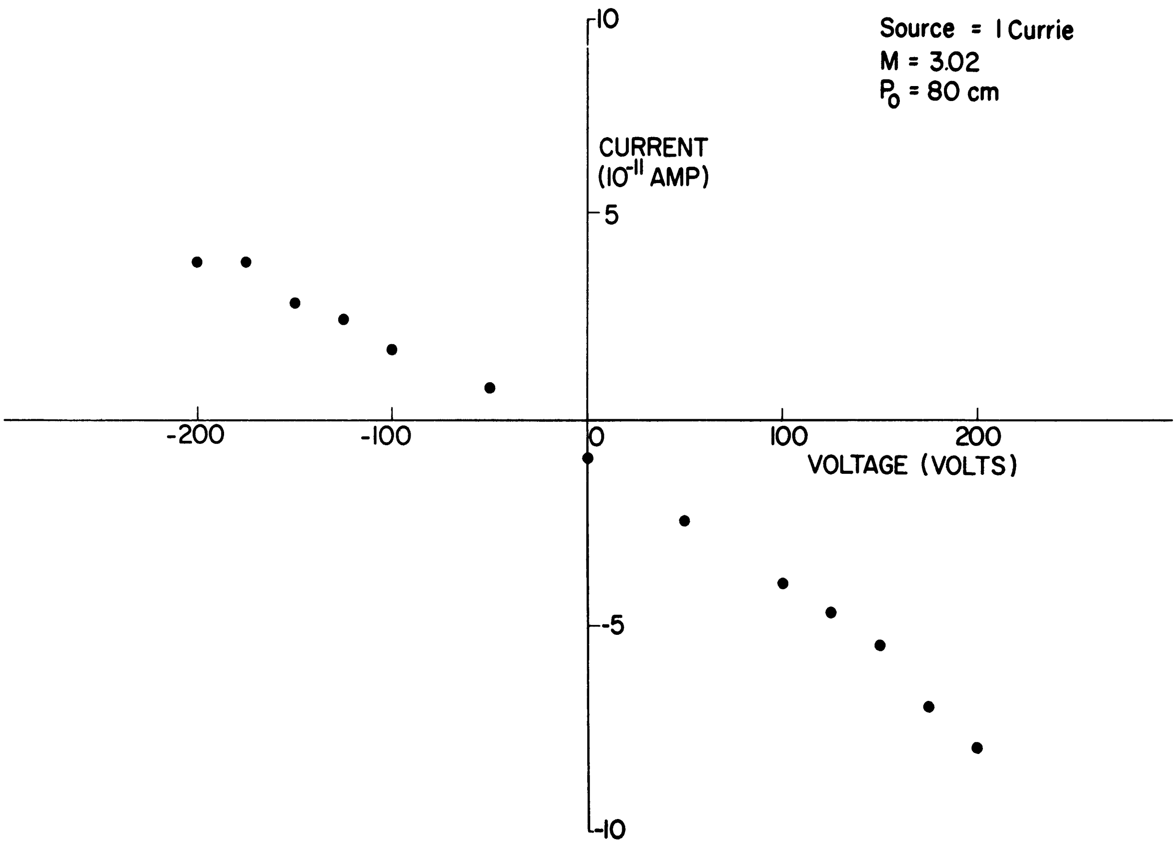

Fig. 4. Measured voltage-current characteristic at M=3.02 for high range of applied voltages.

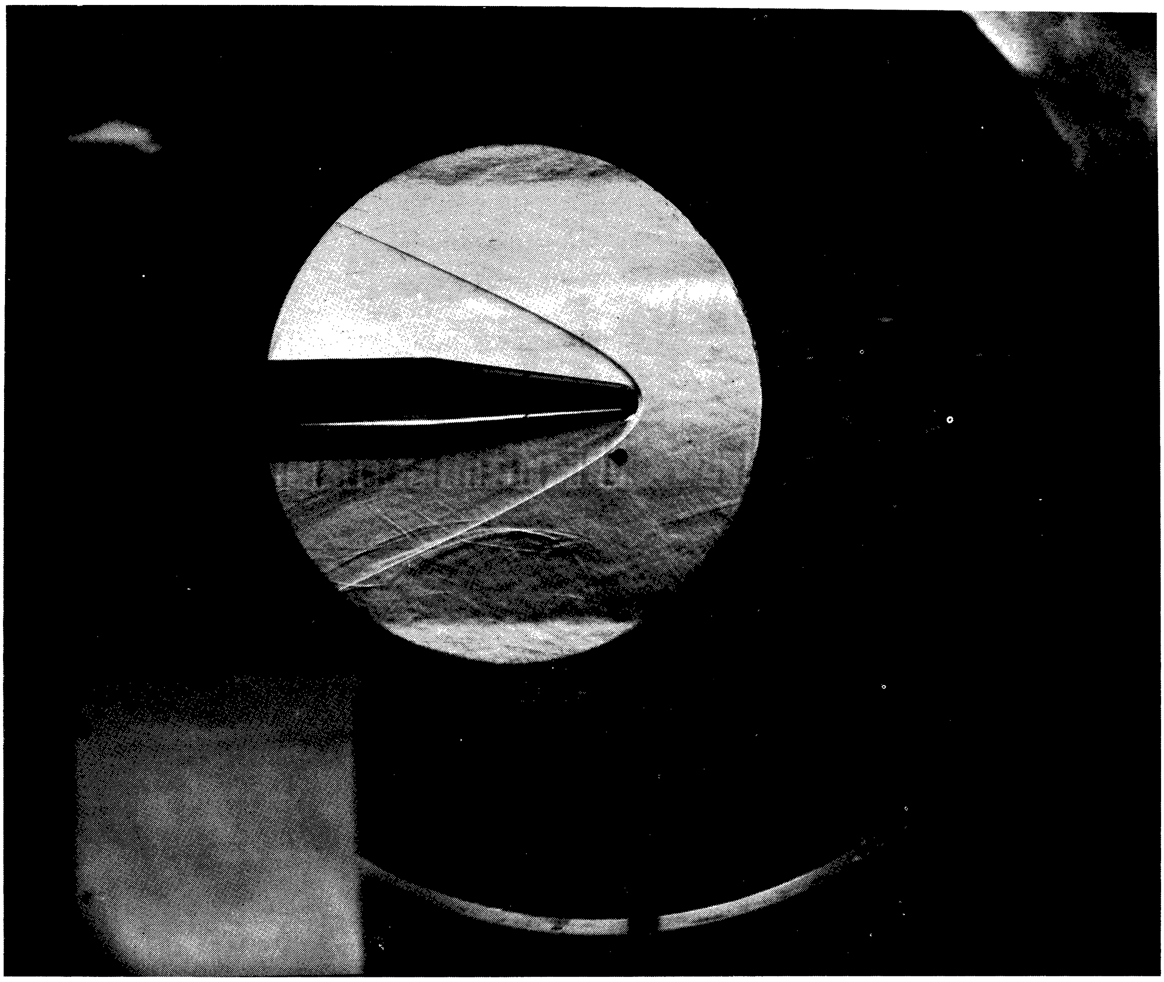

Fig. 5. Schlieren photograph of probe at M=3.02.

4. MATHEMATICAL INVESTIGATION OF THE CURRENT COLLECTING CHARACTERISTICS OF A MOVING PROBE

4.1 THE PHYSICAL PROBLEM

To formulate a theoretical treatment for the collection characteristics of the probe discussed in Section 3, we consider a rounded electrode moving with supersonic velocity through a dense neutral gas containing a low density plasma. The principal features of the physical environment near such a body are indicated in Fig. 6.

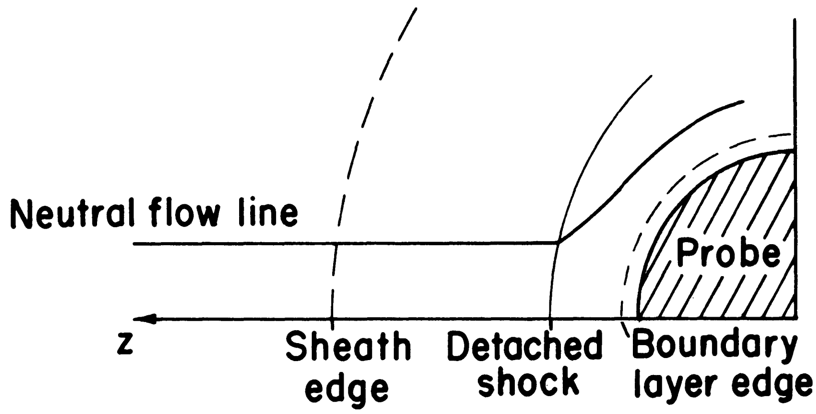

Fig. 6. Representation of the physical environment in front of a supersonic probe.

Here the flow of the nonionized component of the gas is uniform outside the shock, changes to a region of compressible flow behind this, and passes over into the boundary layer near the probe surface.

Significant electrical effects on the ionized components of the flow are restricted to a region around the probe designated the sheath. The scale of this region of electrical influence is determined mainly by the temperatures and densities of the charged particle components and by the potential of the probe relative to the plasma; for sufficiently low densities and/or high probe potentials, this region may extend well beyond the shock. Consequently, within the sheath, strong ionic currents may be created, resulting in a net current to the probe.

Our concern in the following work is to relate the charged particle densities in the undisturbed plasma to the current collected by the probe as a function of the probe voltage.

4.2 MATHEMATICAL FORMULATION

Since we wish to apply our results to data from a probe in the D-region of the ionosphere, the following assumptions regarding the gas are considered justified:

a. The degree of ionization of the gas is small so that the flow of the neutral particle component is unaffected by the ionic currents;

b. The neutral particle density is high enough so that ion migration is governed by mobility and diffusion;

c. The shock is nonionizing and the flow is frozen;

d. The entire system is in a steady state;

e. The Einstein relation between mobility and diffusion constants is valid;

f. effects of magnetic fields are negligible;

g. Each ionic species and the neutral gas may be considered to have a well defined temperature.

The following two further assumptions are made to simplify calculations, though neither is essential in principle to the development:

a. Only positive and negative ions of equal masses are present in the plasma;

b. The plasma components are in thermal equilibrium with the neutral component.

Under these assumptions we may consider the system governed by the equations of charge conservation for each species and by the Poisson equation, written respectively:

$$\nabla' \cdot (\overline{V}'\sigma' - K\sigma'\nabla'\Phi' - D\nabla'\sigma') = 0$$

$$\nabla' \cdot (\overline{V}'\zeta' + K\zeta'\nabla'\Phi' - D\nabla'\zeta') = 0 \qquad (4.2\text{-}1)$$

$$\nabla' \cdot \nabla'\Phi' = \frac{\zeta' - \sigma'}{\epsilon} .$$

The boundary conditions for the system are:

on the probe surface[2,5]

$$\sigma' = \zeta' = 0, \quad \Phi' = \Phi_p'; \tag{4.2-2}$$

at great distances from the probe:

$$\sigma' = \sigma_\infty', \quad \zeta' = \zeta_\infty', \quad \Phi' = 0.$$

Written in terms of the appropriate dimensionless variables, the constants K, D and ϵ can be absorbed (see nomenclature) and the system of differential equations may be written:

$$\begin{aligned} \nabla\cdot(\overline{V}\sigma-\sigma\nabla\Phi-\nabla\sigma) &= 0 \\ \nabla\cdot(\overline{V}\zeta+\zeta\nabla\Phi-\nabla\zeta) &= 0 \\ \nabla\cdot\nabla\Phi &= \zeta-\sigma, \end{aligned} \tag{4.2-3}$$

while the boundary conditions become:

on the probe surface

$$\sigma = \zeta = 0, \quad \Phi = \Phi_p, \tag{4.2-4}$$

at large distances from the probe

$$\sigma_\infty = \zeta_\infty = 1, \quad \Phi = 0$$

Throughout the remainder of this report all quantities will be considered in dimensionless form.

4.3 DISCUSSION OF PROBLEM

The problem as formulated is complicated in particular by the three flow regimes of the neutral gas which must be considered. Up to the present time, theoretical work has been done only on certain aspects of the problem as a whole.

Talbot[1] considers a small planar probe at the stagnation point of a blunt body in a low density supersonic flow. He assumes that the sheath is entirely within the boundary layer and that its thickness is much less than an ionic mean free path.

Chung[2] and Pollin[3] treat a similar problem, but consider ion motion in the sheath to be governed by mobility and diffusion. Again, the sheath is taken as imbedded in the boundary layer. In addition, Pollin considers ionization caused by a strong shock.

At the other extreme, Cohen,[4] and Su and Lam[5] have given the continuum treatment for a stationary sphere.

A more general treatment for an arbitrary low velocity probe in a continuum plasma has been given by Lam.[6] Considering only incompressible flow of the neutral gas, a complete solution to the problem is provided, making no assumptions about the range of the electrical effects of the probe.

Unfortunately the various simplifying assumptions made in the above works render their results inextensible to the problem here considered. Indeed, an exact analytical solution to the entire problem seems out of the question. For this reason, this report describes work done toward its solution by a numerical method.

5. THE "FLOW LINE" METHOD

5.1 OUTLINE OF METHOD

The object of this method is to determine the flow of the plasma components by a series of approximations to the charge and potential distributions about the probe. Starting with the potential field of the probe (taken as a spherical conductor) in free space, flow lines of small elements of the plasma are obtained. Considering the resulting space charge distribution, a new potential field is determined which is in turn used to find new flow lines. The process is to be continued until the variations in succeeding approximations are considered sufficiently small. The current to the probe can then be obtained by calculating the current in the flux tubes containing all flow lines which terminate on the probe surface.

To determine the desired flow lines we apply the divergence Eqns. (4.2-3), to current flux tubes. These equations may be interpreted as expressing the constancy of current in any given tube. From these, we take the current densities for positive and negative species:

$$\bar{J} = (\bar{V}-\nabla\Phi)\sigma-\nabla\sigma$$

$$-\bar{L} = (\bar{V}+\nabla\Phi)\zeta-\nabla\zeta. \qquad (5.1\text{-}1)$$

Here the velocity field $\bar{V}$ of the neutral gas is considered known; the flow ahead of the shock is uniform, while that between probe and shock can be determined numerically,[7,8,9] and entered in the computer as a table.

In the supersonic region of the flow the convective contribution in Eqns. (5.1-1) will dominate the others. Lam[6] has shown, by his "outer" solution, that in such a region the charge densities are uniform, while the potential is harmonic. Thus, we can expect the diffusive terms in Eqns. (5.1-1) to be smaller than the mobility terms except near the probe. Consequently, as a first approximation, we can consider large diffusive effects to be confined to the region behind the shock where the neutral flow is most complex.

This suggest that the program be constructed in two phases:

I. The determination of flow lines in a region of uniform neutral flow, neglecting diffusive effects entirely;

II. Extension of the above to include the flow region behind the shock and density gradient terms over the entire flow field.

This breakdown has several advantages:

a. The phase I program alone should provide good estimates of the actual flow lines in the region considered. Further because the shock standoff distance is small a reasonable estimate of expected probe current can then be obtained for sufficiently large probe potentials simply by extending the flow lines for the attracted ion species down to the probe surface and neglecting the retarded species altogether.

b. By excluding diffusive contributions ahead of the shock analytical solutions for the initial flow lines can be obtained. Comparing these with the corresponding results of the phase I program, the error in the computed flow lines can be estimated;

c. To extend the phase I program to cover the entire flow field (phase II), two essentially similar interpolation routines must be introduced (see Section 8.1). Upon their insertion into the phase I program the general flow line program is completed.

This report deals only with the phase I program.

5.2 DETERMINATION OF FLOW LINES—PHASE I

In the following we treat flow lines of positive particles only; the development for negative species parallels this exactly with appropriate adjustments of signs.

Neglecting the diffusive term in the expression for the positive ion current density in Eqn. (5.1-1) we have:

$$\bar{J} = (\bar{V} - \nabla\Phi)\sigma. \qquad (5.2\text{-}1)$$

From this, the charges can be considered to move as the result of a composite velocity term:

$$\bar{v} = \bar{V} - \nabla\Phi. \qquad (5.2\text{-}2)$$

Integrating this over a small but finite time increment δt we have:

$$\delta\bar{\ell} = (\bar{V} - \nabla\Phi)\delta t + O(\delta t^2) \qquad (5.2\text{-}3)$$

where $\delta\bar{\ell}$ is the change in position of the charge element during time δt.

Taking a cylindrical coordinate system (r, ϕ, z) with origin at the center of the probe and z-axis directed into the flow, the neutral flow vector and potential gradient become respectively:

$$\overline{V} = -V\,\hat{z} \qquad (5.2\text{-}4)$$

and

$$\nabla\Phi = \frac{\partial\Phi}{\partial r}\,\hat{r} + \frac{\partial\Phi}{\partial z}\,\hat{z}, \qquad (5.2\text{-}5)$$

where $\hat{r}$ and $\hat{z}$ are unit vectors in the r and z directions respectively.

Knowing the potential field (see Section 5.4) the gradients in Eqn. (5.2-5) are found in the program by using a difference method.* Desiring the gradients at some point P, and taking a difference parameter Δ (see Fig. 7) we have:

$$\left.\frac{\partial\Phi}{\partial r}\right|_P = \frac{\Phi_4-\Phi_2}{2\Delta} + O(\Delta^2)$$

$$\left.\frac{\partial\Phi}{\partial z}\right|_P = \frac{\Phi_1-\Phi_3}{2\Delta} + O(\Delta^2) \qquad (5.2\text{-}6)$$

where Φ_i represents the potential at a point i at a distance Δ along lines parallel to the coordinate axes.

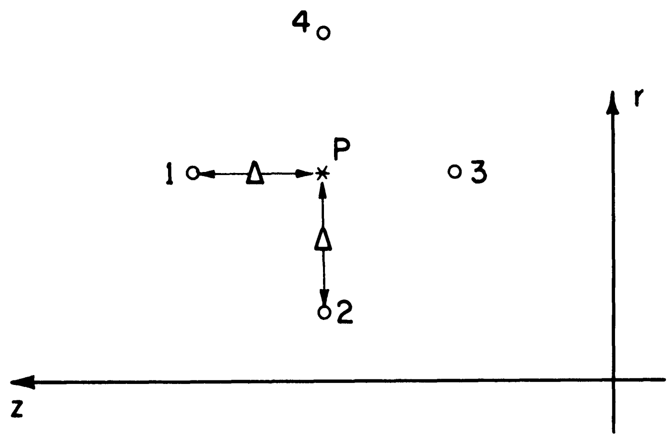

Fig. 7. The difference scheme for potential gradient calculations.

The quantity Δ is chosen to be consistent with the point spacings in the trajectory field. Starting points for the trajectories (taken along a line of constant z far ahead of the probe) are spaced so that:

$$\delta r = V\,\delta t \qquad (5.2\text{-}7)$$

making the r and z spacings of the trajectory points of the same order. Δ is

*The only variation in this procedure occurs in the determination of the initial trajectory field. In this case an analytical expression for Φ is assumed (see part 6).

then written as:

$$\Delta = H\,V\,\delta t \qquad (5.2\text{-}8)$$

where H is an input constant, usually taken as 0.5. Thus, Δ is of order δt.

Consequently, using Eqns. (5.2-6), Eqn. (5.2-3) gives us:

$$\delta\overline{\ell} = \left[-\frac{\Phi_4-\Phi_2}{2\Delta}\,\hat{r} - \left(V+\frac{\Phi_1-\Phi_3}{2\Delta}\right)\hat{z}\right]\delta t, \qquad (5.2\text{-}9)$$

which is accurate to terms in δt^2. Indeed, since the error incurred through the approximation (5.2-6) will contribute only a term in δt^3 to the above, the second order error term arises only from Eqn. (5.2-3), and has the form:

$$\overline{\epsilon} = (\overline{v}\cdot\nabla)\overline{v}\,\frac{\delta t^2}{2}\,. \qquad (5.2\text{-}10)$$

To obtain the flow lines, Eqn. (5.2-9) is applied at a given point to determine the next. Reapplying the equation at the new point another is found, and the process is continued until the flow line is terminated. If one considers the flow line to be generated over a fixed time interval $t_n = n\delta t$, while letting n increase (by taking successively finer and finer steps) then the accumulated error behaves as

$$\overline{\epsilon}_n = \frac{1}{n}\,(\overline{v}\cdot\nabla)\overline{v}\,\frac{t_n^2}{2}, \qquad (5.2\text{-}11)$$

so that the total error over the given time interval decreases inversely as the number of steps in the interval.

Because of limited storage facilities in the computer, the region of study must be restricted to a finite volume of space about the probe. Consequently, a region is considered which is bounded in the z direction by two planes normal to the z axis, one ahead of and one behind the probe, and radially by imposing a certain maximum on the initial radial coordinates of the flow lines. The positions of these planes and the value of the maximum radius are obtained below.

The initial points for the flow lines can be chosen by considering the flow along the axis. Here $r \equiv o$, and the initial z coordinate may be determined by requiring that the mobility term $(\nabla\Phi)$ resulting from the starting potential be a certain fraction p of the free stream velocity V:

$$p = \frac{|\nabla\Phi|}{V}\,. \qquad (5.2\text{-}12)$$

The initial r coordinate for the flow line farthest from the axis may then be taken as, say, twice the value of z so determined, to allow for the greater range of influence of the potential field normal to the flow. Since the terminal value of z is fixed by the parameters of the problem, as explained below, the value of p is chosen to make the total number of points on the flow lines compatible with the available storage space in the computer.

The terminal z coordinate of the flow line, z_{min}, is determined by other means. In using the first approximation to the potential, it is found that the flow lines of the repelled charge species are deflected so as never to close in again behind the probe. Since this does not occur with the flow lines of the attracted species, the result is an infinite sheath trailing behind the probe. This is clearly nonphysical, and its elimination provides the criterion used for terminating the flow lines.

On physical grounds the probe must cause a disturbance in the plasma charge distribution which is commensurate with its own charge. Thus, the charge imbalance in the sheath must be equal to the charge residing on the sphere:

$$Q_{sphere} = - Q_{sheath} \qquad (5.2\text{-}13)$$

Satisfying this condition requires that the charge "tail" behind the probe be cut off at a distance which can be calculated (see Section 6.4). This also restores charge neutrality in the plasma at infinity, as required by the boundary conditions.

5.3 DETERMINATION OF CHARGE DENSITIES

Knowing the flow lines, the variations in charge density along them can be obtained.

Since the flow far ahead of the probe is uniform each flow line in that region is parallel to and is characterized by its distance from the z axis. Let this characteristic distance be r_o.

Recalling the symmetry of the problem, each flow line is recognized as a section of a surface of revolution about the axis. Two such surfaces whose characteristic distances (radii) differ by an infinitesimal amount, dr_o, form a flux tube. By Gauss' Theorem and the first of Eqns. (5.1-1) we may write for such a tube:

$$\int_\tau \nabla \cdot \overline{J} \, d\tau = \int_A \overline{J} \cdot d\overline{A} = 0. \qquad (5.3\text{-}1)$$

Here we consider a volume τ obtained by twice slicing the flux tube transversely. The only portions of the surface of this volume (denoted A) which contribute to the above integral are these transverse surfaces. For convenience we take these surfaces as being everywhere orthogonal to the trajectories. Considering one such surface infinitely far upstream of the probe, and the other a finite distance from it, we may write Eqn. (5.3-1):

$$J_\infty \, dA_\infty = J \, dA = I = \text{constant}, \qquad (5.3\text{-}2)$$

where I is the current in the flux tube and the scalar product is neglected because $\bar{J}$ and $d\bar{A}$ are parallel.

By symmetry and using Eqns. (5.2-1) and (5.2-2), Eqn. (5.3-2) may be written:

$$I = \sigma_\infty V 2\pi r_o dr_o = \sigma \, v \, 2\pi r \, ds, \qquad (5.3\text{-}3)$$

where ds is the distance between the two "flow line surfaces" at the point (r,z) (see Fig. 8). Since v is known, only ds needs to be determined in order to find the charge densities.

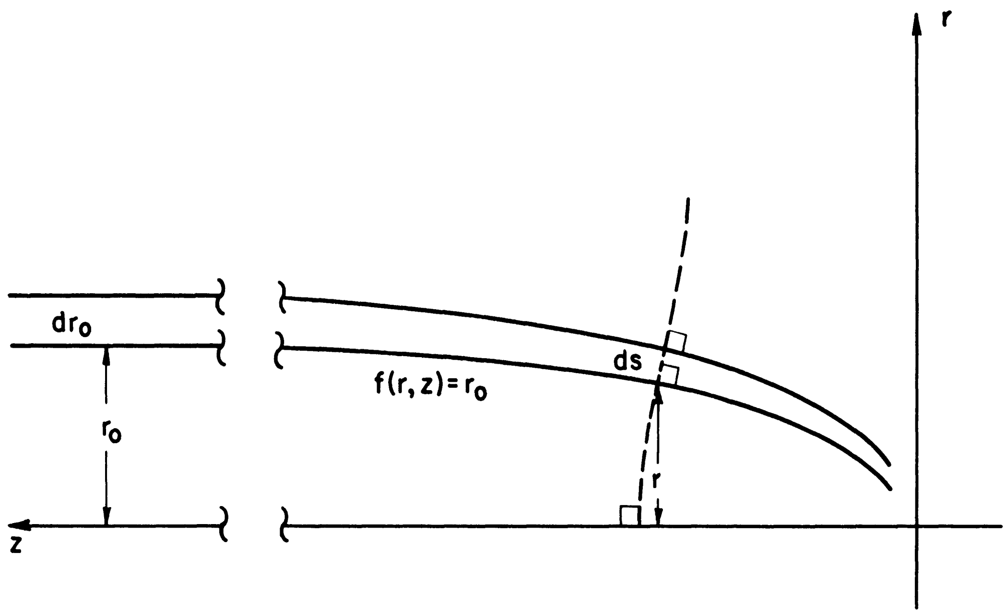

Fig. 8. Parametrization of flow lines.

The equation of a given flow line may be written as:

$$z = z(r, r_o), \qquad (5.3\text{-}4)$$

or, solving for r_o in terms of r and z:

$$r_o = f(r,z). \qquad (5.3\text{-}5)$$

Considering f as a function of its two independent variables and taking its gradient, we have:

$$|\nabla f| = \frac{df}{ds} \tag{5.3-6}$$

where ds is the magnitude of an elemental displacement taken normal to the curves of constant f. From Eqn. (5.3-5) $df \equiv dr_o$, and since we have taken our slicing surfaces normal to the flow lines, the ds of Eqn. (5.3-6) is seen to be the quantity we seek:

$$ds = dr_o / |\nabla f| \tag{5.3-7}$$

Thus, to determine the charge densities from Eqn. (5.3-3) it is sufficient to know the equations of the flow lines and the local flow velocity v.

In the phase I program the densities are not needed explicitly, but are used implicitly in calculating the potential.

5.4 CALCULATION OF POTENTIAL

In order to make use of Eqn. (5.2-9), it is necessary to know the potential distribution in the space surrounding the probe. This field will be governed by the Poisson Equation.

$$\nabla^2 \Phi = \zeta - \sigma \tag{5.4-1}$$

and the boundary conditions.

$$\Phi = \Phi_p \quad \text{at the probe}$$

$$\Phi \to 0 \quad \text{at large distances from the probe} \tag{5.4-2}$$

Assuming the charge densities known, the potential at any point P may be expressed in terms of the probe potential Φ_p and integrals over the space charge distribution:

$$\Phi(P) = \Phi_p \frac{a}{R(P)} - \frac{1}{4\pi} \int \frac{dq}{R_1} + \frac{1}{4\pi} \int \frac{dq'}{R_2} \tag{5.4-3}$$

where

$$dq = (\sigma - \zeta) d\tau \tag{5.4-4}$$

$$dq' = \frac{a}{R} dq, \tag{5.4-5}$$

and a, R, R_1, R_2, R(P) are the nondimensionalized distances shown in Fig. 9.

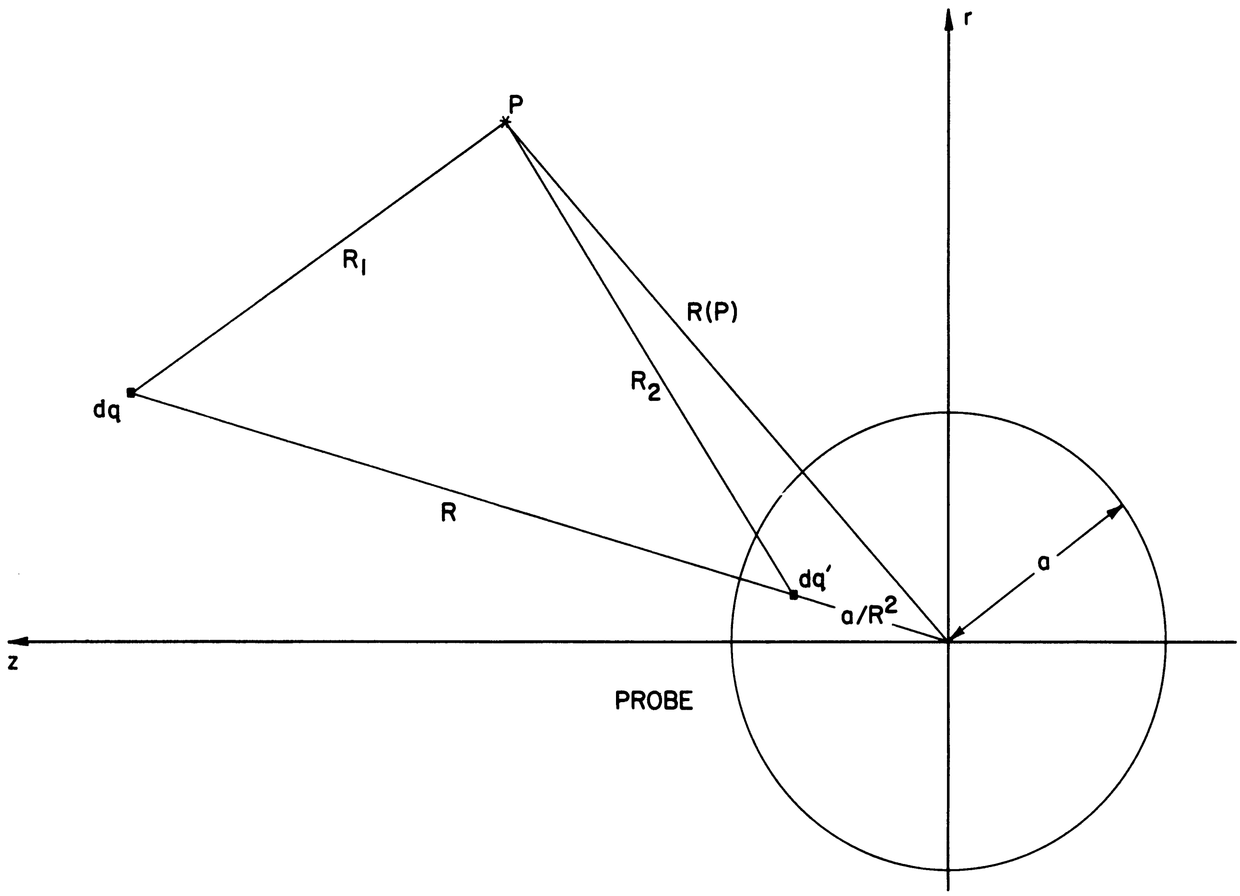

Fig. 9. Variables used in potential integration.

The terms in Eqn. (5.4-3) may be identified as the potentials at P due to the probe, the space charge distribution, and the surface charge induced on the sphere respectively.

In order to use this equation in the program for the calculation of potential, the integrals must be reduced to sums over the points composing the flow lines.

We consider the integrals over the two charge densities in Eqn. (5.4-3) separately. For either species, the flow lines and the corresponding family of "slicing" surfaces we have chosen form an orthogonal net over the r,z plane. The differential volume element may then be conveniently expressed as:

$$d\tau = r\, d\ell\, ds\, d\phi, \qquad (5.4\text{-}6)$$

where ℓ and s measure distances along the flow lines and the orthogonals, respectively, and r is the cylindrical radial coordinate of the volume element. Further, the elemental distance along a flow line may be expressed as:

$$d\ell = v\, dt. \qquad (5.4\text{-}7)$$

Combining Eqns. (5.3-3), (5.4-6), and (5.4-7) we obtain:

$$\sigma \, d\tau = \sigma_\infty \frac{V \, r_o \, dr_o}{v \;\; r \;\; ds} \cdot r \, v \, dt \, ds \, d\phi$$

$$= \sigma_\infty V \, dt \, r_o \, dr_o \, d\phi, \qquad (5.4\text{-}8)$$

so that the integrals of interest take the form:

$$\int \rho \frac{d\tau}{R_i} = V \rho_\infty \int \frac{r_o \, dt \, dr_o \, d\phi}{R_i} \qquad (5.4\text{-}9)$$

where integration extends along a flow line (dt), over all flow lines (dr_o) and around the symmetry axis ($d\phi$). Here ρ and R_i are to be taken respectively as the appropriate charge density and the distance between charge element and field point.

Using the flow lines obtained previously (Section 5.2), Eqn. (5.4-9) is well suited for numerical evaluation. The r_o of each flow line is known, as is the spacing between flow lines δr_o. The step size in the flow lines is determined by the input value of δt. Thus, the integrations over r_o and t in Eqn. (5.4-9) are easily transformed to sums over the points of the flow lines. Only the angular integration need be more thoroughly investigated.

Consider a charge element dq and its image charge in the sphere, dq', as shown in Fig. 10. Let the potential be desired at the point P(r,z,o), let

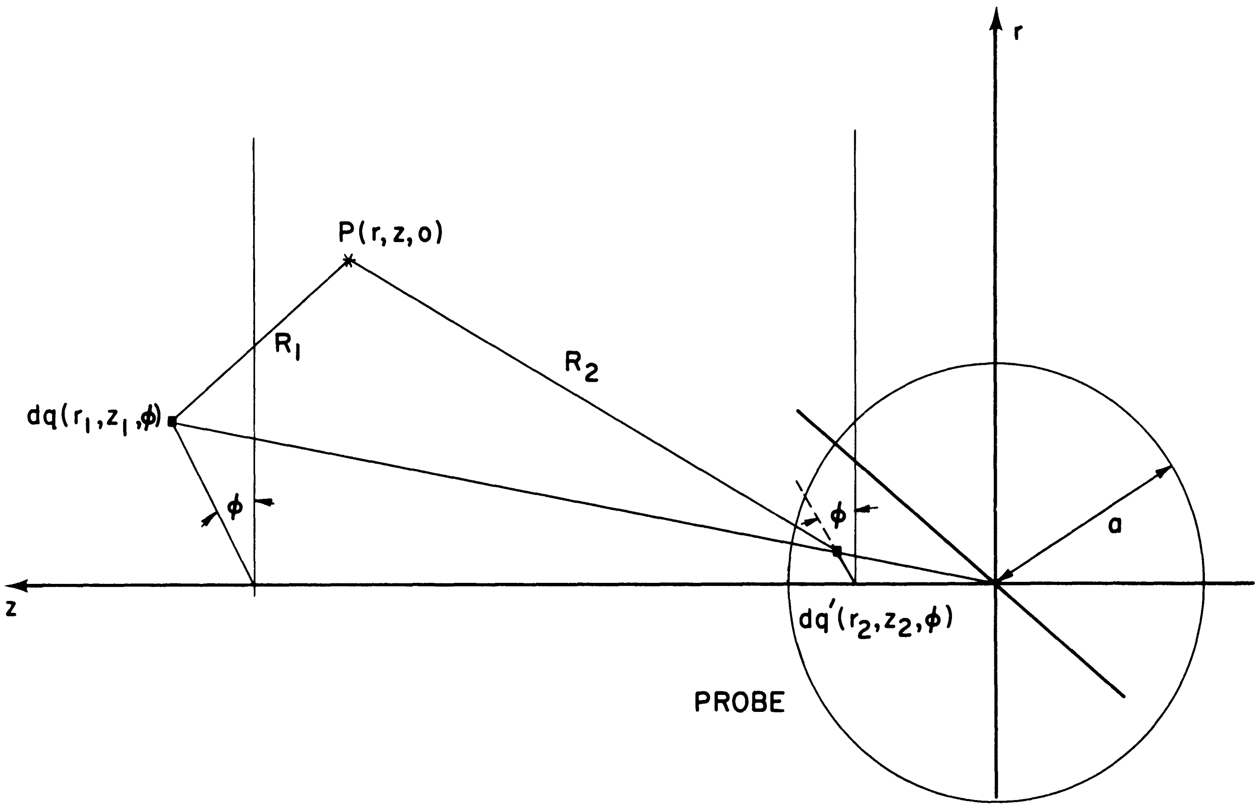

Fig. 10. Variables relating charge with its image charge.

dq be at (r_1, z_1, ϕ), and let dq' be at (r_2, z_2, ϕ). It is easily established from the figure that:

$$R_i^2 = (z-z_i)^2 + r^2 + r_i^2 - 2rr_i \cos\phi$$

$$= A_i - B_i \cos\phi \qquad i = 1,2 \qquad (5.4\text{-}10)$$

where A_i and B_i have the obvious definitions. From the position of the image charge (see Fig. 9) it is known that:

$$r_2 = \frac{a^2}{r_1^2+z_1^2} r_1$$

$$z_2 = \frac{a^2}{r_1^2+z_1^2} z_1. \qquad (5.4\text{-}11)$$

Using relations (5.4-10) and (5.4-11), all integrands in integrals of the form (5.4-9) can be expressed in terms of the coordinates of dq and the point P, i.e., in terms of the flow line point and the field point.

Using the notation of Eqn. (5.4-10) the azimuthal integral in Eqn. (5.4-9) takes the form

$$\int \frac{d\phi}{R_i} = \frac{1}{\sqrt{A_i}} \int_0^{2\pi} \frac{d\phi}{\sqrt{1-\alpha_i \cos\phi}} . \qquad (5.4\text{-}12)$$

where

$$\alpha_i = \frac{B_i}{A_i} \qquad 0 \leq \alpha_i \leq 1. \qquad (5.4\text{-}13)$$

The integral on the right side of Eqn. (5.4-12), may be expressed in terms of the complete elliptic integral of the first kind:

$$\int_0^{2\pi} \frac{d\phi}{\sqrt{1-\alpha_i \cos\phi}} = \frac{4}{\sqrt{1+\alpha_i}} \int_0^{\pi/2} \frac{d\zeta}{\sqrt{1-\frac{2\alpha_i}{1+\alpha_i}\sin^2\zeta}}$$

$$= \frac{4}{\sqrt{1+\alpha_i}} \kappa\left(\frac{2\alpha_i}{1+\alpha_i}\right) \qquad (5.4\text{-}14)$$

Thus, Eqn. (5.4-12) may be written as:

$$\int \frac{d\phi}{R_i} = \frac{4}{\sqrt{A_i+B_i}} \kappa\left(\frac{2\alpha_i}{1+\alpha_i}\right) \tag{5.4-15}$$

In the program this elliptic integral is evaluated by the series:

$$\kappa\left(\frac{2\alpha}{1+\alpha}\right) = \sum_{n=o}^{4} a_n \left(\frac{1-\alpha}{1+\alpha}\right)^n - \ln\left(\frac{1-\alpha}{1+\alpha}\right)\cdot\sum_{n=o}^{4} b_n \left(\frac{1-\alpha}{1+\alpha}\right)^n, \tag{5.4-16}$$

where[10]

$$\begin{aligned}
a_o &= 1.386\ 294\ 361\ 12 & b_o &= .5 \\
a_1 &= .096\ 663\ 442\ 59 & b_1 &= .124\ 985\ 935\ 97 \\
a_2 &= .035\ 900\ 923\ 83 & b_2 &= .068\ 802\ 485\ 76 \\
a_3 &= .037\ 425\ 637\ 13 & b_3 &= .033\ 283\ 553\ 46 \\
a_4 &= .014\ 511\ 962\ 12 & b_4 &= .004\ 417\ 870\ 12
\end{aligned} \tag{5.4-17}$$

Evaluating this series in the IBM 7090 computer using roughly 9 significant figures, the results are considered accurate to about one part in 10^7.

It is noted that the above integral diverges as the logarithm of $(1-\alpha_i)^{-1}$ when $\alpha_i \to 1$, i.e., as the field point approaches a flow line point. Since this divergence is nonphysical, such situations must be treated by a special method.

In evaluating the potential integrals we obtain Eqn. (5.4-12) by considering the charge associated with a given flow line point to be concentrated on a circle concentric with the symmetry axis, rather than distributed in a toroid of finite volume. Since the potential of such a ring diverges as one approaches it, the misbehavior of our integral is explained. Clearly then, our method breaks down when the field point P enters the torus associated with the flow line point (Fig. 11). This provides a criterion for changing the procedure used for finding the potential due to the toroid in question.

Turning again to Fig. 11, the toroid associated with the point Q will generally have a roughly parallelogram-like cross-section with an area of order $(v\delta t)^2$. Since the exact shape of this figure cannot be determined without greatly increased complexity, it is approximated in the program by a circle about the point Q having area $(v\delta t)^2$. The radius of this circle is then given by:

$$r = \frac{v\delta t}{\sqrt{\pi}} \tag{5.4.18}$$

where the value of $v\delta t$ is taken as the separation of the trajectory point Q and the preceding point S. If a point P falls within distance r of Q, the potential at that point is found in the following manner.

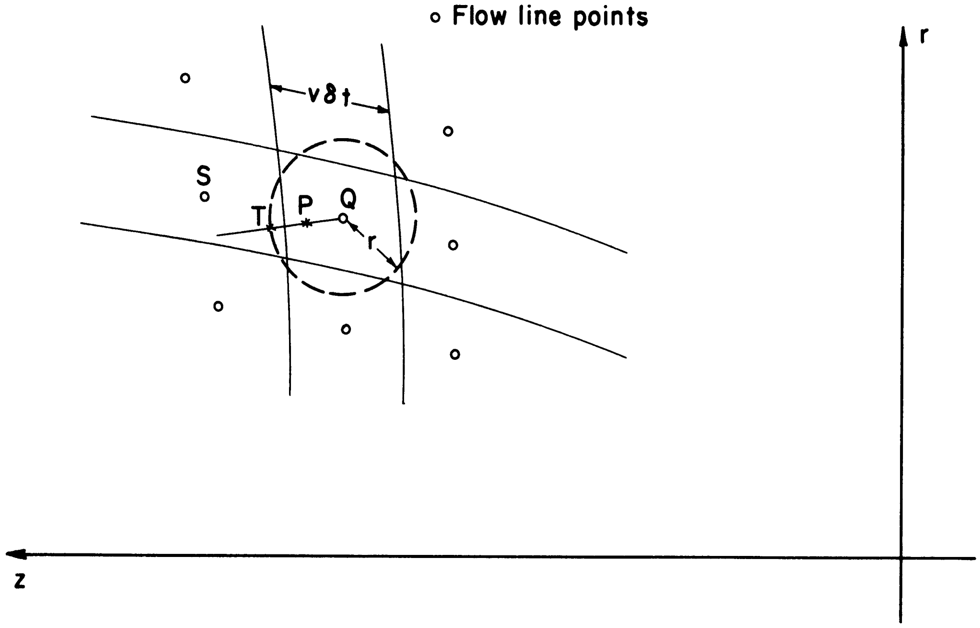

Fig. 11. Section of charge toroid.

The line PQ is constructed and extended through P to intersect the above circle at T. The potential at T is found in the usual manner, and the potential at Q is found as explained below. Then the potential at P is taken as that obtained by linear interpolation between the potentials at Q and T.

To obtain the potential at a point Q on the central circle of the torus, the torus is first approximated by a series of spheres centered on this circle. The potential due to this new charge distribution is taken as an approximation to that of the original toroidal distribution.

The torus is assumed to have major radius R, and minor radius r, given by Eqn. (5.4-18) (see Fig. 12). Measuring from the point Q the axis is cut into segments having length

$$R\delta\phi = \frac{2\pi R}{\left[\frac{\pi R}{r}\right]} \tag{5.4-19}$$

where $[\pi R/r]$ signifies the greatest integer in $\pi R/r$. At the end of each segment determined as above, a sphere of radius r is constructed. Each such sphere is considered to have charge given by:

$$\delta q = \frac{q}{\left[\frac{\pi R}{r}\right]} \tag{5.4-20}$$

where q is the total charge of the complete torus. The flow lines have been generated in such a way that this charge is identically equal to the charge in a torus at the top of the flow line considered, i.e.,

$$q = 2\pi\, r_o\, \delta r_o\, V\, \delta t. \tag{5.4-21}$$

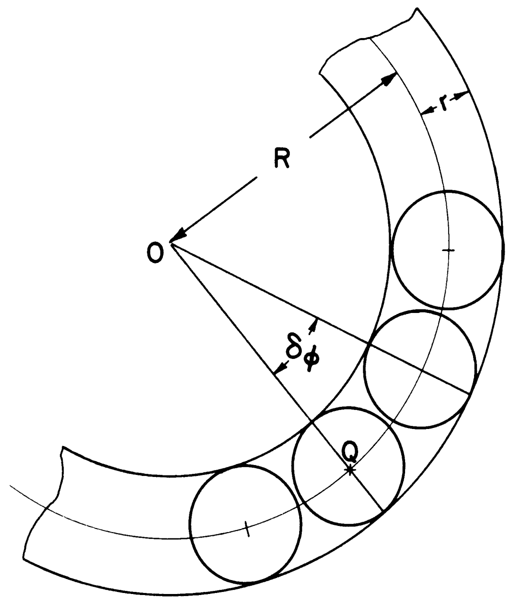

Fig. 12. Construction for integration when field point lies within charge toroid.

Calling

$$\phi_n = n\,\delta\phi, \qquad n = 0,1,\ldots,[\pi \tfrac{R}{r}]-1 \tag{5.4-22}$$

the potential at Q due to this distribution is

$$\Phi = \Phi_o + \frac{1}{4\pi} \sum_{n=1}^{[\pi \frac{R}{r}]-1} \frac{\delta q}{\sqrt{2R^2-2R^2\cos\phi_n}}, \tag{5.4-23}$$

where

$$\Phi_o = \frac{3\, r_o\, \delta r_o\, V\, \delta t}{4r\, [\pi \frac{R}{r}]} \tag{5.4-24}$$

represents the potential at Q due to the sphere of charge δq centered at Q. Thus the total potential at Q due to the torus is:

$$\Phi = \frac{r_o\, V\, \delta r_o\, \delta t}{2\sqrt{2}\,[\pi \frac{R}{r}]} \left\{ \frac{3}{r\sqrt{2}} + \frac{1}{R} \sum_{n=1}^{[\pi \frac{R}{r}]-1} \frac{1}{\sqrt{1-\cos\phi_n}} \right\} . \qquad (5.4\text{-}25)$$

The above relations now allow us to calculate the potential at any point P due to the charge distribution given by the flow lines. The potential expression (5.4-4) becomes:

$$\Phi(P) = \Phi_p \frac{a}{R(P)} + \frac{V\,\delta t}{\pi} \left(\sum_\zeta{}' - \sum_\sigma{}' \right) r_o\, \delta r_o \left\{ \frac{\kappa\left(\frac{2\alpha_1}{1+\alpha_1}\right)}{\sqrt{A_1+B_1}} - \frac{a}{R}\, \frac{\kappa\left(\frac{2\alpha_2}{1+\alpha_2}\right)}{\sqrt{A_2+B_2}} \right\}$$

$$+ \frac{V\,\delta t}{2\sqrt{2}} \left(\sum_\zeta{}'' - \sum_\sigma{}'' \right) \frac{r_o\, \delta r_o}{[\pi \frac{R}{r}]} \left\{ \frac{3}{r\sqrt{2}} + \frac{1}{R} \sum_{n=1}^{[\pi \frac{R}{r}]-1} \frac{1}{\sqrt{1-\cos\phi_n}} \right\} \qquad (5.4\text{-}26)$$

where all symbols are as previously indicated, and $\sum_\sigma{}'$, $\sum_\zeta{}'$ are sums over all flow line points of the σ and ζ species respectively except points which fall into the case treated by Eqn. (5.4-25), which are accounted for by the sums $\sum_\sigma{}''$ and $\sum_\zeta{}''$. The values of r_o and δr_o which are used in the program are computed from the r coordinates at the tops of the flow line considered and of that with the next larger value of r; r_o is taken as the average of these values, and δr_o as the difference. These calculations are performed for the farthest trajectory from the axis by considering another to be located δr_o farther out, where δr_o is taken as the last calculated value of that quantity.

6. INITIAL APPROXIMATIONS USED IN PROGRAMMING THE FLOW LINE METHOD

6.1 INTRODUCTION

In order to start the iterative procedure of the flow line method it is necessary to assume an initial potential field or charge distribution. We assume here an initial potential field: that due to a sphere of potential Φ_p in free space. This is not only reasonable physically but it also enables the flow lines and charge densities of the first iteration to be derived analytically, giving an insight into the operation of the procedure as well as an estimate of the errors involved due to finite step size.

6.2 INITIAL FLOW LINES

In a cylindrical coordinate system the initial potential is given by

$$\Phi = \Phi_p \frac{a}{\sqrt{r^2+z^2}}, \qquad r^2+z^2 \geq a^2 \tag{6.2-1}$$

The paths followed by the charge elements will be described by a function $z = z(r,r_o)$ which, for given r_o, will be everywhere tangent to the local velocity vector $\overline{v}$, as given by Eqn. (5.2-2). This function is determined by integrating the differential equation:

$$\frac{dr}{dz} = \frac{v_r}{v_z} \tag{6.2-2}$$

where v_r and v_z are the r and z components of the vector $\overline{v}$. Using Eqns. (5.2-2), (5.2-4), (5.2-5), and (6.2-1), we find these velocity components to be:

$$v_r = \frac{\Phi_p \, a \, r}{(r^2+z^2)^{3/2}}$$

$$v_z = -V + \frac{\Phi_p \, a \, z}{(r^2+z^2)^{3/2}} . \tag{6.2-3}$$

Substituting these relations in Eqn. (6.2-2), the resulting differential equation is easily integrated. Requiring that $r \to r_o$ as $z \to +\infty$ the constant of integration is evaluated, and the flow line equation is found to be:

$$r_o^2 - r^2 = 2\beta\left(\frac{z}{\sqrt{r^2+z^2}}-1\right), \tag{6.2-4}$$

where:

$$\beta = \frac{\Phi_p a}{V} . \qquad (6.2\text{-}5)$$

The equation for flow lines of the negative species is identical to the above except that the sign of the right side is changed.

Taking β positive (positive probe) the flow lines of positive particles are deflected away from the probe, while those of negative particles are attracted, which results in a region where one species is excluded, i.e., a sheath. It can be shown from the equations of the flow lines that this region starts at a distance ahead of the origin equal to $\sqrt{|\beta|}$, that it extends behind the probe an infinite distance, and that it is always of finite width, having a radius of $2\sqrt{|\beta|}$ at an infinite distance behind the probe. For the ionic species which is attracted to the probe, this radius also corresponds to the r_o of the flow line farthest from the axis which is "collected." In fact, it is easily shown that the flow lines of the positive and negative species are merely the mirror images of one another across the plane z=o (see Figs. 13 and 14).

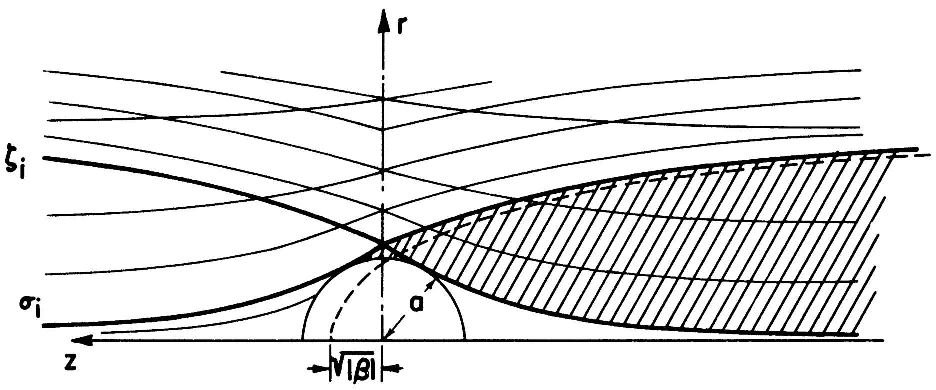

Fig. 13. Flow past sphere, ($\sqrt{|\beta|} < a$).

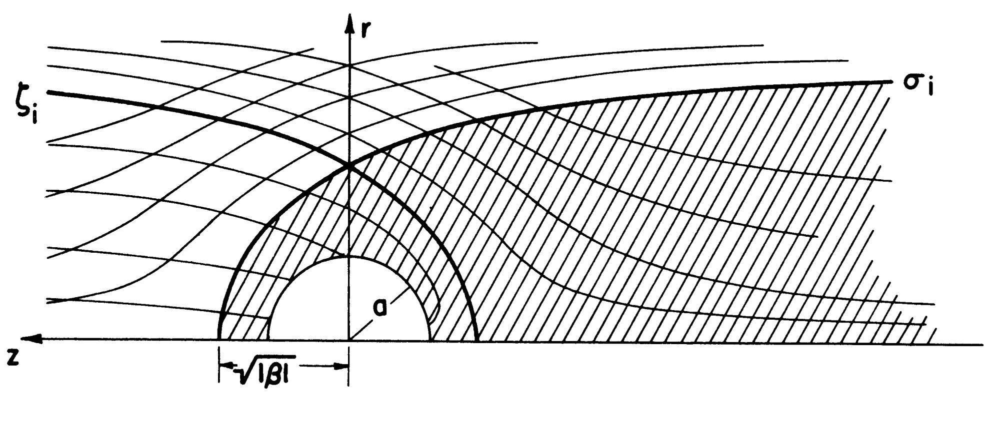

Fig. 14. Flow past sphere, ($\sqrt{|\beta|} > a$).

6.3 CHARGE DISTRIBUTION RESULTING FROM STARTING FLOW LINES

From Section 5.3 we know that the charge density distribution is given by Eqns. (5.3-3), (5.3-5), and (5.3-7). Combining these relations and using the fact that $\sigma_\infty = 1$ we obtain

$$\sigma = \frac{V}{v} \frac{|\nabla r_o^2|}{2r}, \qquad (6.3\text{-}1)$$

since by Eqn. (5.3-5), $f \equiv r_o$.

Solving Eqn. (6.2-4) for r_o^2 and using Eqns. (6.2-3) we find that

$$\frac{\partial r_o^2}{\partial r} = -2r \frac{v_z}{V}$$

$$\frac{\partial r_o^2}{\partial z} = 2r \frac{v_r}{V} \qquad (6.3\text{-}2)$$

so that Eqn. (6.3-1) reduces to:

$$\sigma \equiv 1. \qquad (6.3\text{-}3)$$

A similar relation holds for ζ, so that the charge distribution is everywhere uniform except in the region where one species of particles is excluded. The net density is therefore zero everywhere outside the sheath, and unity inside, where it has the sign opposite to that of the sphere potential.

6.4 TERMINATION OF FLOW LINES

As mentioned in Section 5.2, the nonphysical nature of the infinite trailing sheath provides a criterion for terminating the flow lines. Since both charge densities are uniform everywhere outside the sheath, terminating the flow lines amounts to cutting off the sheath and restoring neutrality to the flow behind it, which also satisfies the boundary condition of charge neutrality at infinity.

Our requirement is that the net charge in the sheath shall be equal in magnitude to the charge on the sphere due to its natural capacitance:

$$Q_{sphere} = -Q_{sheath} \qquad (6.4\text{-}1)$$

Considering the spherical probe to be initially in free space, the non-dimensionalized charge on it due to its own capacitance is easily found to be

$$Q_{sphere} = 4\pi a n_\infty \Phi_p \qquad (6.4\text{-}2)$$

Here the charge is normalized with respect to the electronic charge and n_∞ is the number of charged particles of either species in a cube at infinity having side equal to a Debye length, λ.

To determine the sheath charge for use in Eqn. (6.4-1) we must first find the boundary of the sheath.

Figure 13 indicates some of the flow lines of the first approximation in the vicinity of the probe when $|\beta| < a^2$. We note that the probe intercepts flow lines of both species. Assuming the probe to have a positive potential, the curves labeled σ_i and ζ_i represent the flow lines of positive and negative charges respectively which just graze the probe surface. All flow lines of both species having characteristic radii r_o less than those of the corresponding flow line above are collected; all having values of r_o greater than those of the above are not. Thus the sheath is the region (shaded) between the line σ_i, and the line ζ_i or the probe, whichever is appropriate. In this region there is negative charge only.

To determine the outer edge of the sheath we must find the flow line σ_i, which has a point of tangency with the probe. Let this line have characteristic radius r_o'. At the required point of tangency, call it (r',z'), the following conditions are satisfied:

$$r'^2 + z'^2 = a^2, \tag{6.4-3}$$

and:

$$r_o'^2 - r'^2 = 2\beta\left(\frac{z'}{\sqrt{r'^2+z'^2}} - 1\right). \tag{6.4-4}$$

In addition, the slope of the flow line is equal to that of the sphere here, so that the quantity $\frac{d}{dr} z^2$ is equal for both also. Finding z^2 from Eqns. (6.4-3) and (6.4-4), calculating these derivatives and equating the results we obtain:

$$(4\beta^2 - y^2)^2 = y^4 - 4\beta^2 y^2 + 8\beta^2 r'^2 y, \tag{6.4-5}$$

where:

$$y = r_o'^2 - r'^2 + 2\beta. \tag{6.4-6}$$

Solving the system of Eqns. (6.4-3) through (6.4-6) we obtain

$$r' = \sqrt{a^2 - \frac{\beta^2}{a^2}}$$

$$z' = \frac{\beta}{a} \tag{6.4-7}$$

$$r_o' = a - \frac{\beta}{a}.$$

The outer boundary of the sheath is thus determined.

The inner boundary of the sheath consists of two parts. Because of the symmetry of the flow lines of the different species about the plane z=o, the line ζ_i of Fig. 13 is tangent to the sphere at the point $(r', -z')$. Thus, the inner boundary of the sheath is the probe surface between the points (r', z') and $(r', -z')$, and is the flow line ζ_i for all values of $z < -z'$.

The value of r_o for this flow line, call it r_o'', can be found rather simply in terms of r'_o. We consider the flow line equation for negative ions:

$$r_o^2 - r^2 = -2\beta\left(\frac{z}{\sqrt{r^2+z^2}} - 1\right). \qquad (6.4\text{-}8)$$

Letting z go to minus infinity and denoting the value of r in this limit by r_∞ we have:

$$r_o^2 - r_\infty^2 = 4\beta. \qquad (6.4\text{-}9)$$

Because of the previously mentioned symmetry of the flow lines we know that for the ζ_i trajectory $r_\infty = r_o'$, so that Eqn. (6.4-9) gives us:

$$r_o''^2 = 4\beta + r_o'^2. \qquad (6.4\text{-}10)$$

Thus, the boundaries of the charge distribution in the sheath are known.

With this information we can now turn to the calculation of the sheath charge as required in Eqn. (6.4-1). Considering all flow lines terminated at some plane $z = z_{min}$, the sheath charge may be expressed in terms of integrals:

$$Q_{sheath} = -\pi n \begin{cases} \displaystyle\int_{z_{min}}^{z'} dz \int_{a^2-z^2}^{r_2^2(z)} d\, r^2 & |\beta| < a^2;\ z' > z_{min} > -a \\[2ex] \displaystyle\int_{-z'}^{z'} dz \int_{a^2-z^2}^{r_2^2(z)} d\, r^2 + \int_{z_{min}}^{-z'} dz \int_{r_1^2(z)}^{r_2^2(z)} d\, r^2 & |\beta| < a^2;\ z_{min} < -a \end{cases} \qquad (6.4\text{-}11)$$

where n represents the number of ions per Debye cube in the sheath, and $r_1^2(z)$ and $r_2^2(z)$ are obtained from the equations for ζ_i and σ_i respectively, as shown below.

Letting

$$\mu = r_o'^2 + 2\beta \qquad (6.4\text{-}12)$$

and expanding either of the equations for σ_i or ζ_i we obtain a single cubic equation in r^2:

$$(r^2)^3+(z^2-2\mu)(r^2)^2+\mu(\mu-2z^2)(r^2)+z^2(\mu^2-4\beta^2) = 0. \qquad (6.4\text{-}13)$$

For values of the parameters in this equation which are of interest to us ($|\beta| > 0$; r_o^2, $z^2 > 0$) there are three real solutions for r^2:

$$r^2(k,z) = \frac{2(r_0^2+z^2+2\beta)}{3}\left[1+\cos\left\{\frac{2k\pi + \mathrm{Cos}^{-1}\left(\frac{54\beta^2z^2}{(r_0^2+z^2+2\beta)^3}-1\right)}{3}\right\}\right] - z^2$$

$$k = 0,1,2 \qquad (6.4\text{-}14)$$

Considering appropriate limits of these solutions we find that:

$$r_1^2 = r^2(0,z)$$
$$r_2^2 = r^2(2,z) \qquad (6.4\text{-}15)$$

while the solution $r^2(1,z)$ is physically impossible.

In the event that $|\beta| \geq a^2$, Fig. 13 is altered (see Fig. 14). In this case all of the σ flow lines miss the probe entirely. In addition, there is no region behind the probe which is free of charge, so that the range of integration for the sheath charge integral extends from the axis to σ_i except between $a < z < -a$ where it is bounded on the inside by the sphere.

In this case flow line σ_i has $r_o' = 0$, so that μ in Eqn. (6.4-12) reduces to 2β. Equation (6.4-13) then becomes

$$(r^2)\ [(r^2)^2+(z^2-4\beta)(r^2)+4\beta(\beta-z^2)] = 0, \qquad (6.4\text{-}16)$$

and the solutions of interest are:

$$r_1^2(z) = 0$$
$$r_2(z) = 2\beta - \frac{z^2}{2} - \frac{z}{2}\sqrt{8\beta+z^2}\ . \qquad (6.4\text{-}17)$$

Using these results, the sheath charge integral now takes the forms

$$
Q_{sheath} = -\pi n \begin{cases} \displaystyle\int_{z_{min}}^{\sqrt{|\beta|}} dz \int_{0}^{r_2^2(z)} d\ r^2 & |\beta| \geq a^2;\ \sqrt{|\beta|} \geq z_{min} > a \\ \displaystyle\int_{z_{min}}^{\sqrt{|\beta|}} dz \int_{0}^{r_2^2(z)} d\ r^2 - \int_{z_{min}}^{a} dz \int_{0}^{a^2-z^2} d\ r^2 & |\beta| \geq a^2;\ a > z_{min} > -a \\ \displaystyle\int_{z_{min}}^{\sqrt{|\beta|}} dz \int_{0}^{r_2^2(z)} d\ r^2 - \int_{-a}^{a} dz \int_{0}^{a^2-z^2} d\ r^2 & |\beta| \geq a^2;\ z_{min} < -a \end{cases} \qquad (6.4\text{-}18)
$$

where $r_2^2(z)$ is given by Eqn. (6.4-17).

Thus, depending on the relative magnitudes of a^2 and β, the appropriate form of Eqns. (6.4-11) or (6.4-18) is used with Eqn. (6.4-2) in Eqn. (6.4-1). This yields an equation for z_{min} which involves only the parameters of the problem; when solved this provides the stopping point for the flow lines.

In the case where $|\beta| < a^2$ the evaluation of the charge integral is extremely difficult because of the complicated nature of the limits r_1^2 and r_2^2. However, if $|\beta| \ll a^2$ an approximation may be made which reduces the difficulty considerably and the integral may be evaluated. When $|\beta| > a^2$ the sheath charge integral can be evaluated directly. We now consider these cases separately.

If $|\beta| \ll a^2$ $\left(a \gg \frac{|\Phi_p|}{V}\right)$ the two flow lines determining the sheath will be tangent to the probe very near $(r,z) = (a,o)$. In the limit of $\Phi_p = 0$ these flow lines will satisfy this condition exactly and will be everywhere parallel to the z-axis. We consider cases near this limit, taking $|\beta|$ to be small.

Demanding that the two flow lines of interest pass through the point (a,0), the flow line equations give us the relations

$$
r_o^2 - a^2 = \pm 2\beta \qquad (6.4\text{-}19)
$$

where the upper sign is valid for flow lines of positive species, the lower for negative species. Substituting these results in the flow line equations we obtain:

$$
a^2 - r^2 = \frac{\pm 2\beta z}{\sqrt{r^2+z^2}} \ . \qquad (6.4\text{-}20)
$$

In the limit we are considering r will not deviate appreciably from its value at z = 0, so we set r = a in the radical of Eqn. (6.4-20) to obtain:

$$r^2 = a^2 \mp \frac{2\beta z}{\sqrt{a^2+z^2}} \quad . \tag{6.4-21}$$

This gives a good approximation to r^2 for all z, since near z = 0, r is very nearly equal to a, and for large negative z the importance of the r^2 in the radical is diminished so that the error introduced by the substitution r = a is very small.

Using Eqn. (6.4-21), the sheath charge integrals (6.4-11) reduce to:

$$Q_{sheath} \approx -\pi n \int_{z_{min}}^{0} dz \int_{a^2 + \frac{2\beta z}{\sqrt{a^2+z^2}}}^{a^2 - \frac{2\beta z}{\sqrt{a^2+z^2}}} dr^2 \qquad z_{min} \leq 0$$

$$= -4\pi n\beta a \left\{ \sqrt{1+x^2} - 1 \right\} \tag{6.4-22}$$

where:

$$x = \frac{z_{min}}{a} \quad . \tag{6.4-23}$$

Substituting Eqns. (6.4-21), (6.4-22), and (6.4-23) into Eqn. (6.4-1) and rearranging terms we have:

$$\frac{\Phi_p}{\beta} = \sqrt{1+x^2} - 1 = f(x) \qquad x \leq 0 \tag{6.4-24}$$

which enables us to solve for z_{min}. We note that the asympototic form of f(x) for large negative x, call it $f_\infty(x)$, is

$$f_\infty(x) = -x-1 \qquad x \to -\infty \tag{6.4-25}$$

When $|\beta| > a^2$, we use Eqns. (6.4-18) for the sheath charge. These can be immediately integrated to give

$$Q_{sheath} = -\frac{\pi n\beta^{3/2}}{6} \left[t^3 + (8+t^2)^{3/2} - 12t - 16 \right]$$

$$+ \frac{\pi n\beta^{3/2}}{3} \begin{cases} 0 & 1 \geq \gamma^2 \quad 1 > t > \gamma \\ t^3 - 3\gamma^2 t + 2\gamma^3 & 1 \geq \gamma^2 \quad \gamma > t > -\gamma \\ 4\gamma^3 & 1 \geq \gamma^2 \quad t < -\gamma \end{cases} \tag{6.4-26}$$

where

$$t = \frac{z_{min}}{\sqrt{|\beta|}}, \qquad \gamma = \frac{a}{\sqrt{|\beta|}} \quad . \tag{6.4-27}$$

Substituting Eqns. (6.4-27) and (6.4-26) into Eqns. (6.4-1) and (6.4-2), and rearranging terms we have

$$24\gamma \frac{\Phi_p}{\beta} = g(t) - \begin{cases} 0 & 1\geq \gamma^2 \quad 1>t>\gamma \\ 2h(\gamma,t) & 1\geq \gamma^2 \quad \gamma>t>-\gamma \\ 8\gamma^3 & 1\geq \gamma^2 \quad t<-\gamma \end{cases} \tag{6.4-28}$$

where

$$g(t) = t^3+(8+t^2)^{3/2}-12t-16 \tag{6.4-29}$$

$$h(\gamma,t) = t^3-3\gamma^2 t+2\gamma^3 . \tag{6.4-30}$$

The asymptotic form of g(t) is

$$g_\infty(t) = -24t-16 \qquad t \rightarrow -\infty . \tag{6.4-31}$$

Having obtained solutions of Eqn. (6.4-1) for $|\beta| \geq a^2$ and $|\beta| \ll a^2$ it is of interest to see whether the results can be adapted to the intermediate case of $|\beta| \lesssim a^2$. Considering the relations for x, t and γ (Eqns. (6.4-23) and (6.4-27)) we have

$$t = \gamma x. \tag{6.4-32}$$

Defining:

$$\eta = \frac{\Phi_p}{\beta}, \tag{6.4-33}$$

Eqn. (6.4-24) can be solved for t:

$$\begin{aligned} t &= \gamma f^{-1}(\eta) \\ &= -\gamma \sqrt{(\eta+1)^2-1}. \end{aligned} \tag{6.4-34}$$

Turning to Eqn. (6.4-28) we consider values of γ beyond the stated range, i.e., $\gamma > 1$. From the nature of $h(\gamma,t)$ we know that

$$24\eta\gamma \leq g(t) \leq 24\eta\gamma+8\gamma^3 , \tag{6.4-35}$$

and hence, by the monotone property of g(t), that:

$$g^{-1}(24\eta\gamma) \geq t \geq g^{-1}(24\eta\gamma+8\gamma^3). \qquad (6.4\text{-}36)$$

Using Eqn. (6.4-34) and the inequalities (6.4-36), curves of t vs γ are given in Figs. 15, 16, and 17 for three values of η. The curves have been extended beyond their ranges of definition in γ for purposes of comparison. These indicate that for values of $\eta \geq 10$ the percentage variation between the values of t determined from f and g is quite small in the intermediate range of $1 \leq \gamma \leq 3$. Thus, extension of the use of g(t) to values of up to $\gamma = 1.2$ (see Fig. 15) in the form

$$g(t) = 24\eta\gamma+8\gamma^3 \qquad 1 \leq \gamma \leq 1.2 \qquad (6.4\text{-}37)$$

and the use of f(x) for values of $\gamma > 1.2$ can be considered to give a good approximation for determining z_{min} in the intermediate range of γ.

The restriction that $\eta \geq 10$ is not a serious one in practical cases of interest, since it will be satisfied by most rocket mounted probes, e.g., considering a probe at an altitude of 70 km with $V' \geq 100$ m/sec, $\Phi_p' = 10$, $a' = 1.3$ cm, $T' = 300°K$, and $n_\infty' = 1.3 \times 10^4/cm^3$ of singly ionized O_2, we find that $\eta \geq 60$.

In order to obtain fast approximate solutions of the z_{min} equations, graphs of the functions f(x), g(t), and g(t) - 2h(γ,t) are given in Figs. 18 through 22. To obtain a graphical solution for z_{min} the value of $|\beta|$ is calculated from the given data of the probelm and compared with a^2. If $|\beta| \ll a^2$, the parameter on the left side of Eqn. (6.4-24) is computed and the appropriate value of x determined from the graph of f(x) in Fig. 18, or from the asymptotic relation for f(x). Then z_{min} is found from Eqn. (6.4-23).

If $|\beta| \geq a^2$, the parameter γ is evaluated from Eqn. (6.4-27). This determines a unique "branch" of the g(t)-2h(γ,t) curve of Fig. 22. Computing the parameter on the left side of Eqn. (6.4-28), this figure should be consulted to find the appropriate value of t, interpolating between the curves for different values of γ if necessary. In the event that the parameter $24\gamma \frac{\Phi p}{\beta}$ is so large that the g(t)-2h(γ,t) curves are not extended sufficiently far along the negative t axis to allow solution, $8\gamma^3$ should be added to it, and the value of t read directly from the g(t) curve (Figs. 19, 20, and 21) or obtained from the asymptotic relation (6.4-31).

When the values of a and β are such that γ falls between the limiting cases discussed above, the curves are used in accordance with the results discussed in the paragraph following Eqn. (6.4-36).

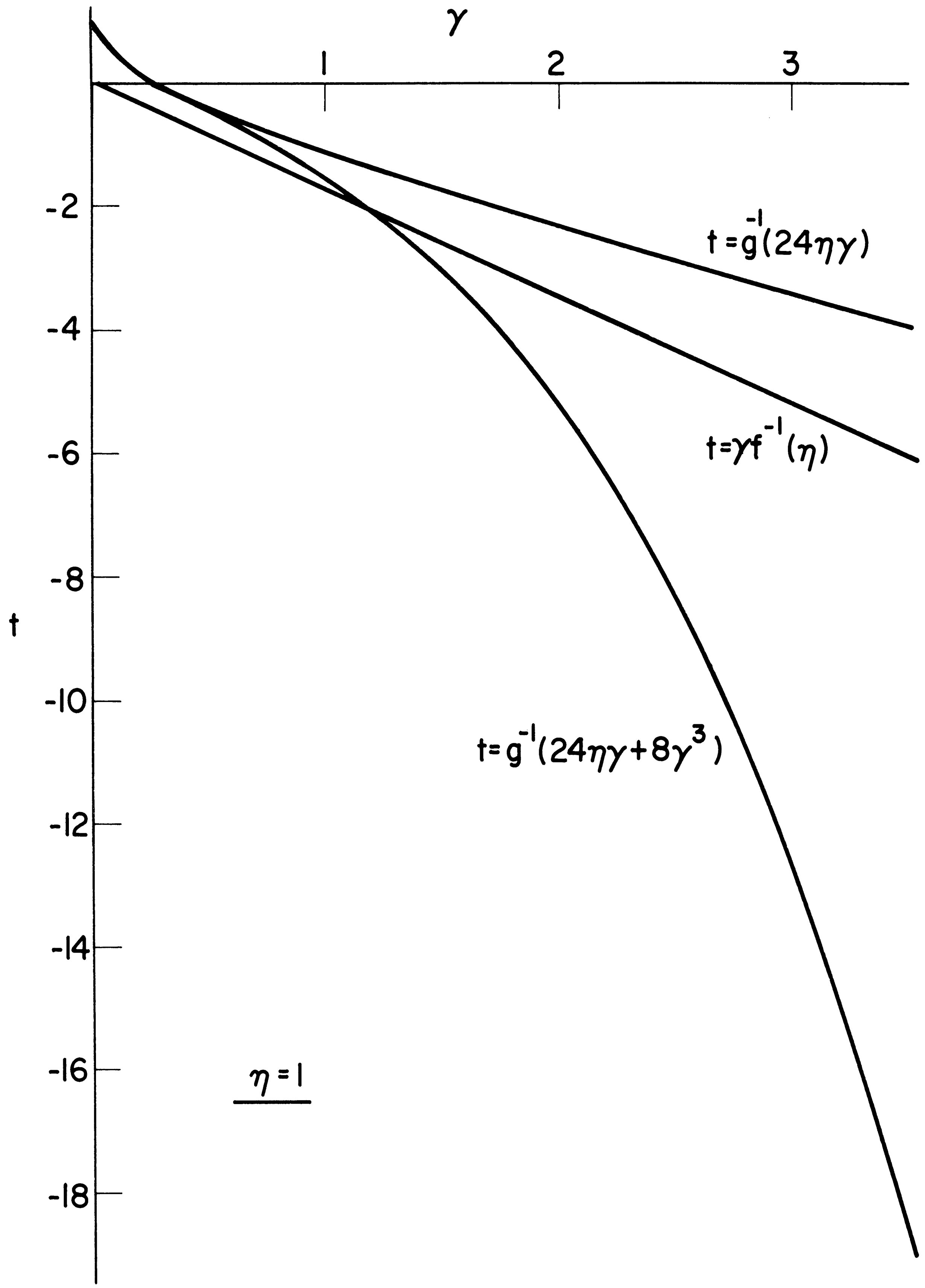

Fig. 15. Curve of t vs γ, (η=1).

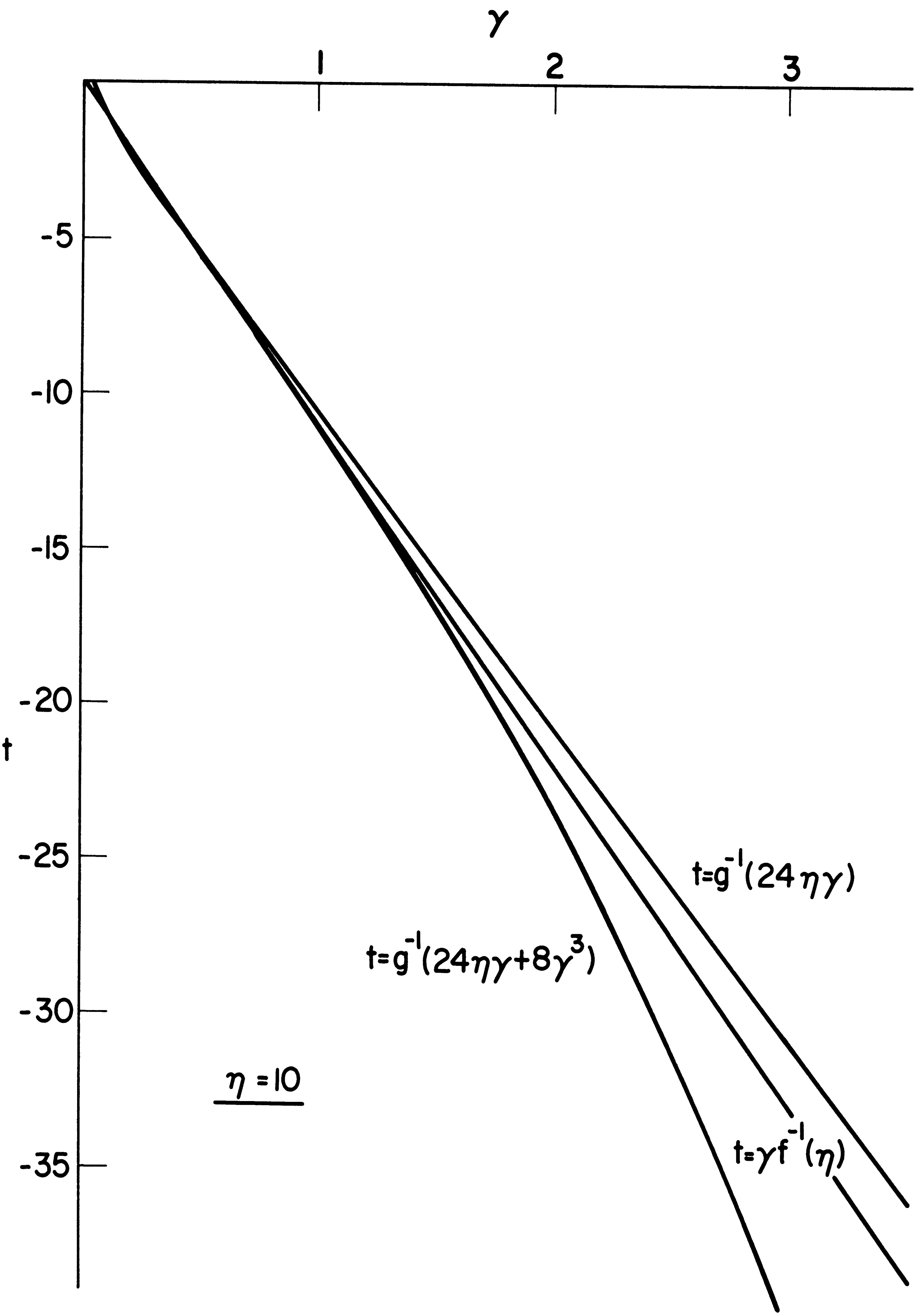

Fig. 16. Curve of t vs γ, (η=10).

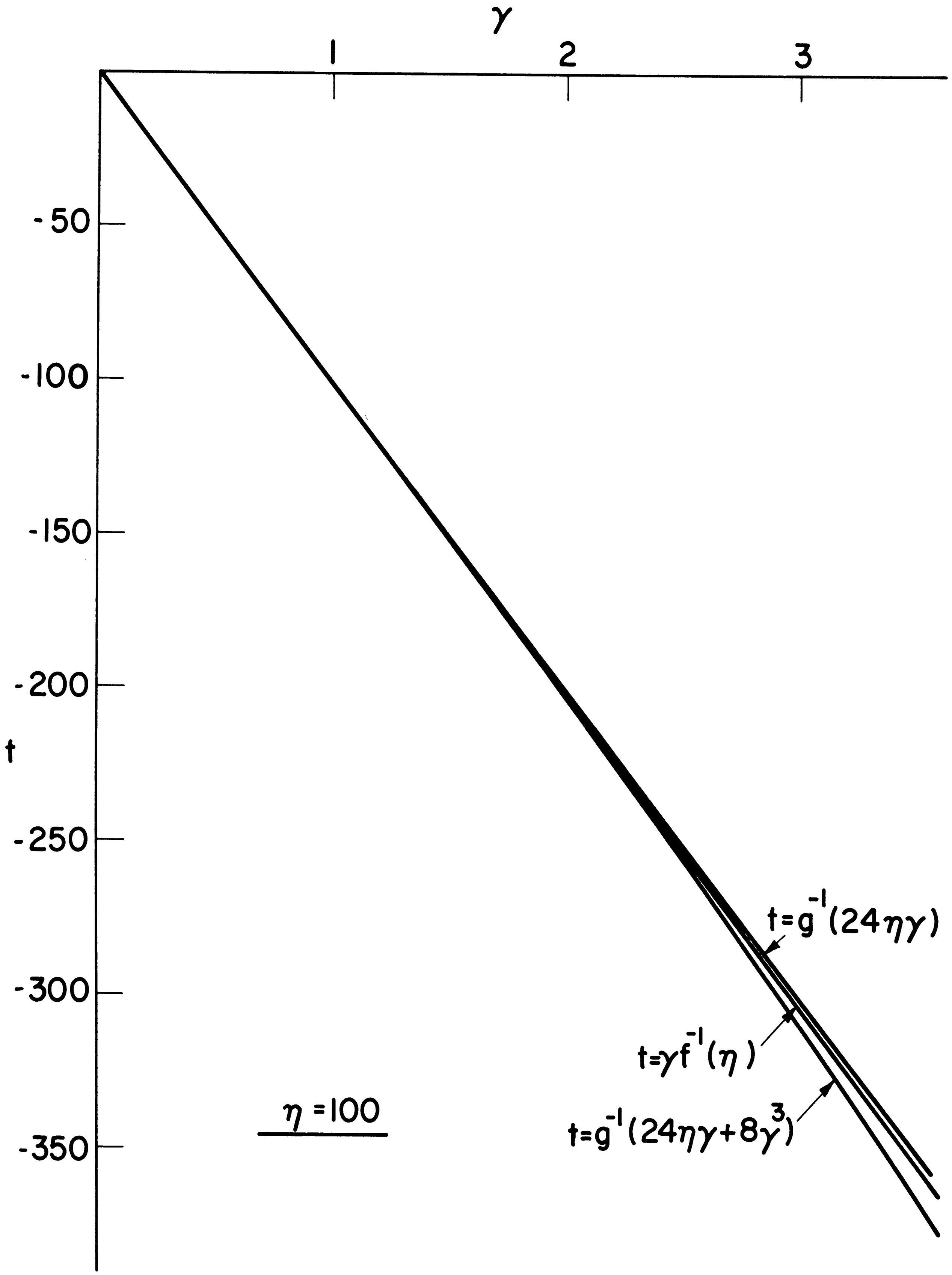

Fig. 17. Curve of t vs γ, (η=100).

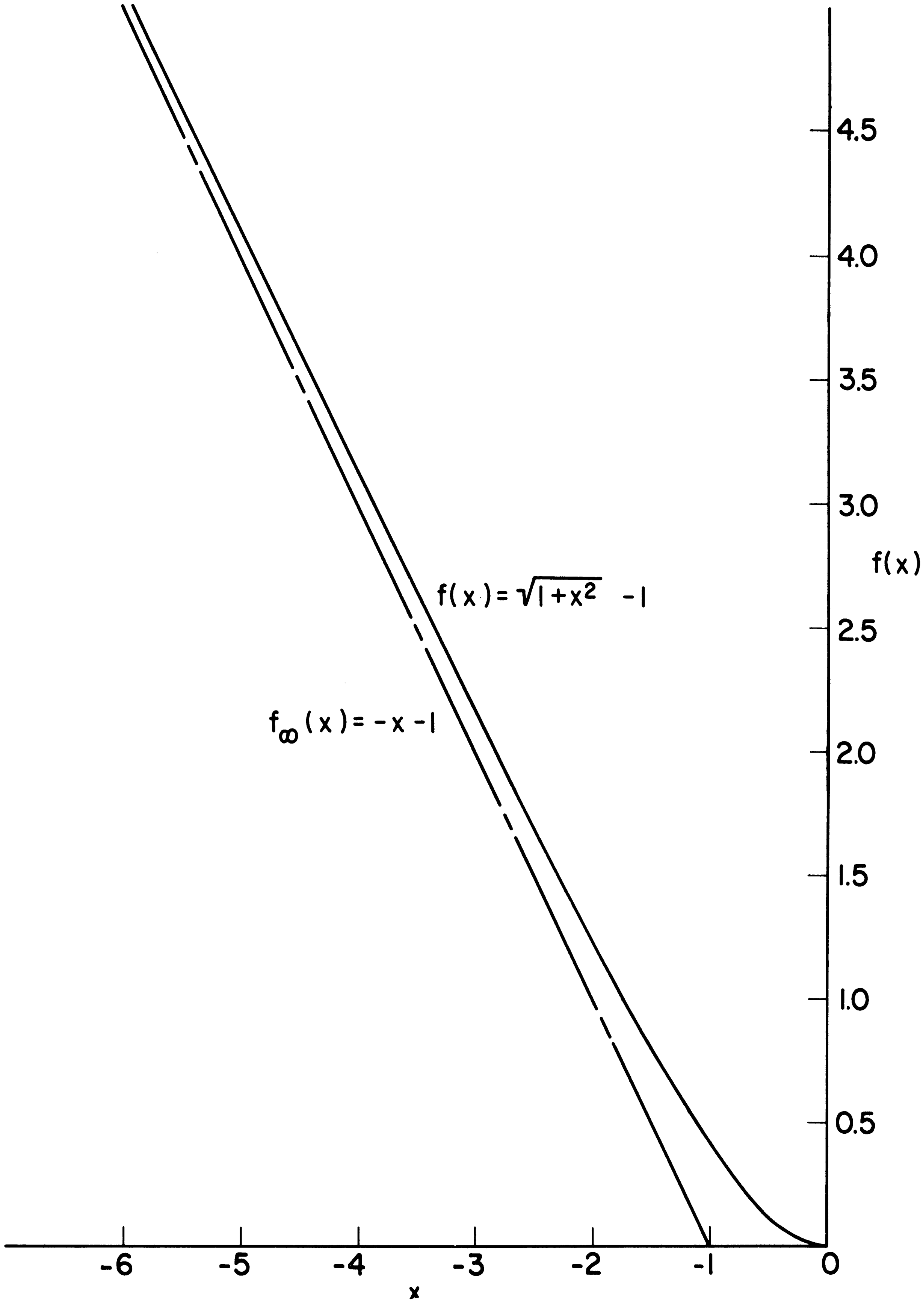

Fig. 18. Curve of f(x) vs x.

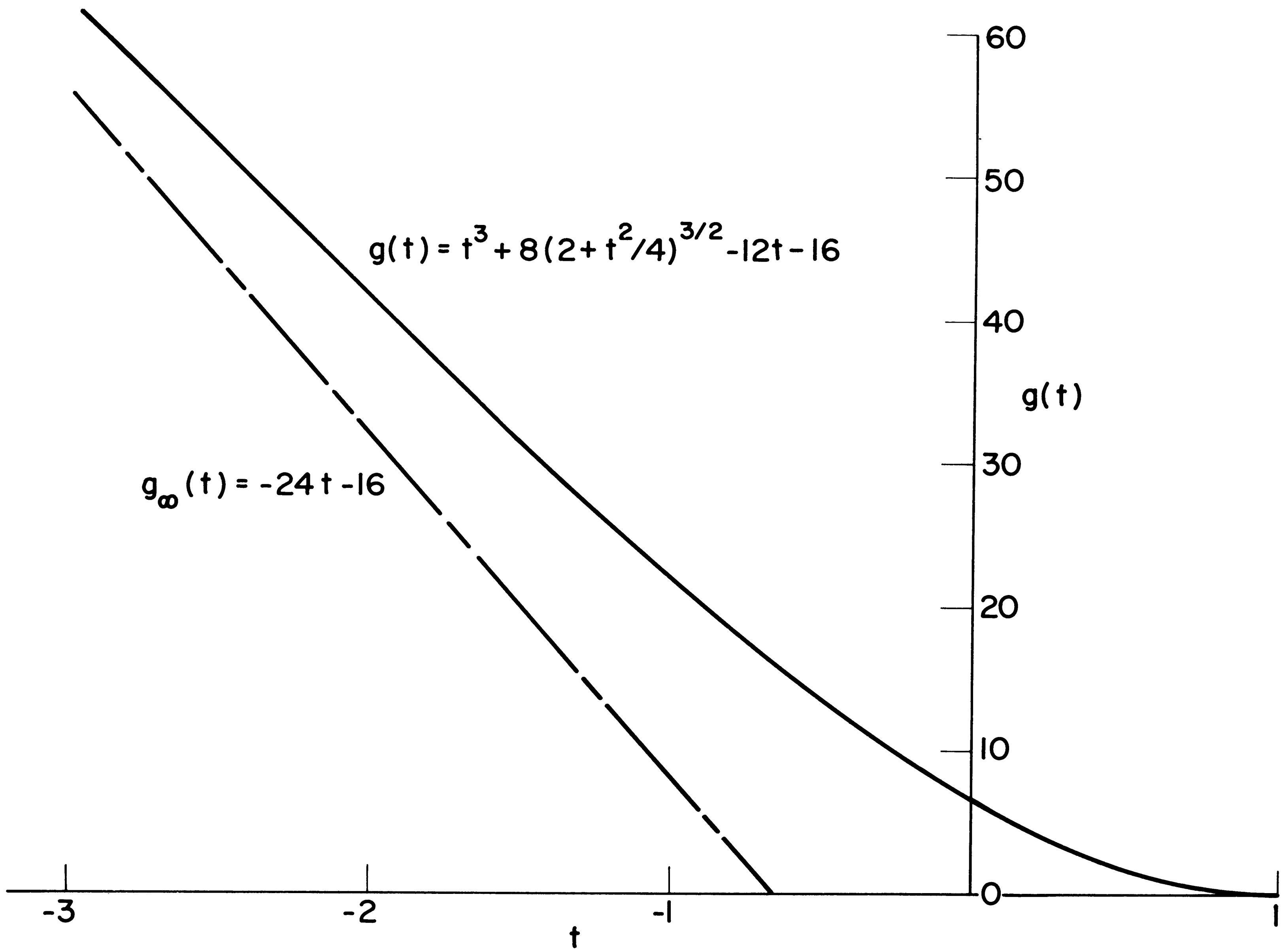

Fig. 19. Curve of g(t) vs -t, (γ=0).

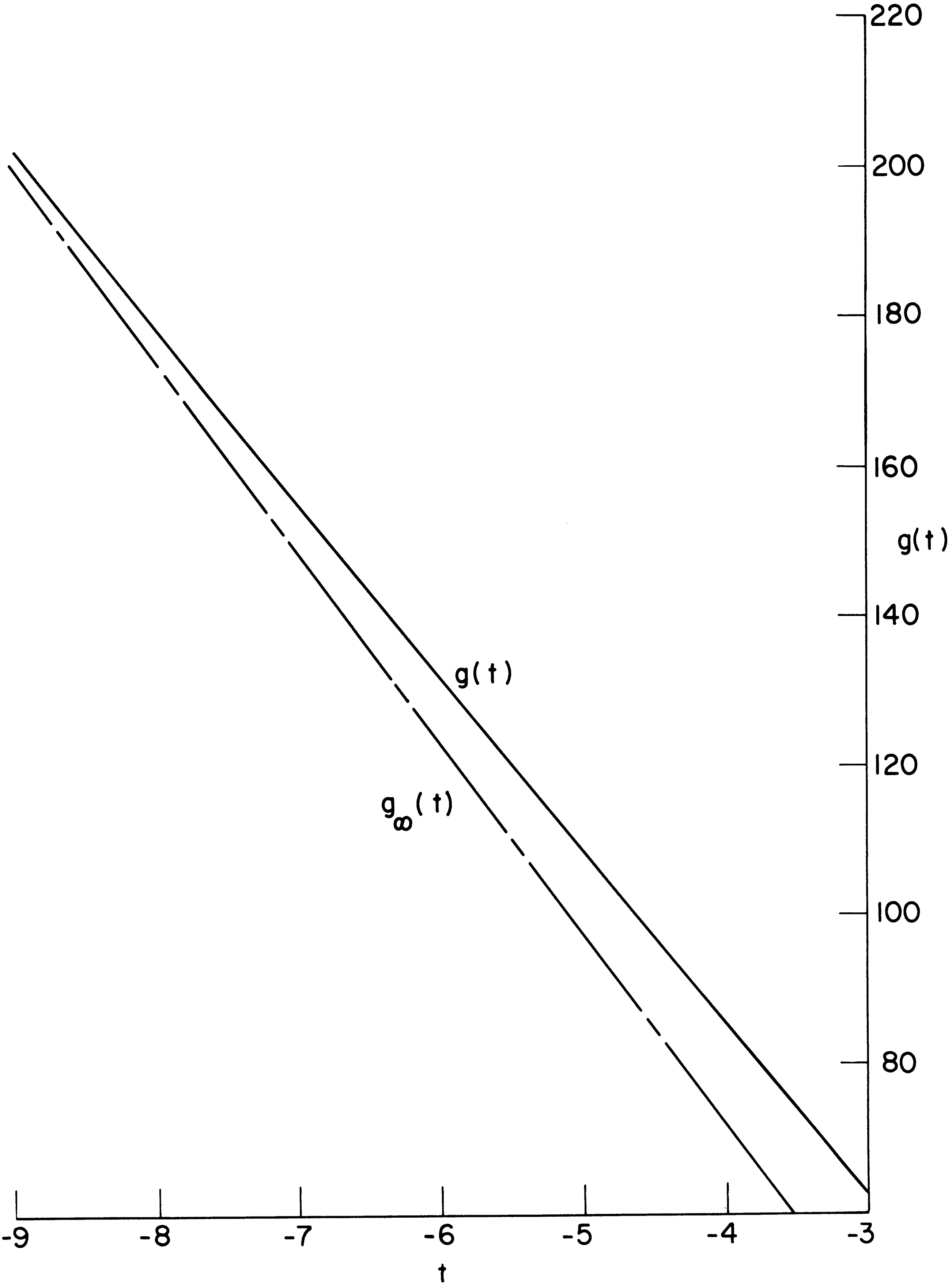

Fig. 20. Curve of g(t) vs -t, (γ=0).

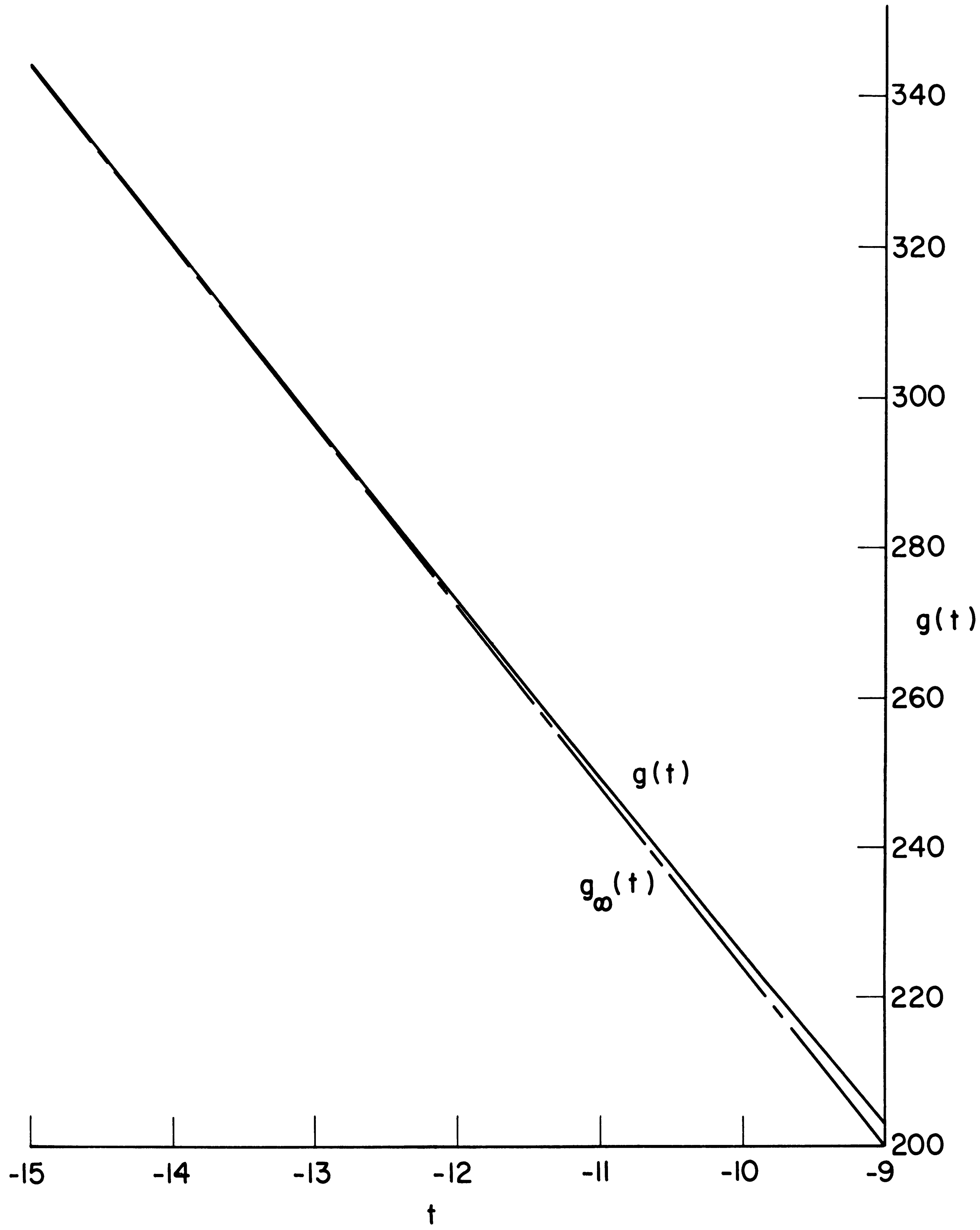

Fig. 21. Curve of g(t) vs -t, (γ=0).

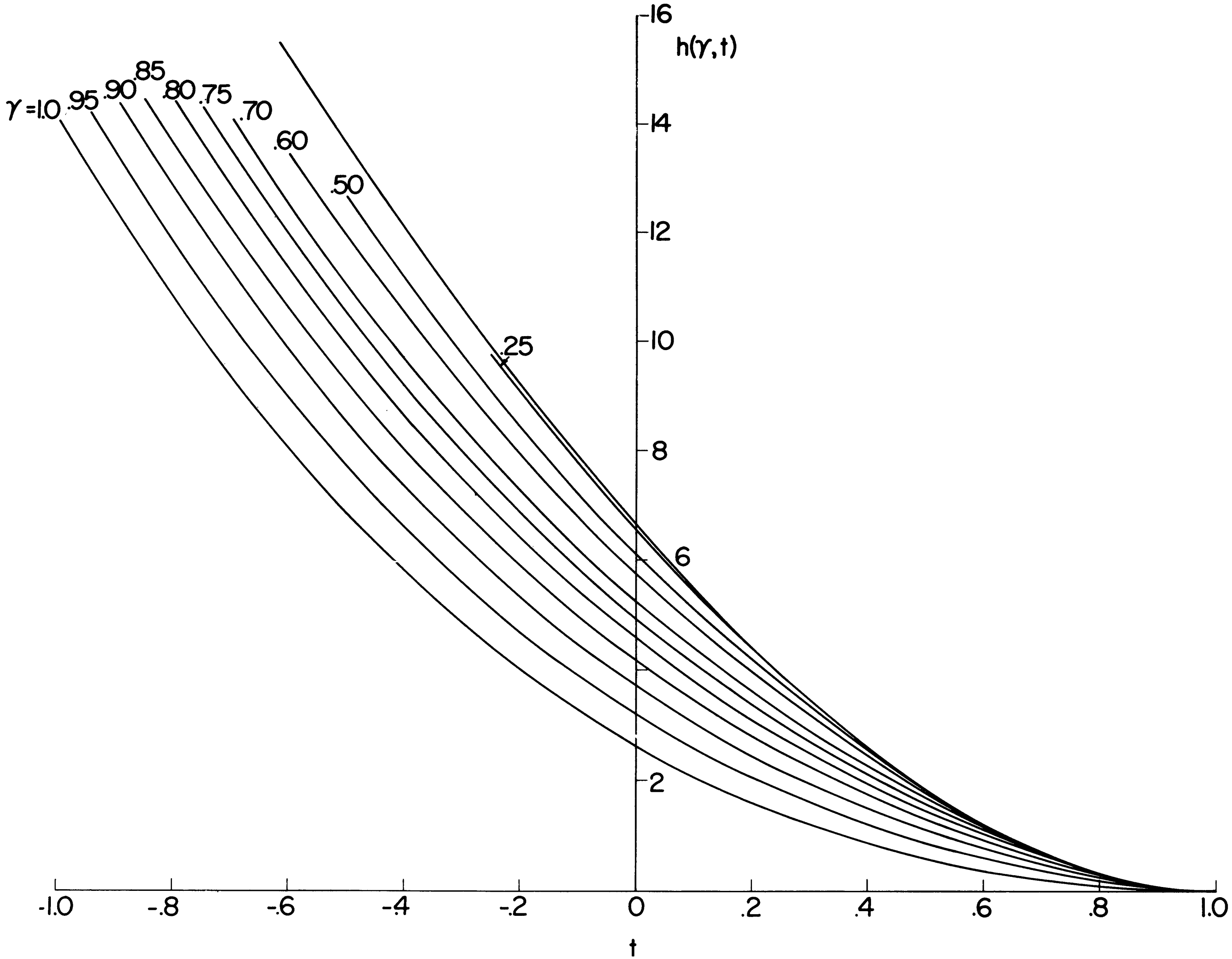

Fig. 22. Curve of $h(\gamma,t)$ vs $-t$, $(\gamma \neq 0)$.

7. COMPUTER PROGRAM AND NUMERICAL RESULTS

7.1 COMPUTER PROGRAM

The input parameters for the program are:

1. V = probe velocity (dimensionless)
2. PHI = Φ_p = probe potential (dimensionless)
3. DELTAT = δt (dimensionless)
4. A = a = probe radius
5. ZMIN = z_{min} (dimensionless)
6. H = spacing parameter for derivative calculations.
7. NUM = number of starting points to be used in generating flow lines.
8. NMAX = maximum number of points per flow line, set by computer storage restrictions.
9. NITER = number of iterations to be made after computing initial flow lines.
10. PSW = intermediate output switch.
11. (RI, ZI) = starting points for flow lines (NUM pairs will be read).

From the starting points (RI, ZI) the program first computes an initial approximation to the flow lines from the neutral flow velocity and probe potential. These flow lines are stored in two pairs of arrays: RSA, ZSA and RZA, ZZA. The first letter of each array name indicates SIGMA (positive charge) or ZETA (negative charge).

Next a new approximation to the flow lines is made by using the same starting points and taking into account the charge distribution from the previous approximation. These new approximations are stored in arrays RSB, ZSB, RZB, and ZZB. If the number of new approximations is less than NITER, the "B" arrays are shifted into the "A" arrays and the next iteration is calculated and stored in the "B" arrays.

During calculation of all approximations to the flow lines, a flow line is terminated at the last point before any of the following occur:

1. The calculated increment in Z is positive for the flow line along the vertical axis.

2. R is negative.

3. Z is less than ZMIN.

4. The flow line intersects the probe.

5. More than NMAX points are calculated.

After each approximation to the flow lines is completed, it is written on the output tape. Because each iteration uses many minutes of computer time, it is sometimes desirable to print out each new flow line point as it is generated. Assigning a non-zero value to PSW accomplishes this, and allows the program to be stopped at any time without loss of output.

For details of the method see the flow diagram and program listing in the Appendix. Subroutines which are not expanded in the flow diagram or the program listing are part of The University of Michigan Computing Center Executive System.

7.2 PRESENTATION OF SAMPLE RUN

At the time of writing this report, results of programming the procedure previously discussed are not satisfactory. The output of a run using the program discussed in Section 4.1 is presented in Figs. 23 through 26; the dots indicate the computed points. Note also that the r and z axes are scaled differently.

Here the values of the parameters used are $V=15$, $\Phi_p=+10$, $a=3$, $\delta t=\frac{1}{6}$, $H=\frac{1}{2}$. It is found in this case that $|\beta| < a^2$, so the sheath cutoff distance is determined using Fig. 14; this gives $z_{min} = -17.5$. The starting coordinates for the flow lines are arbitrarily chosen to be $z=+30$, $r=0,2,4,\ldots,12$.

Figures 23 and 24 show the flow lines as computed using only the free space potential due to the probe. Figures 25 and 26 show the first iteration, using the fields of the previous figures in addition to the potential of the probe. Total running time on an IBM 7090 computer for the two iterations was 15 min. The results shown in Figs. 25 and 26 have several salient features:

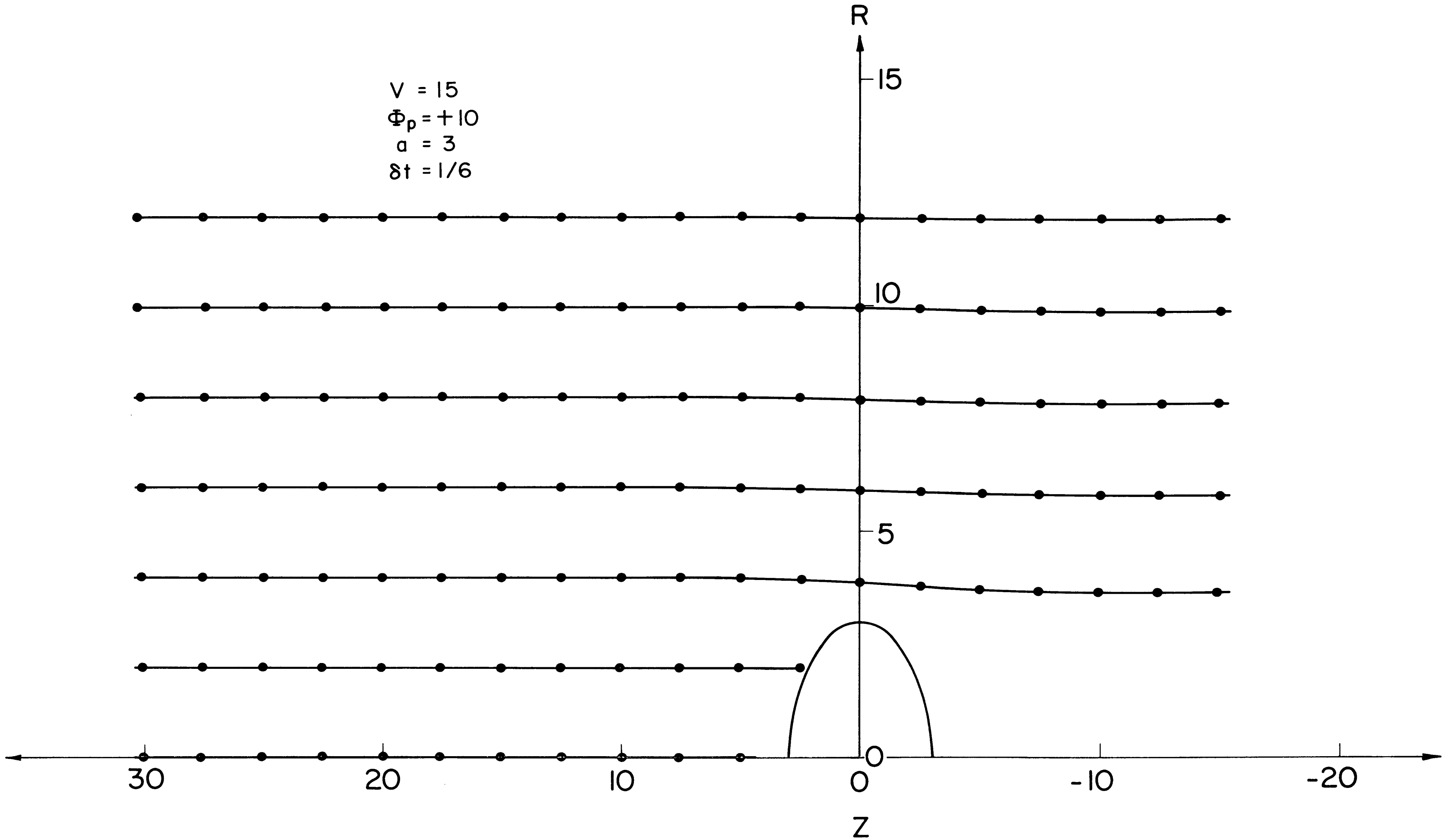

Fig. 23. σ flow lines (initial approximation).

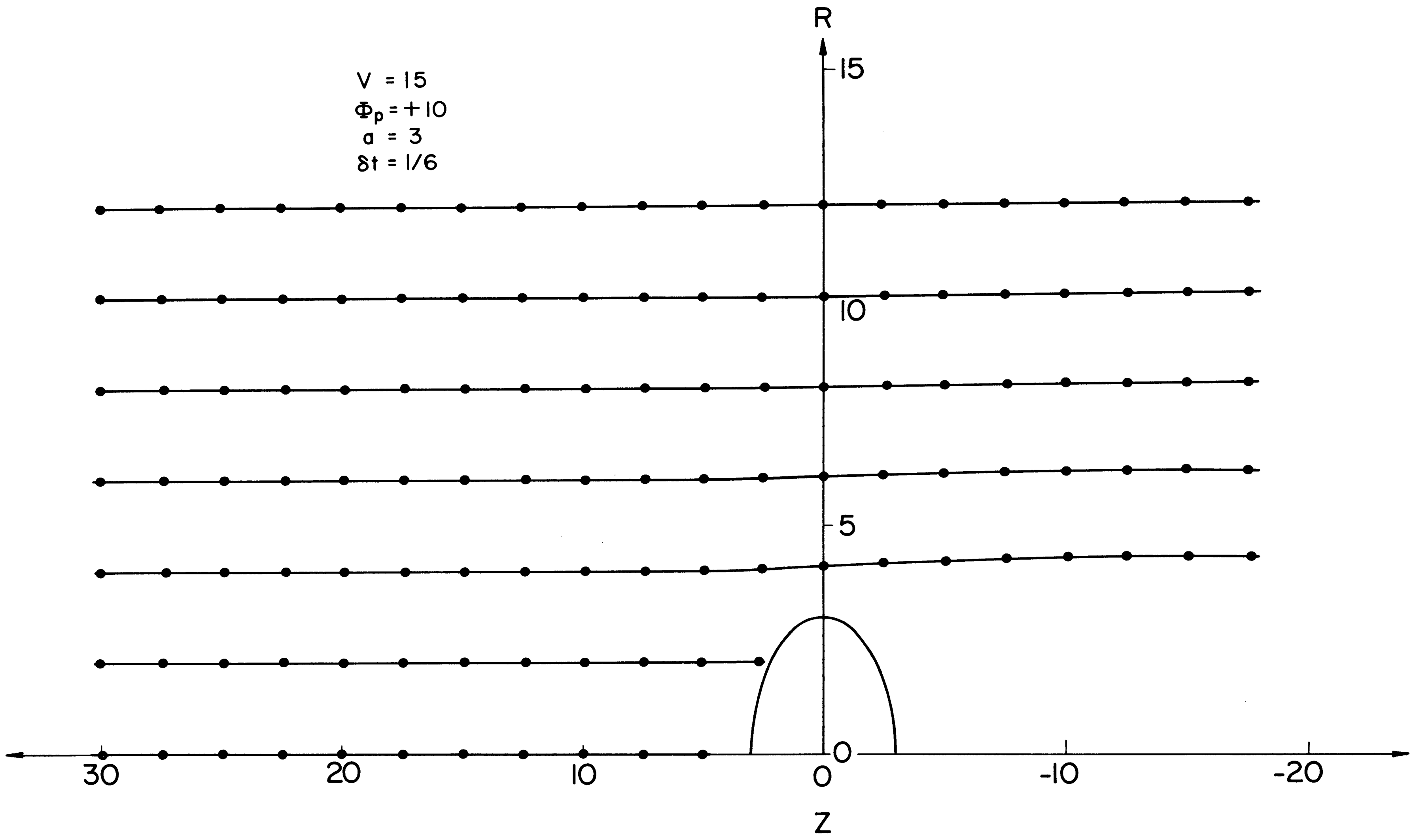

Fig. 24. ζ flow lines (initial approximation).

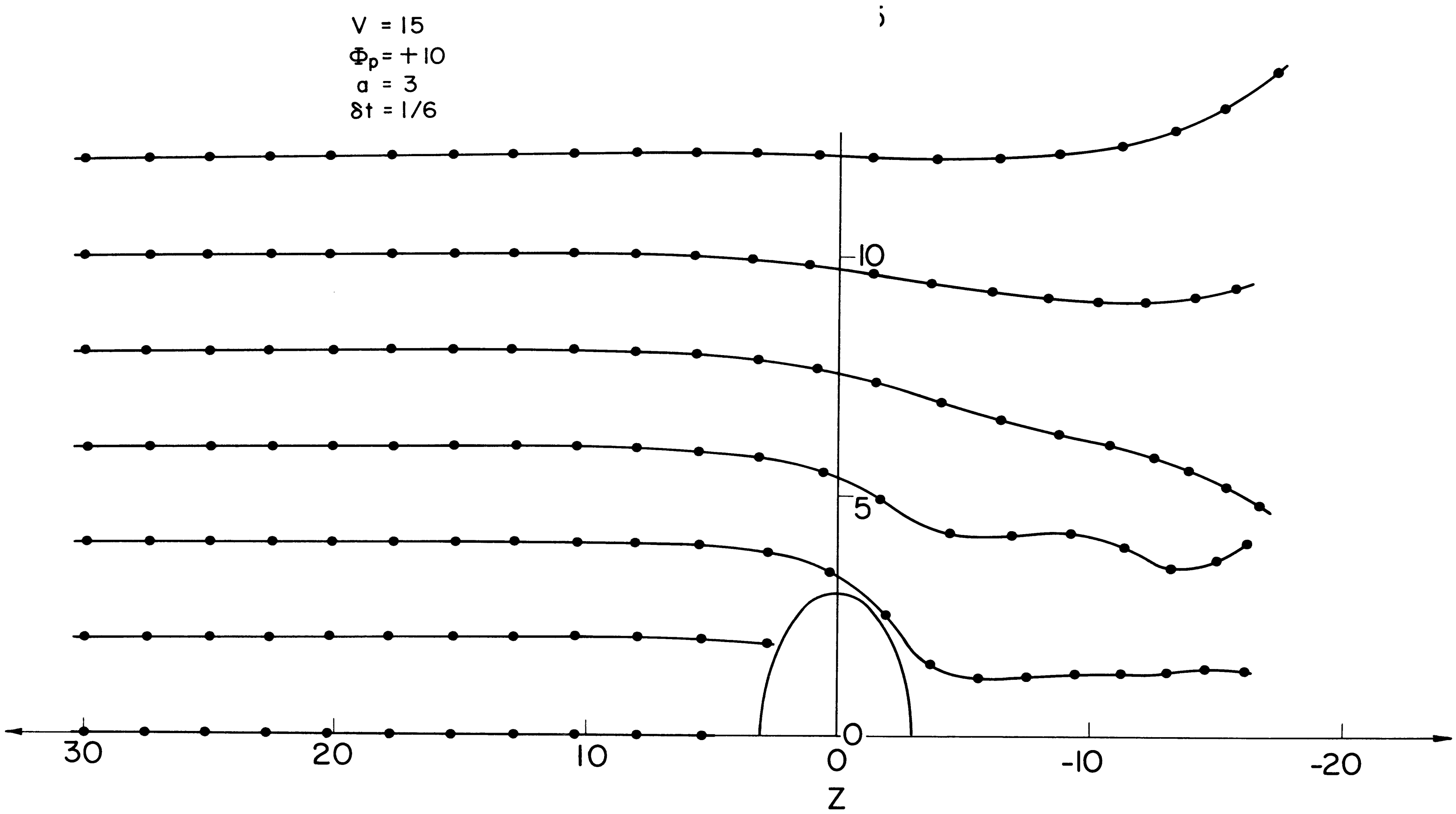

Fig. 25. σ flow lines (first iteration).

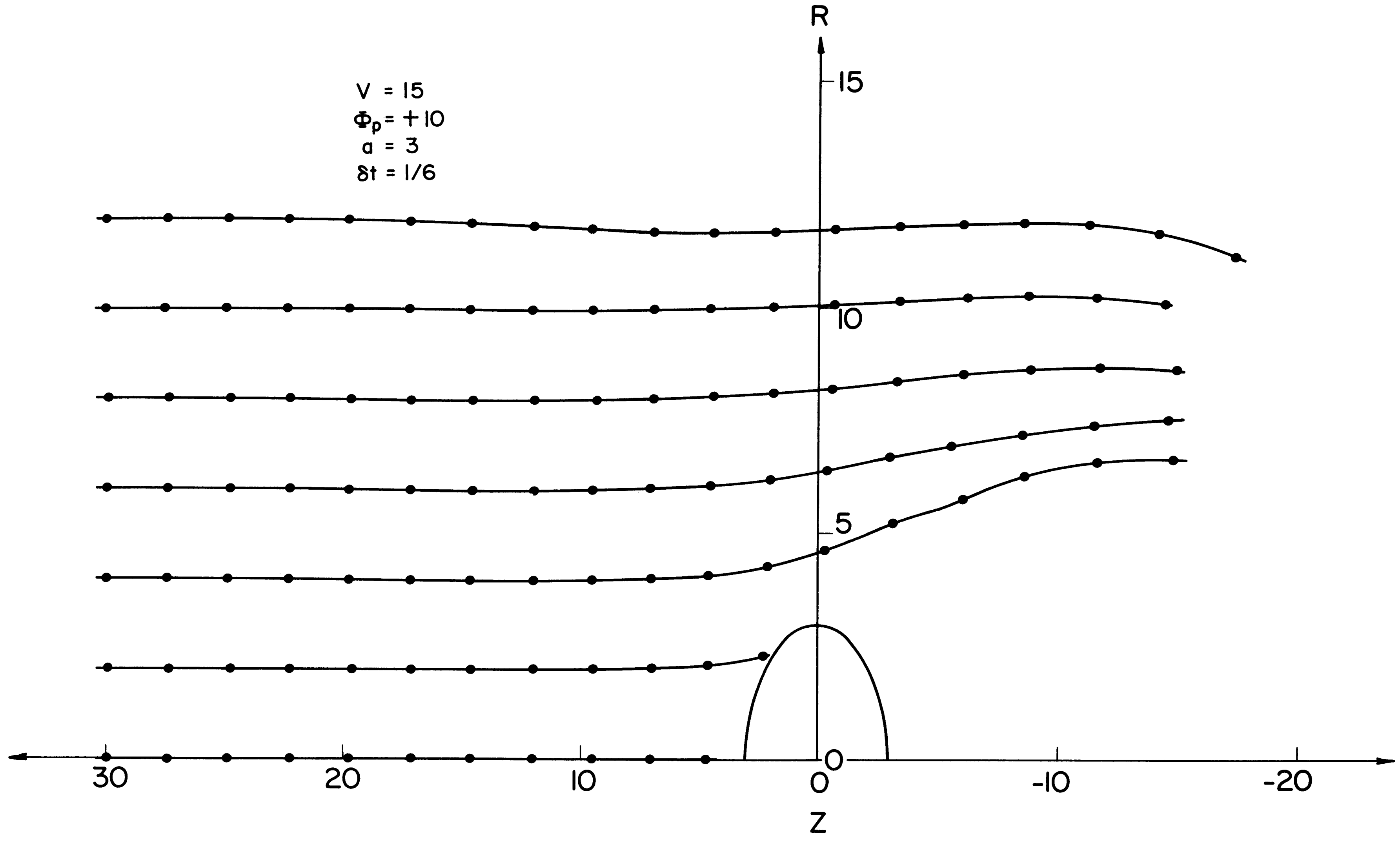

Fig. 26. ζ flow lines (first iteration).

1. The sigma flow line starting with r=6 has several irregularities near the lower end;

2. the magnitude of the overall interaction is markedly increased, as exemplified by the highly distorted flow lines;

3. near the probe the positive (negative) species are attracted (repelled) in the second iteration; and

4. the strength of the interaction seems to increase with distance from the probe, as indicated by the increasing distortion of the flow lines which begin with successively larger values of r.

At present, these effects, all of which appear to be non-physical have not been satisfactorily explained. Until these are resolved, further iterations do not appear warranted.

8. EXTENSIONS AND CONCLUSIONS

8.1 EXTENSION TO PHASE II

The extension of the phase I program to include nonuniform flow and diffusion can be achieved by considering these effects independently.

In principle the complications necessary in the program because of the change in the neutral flow regime at and behind the shock are of a relatively simple nature. In passing through the shock both the flow velocity and the density change discontinuously. Thus, the first necessary alteration to the phase I program is the determination of the intercepts of the flow lines and the shock. This involves checking the points along a flow line to locate the first point falling behind the shock, and then by say, linear interpolation, finding the point of intersection P of the flow line and the shock front (Fig. 27). The point so located should then be used as an "initial" point for further determination of the flow line behind the shock.

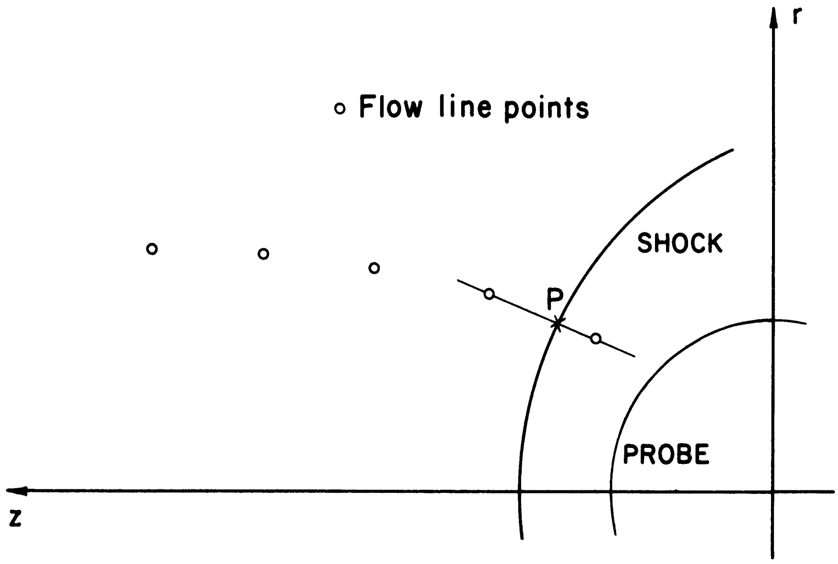

Fig. 27. Flow lines crossing shock.

The addition of an interpolation routine is also necessary in order to determine the neutral flow velocity at flow line points behind the shock. This will be required because such points cannot generally be expected to coincide with any of the points at which the neutral velocity is available, since the velocity field is entered in the computer as a table. Such an interpolation routine might be constructed as follows.

Consider a flow line point P at which the neutral stream velocity is desired (see Fig. 28). Let the three points nearest to P at which the velocity

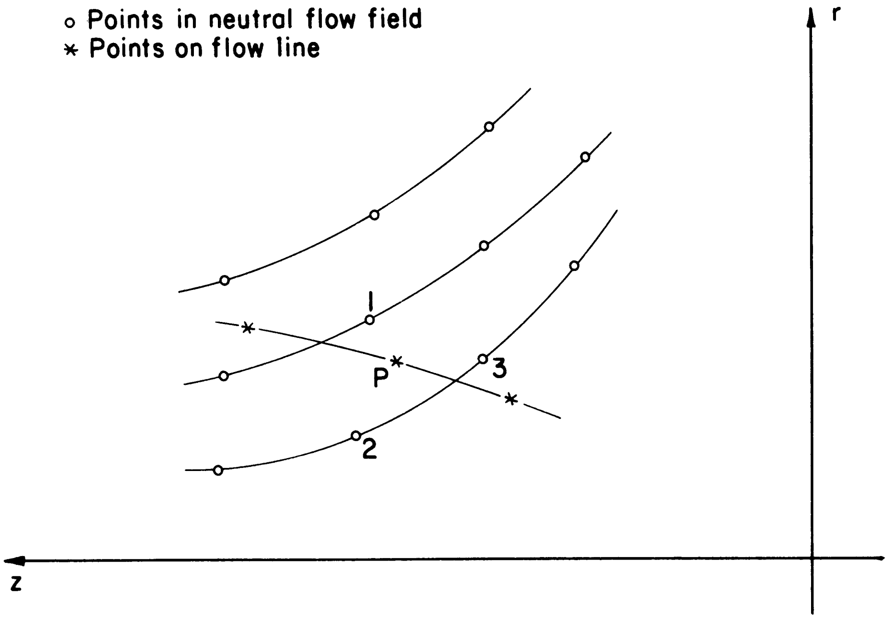

Fig. 28. The three points of tabulated velocity field which are nearest to point P.

field is tabulated be indicated by 1, 2, and 3. Making a Taylor series expansion in the components of the velocity about the point P we have to first order:

$$V_{ri} = V_P + \frac{\partial V}{\partial r}\Big|_P \delta r_i + \frac{\partial V}{\partial z}\Big|_P \delta z_i \qquad i = 1,2,3 \qquad (8.1\text{-}1)$$

where V_{ri} denotes the r component of the velocity vector at the point i and δr_i, δz_i are the appropriate displacements of the points i from point P. This linear system can now be solved for the radial velocity components at the point P. A similar procedure can be used to find the required z-components of the vector $\overline{V}$.

It should be noted that the real difficulty in the above is the machine determination of the nearest neighbor points 1,2, and 3. This could perhaps be done by searching the velocity table for points within a specified distance of P, which is, say, twice the maximum distance between points in the velocity table. Decrementing this distance by small amounts, some of the points so determined could be excluded until the three necessary points were found.

The contribution to the current density due to density gradients can be found by an interpolation technique similar to the above. Rearranging Eqns. (5.1-1) the current densities may be written:

$$\overline{J} = (\overline{V} - \nabla\Phi - \frac{\nabla\sigma}{\sigma})\,\sigma$$

$$-\overline{L} = (\overline{V} + \nabla\Phi - \frac{\nabla\zeta}{\zeta})\,\zeta. \qquad (8.1\text{-}2)$$

We see then, that the contribution to the velocity of the charges due to diffusion is given by the ratio of the density gradient to the density itself (assuming the density is finite). Setting up a linear system analogous to Eqns. (8.1-1) for the charge densities, these contributions can be easily found.

Since we assume the ionized flow to be frozen, the ion densities will change directly with the neutral density increase across the shock. For computer calculations we must therefore consider the neutral flow velocity and the densities to be double valued at the shock (point P of Fig. 23), using the shock as a bounding surface between the two regions of the flow. In calculating charge density gradients ahead of the shock, the "nearest" neighbor points considered must be restricted to the region ahead of the shock or on the shock itself as approached from the front. Similarly, behind the shock calculations must use only values in the region behind the shock or values along the shock which have been corrected for the changes caused by passing through the shock.

Further corrections might also be included for such effects as the variation in diffusion (and thus mobility) constants due to the density variation behind the shock.

8.2 FURTHER EXTENSIONS AND CONCLUSIONS

The major portion of this report has been concerned with a spherical probe, and with the free space potential of such a body as the potential approximation initiating the iterative procedure. In principle the extension of the program to utilize different configurations and potentials is straightforward. Changes would be necessary in sections of the program in which the initial flow lines are computed (by changing the initial potential function).

Even if the spherical probe is retained, an extension of the process used for determining the flow line cutoff point z_{min} would be desirable. In general the charge distribution on and about the probe will be altered with each iteration. Consequently, new calculations of the charge imbalance in the plasma and of the net charge on the sphere (including for consistency the charge induced by the previous spatial distribution) should be used to obtain a new approximation to z_{min}. This would require an additional section in the program for performing the necessary numerical integrations and for obtaining the desired cutoff value from them. The numerical integrations might easily utilize the density computations mentioned in connection with the phase II extension of the program.

Some serious points concerning the validity of the entire procedure must be mentioned. The whole method evolves from the observation that if the potential Φ is known, then the system (4.2-3) can be solved for σ and ζ, or alternatively if the charge densities are known, the Poisson equation can be solved for the potential. This suggests solving the system by successive approximations, as has been done in this report. This process has the advantage of resolving the problem into the solution of a sequence of linear equations, rather than of a coupled system. However, this approach immediately raises the following questions: do there exist functions which can be used as initial potentials for which the process will ultimately converge to the solution of the system (4.2-3) with its boundary conditions, and if so, what are they? These questions remain unanswered; results of running the computer program evolved in this report (see Section 7.1) are not sufficient to indicate possible resolution of these important points at this time.

BIBLIOGRAPHY

1. Talbot, L., "Theory of the Stagnation-Point Langmuir Probe," Phys. Fluids, 3, 289, 1960.

2. Chung, P. M., Electrical Characteristics of Couette and Stagnation Boundary Layer Flows of Weakly Ionized Gases, Aerospace Corporation, Report No. TDR - 169 (3230-12)TN-2, October 1962.

3. Pollin, I., The Stagnation-Point Langmuir Probe in a Shock Tube—Theory and Measurements, Harry Diamond Laboratories, TR-1103, June 1963 (AD 416 346).

4. Cohen, I. M., "Asymptotic Theory of Spherical Electrostatic Probes in a Slightly Ionized, Collision-Dominated Gas," Phys. Fluids 6, 1492, 1963.

5. Su, C. H., and Lam, S. H., "Continuum Theory of Spherical Electrostatic Probes," Phys. Fluids 6, 1479, 1963.

6. Lam, S. H., "A General Theory for the Flow of Weakly Ionized Gases," AIAA Jour., 2, 256, 1964.

7. Lieberman, E., Description of IBM 709/90/94 Computer Programs and Analysis for Flow Fields About Bodies of Revolution in Hypersonic Flight, General Applied Science Laboratories, Technical Report No. 340, May 1963.

8. Garabedian, P. R., Numerical Construction of Detached Shock Waves, Stanford University, Applied Mathematics and Statistics Laboratory, Technical Report No. 55, September 1956.

9. Nelson, P., Jr., An Iterative Method for Approximating the Flow Field About a Supersonic Blunt Body, Brown Engineering Co., TN R-72, October 1963 (AD 435 078).

10. Hastings, C., Jr., "Approximations for Digital Computers," Princeton University Press, 1955.

APPENDIX

FLOW DIAGRAM AND PROGRAM LISTING

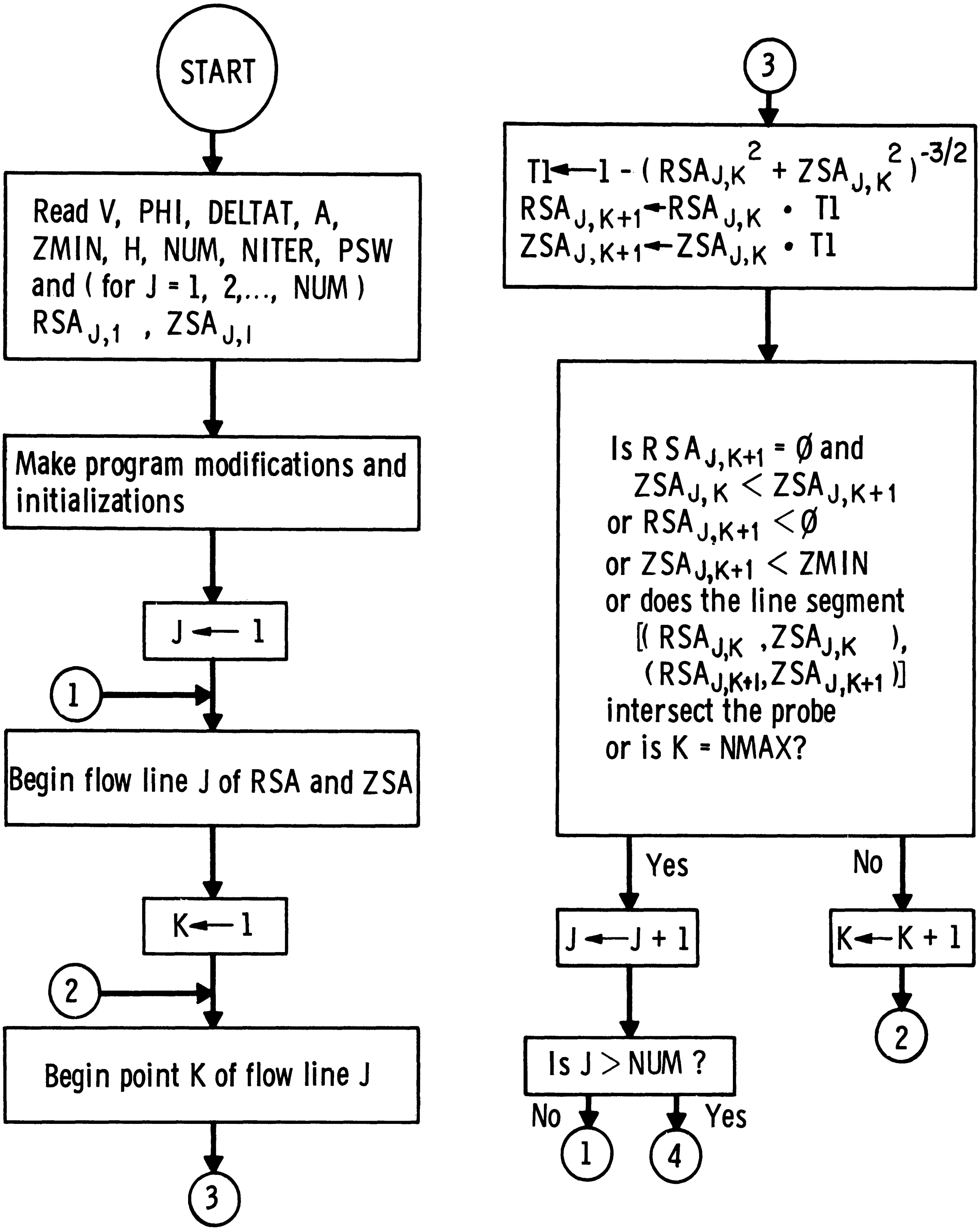
START
Read V, PHI, DELTAT, A, ZMIN, H, NUM, NITER, PSW and (for J = 1, 2,..., NUM) $RSA_{J,1}$, $ZSA_{J,1}$
Make program modifications and initializations
J ← 1
1
Begin flow line J of RSA and ZSA
K ← 1
2
Begin point K of flow line J
3
3
$T1 \leftarrow 1 - (RSA_{J,K}^2 + ZSA_{J,K}^2)^{-3/2}$
$RSA_{J,K+1} \leftarrow RSA_{J,K} \cdot T1$
$ZSA_{J,K+1} \leftarrow ZSA_{J,K} \cdot T1$
Is $RSA_{J,K+1} = \emptyset$ and $ZSA_{J,K} < ZSA_{J,K+1}$ or $RSA_{J,K+1} < \emptyset$ or $ZSA_{J,K+1} < ZMIN$ or does the line segment $[(RSA_{J,K}, ZSA_{J,K}), (RSA_{J,K+1}, ZSA_{J,K+1})]$ intersect the probe or is K = NMAX?
Yes
No
J ← J + 1
K ← K + 1
2
Is J > NUM ?
No
Yes
1
4

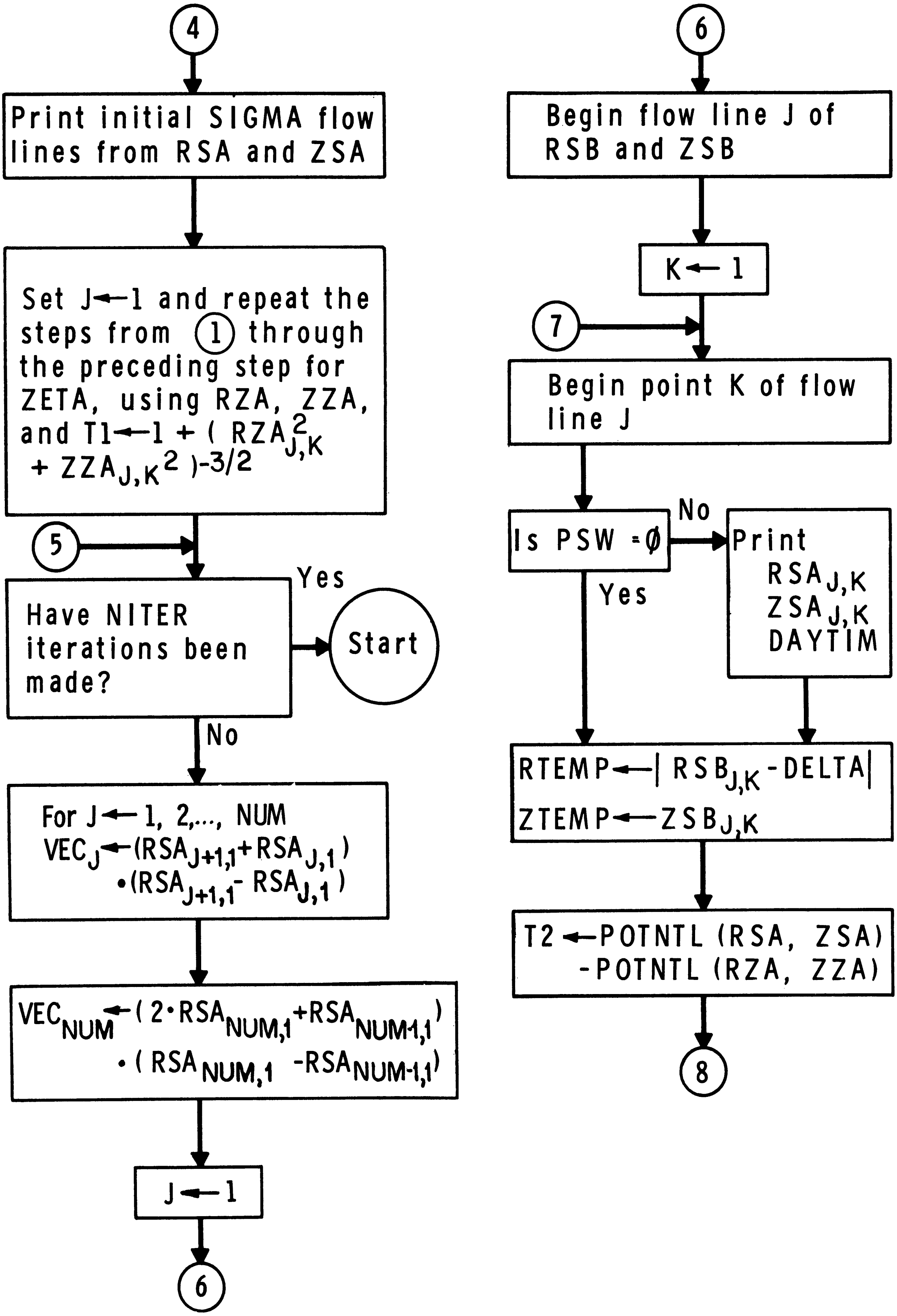
4
Print initial SIGMA flow lines from RSA and ZSA
Set J←1 and repeat the steps from (1) through the preceding step for ZETA, using RZA, ZZA, and T1←1 + (RZA$^2_{J,K}$ + ZZA$_{J,K}$^{2})-3/2
5
Have NITER iterations been made?
Yes
Start
No
For J←1, 2,..., NUM
VEC$_J$←(RSA$_{J+1,1}$+RSA$_{J,1}$)
•(RSA$_{J+1,1}$- RSA$_{J,1}$)
VEC$_{NUM}$←(2•RSA$_{NUM,1}$+RSA$_{NUM-1,1}$)
• (RSA$_{NUM,1}$ -RSA$_{NUM-1,1}$)
J←1
6
6
Begin flow line J of RSB and ZSB
K←1
7
Begin point K of flow line J
Is PSW =∅
No
Yes
Print
RSA$_{J,K}$
ZSA$_{J,K}$
DAYTIM
RTEMP←| RSB$_{J,K}$ -DELTA|
ZTEMP←ZSB$_{J,K}$
T2←POTNTL (RSA, ZSA)
-POTNTL (RZA, ZZA)
8

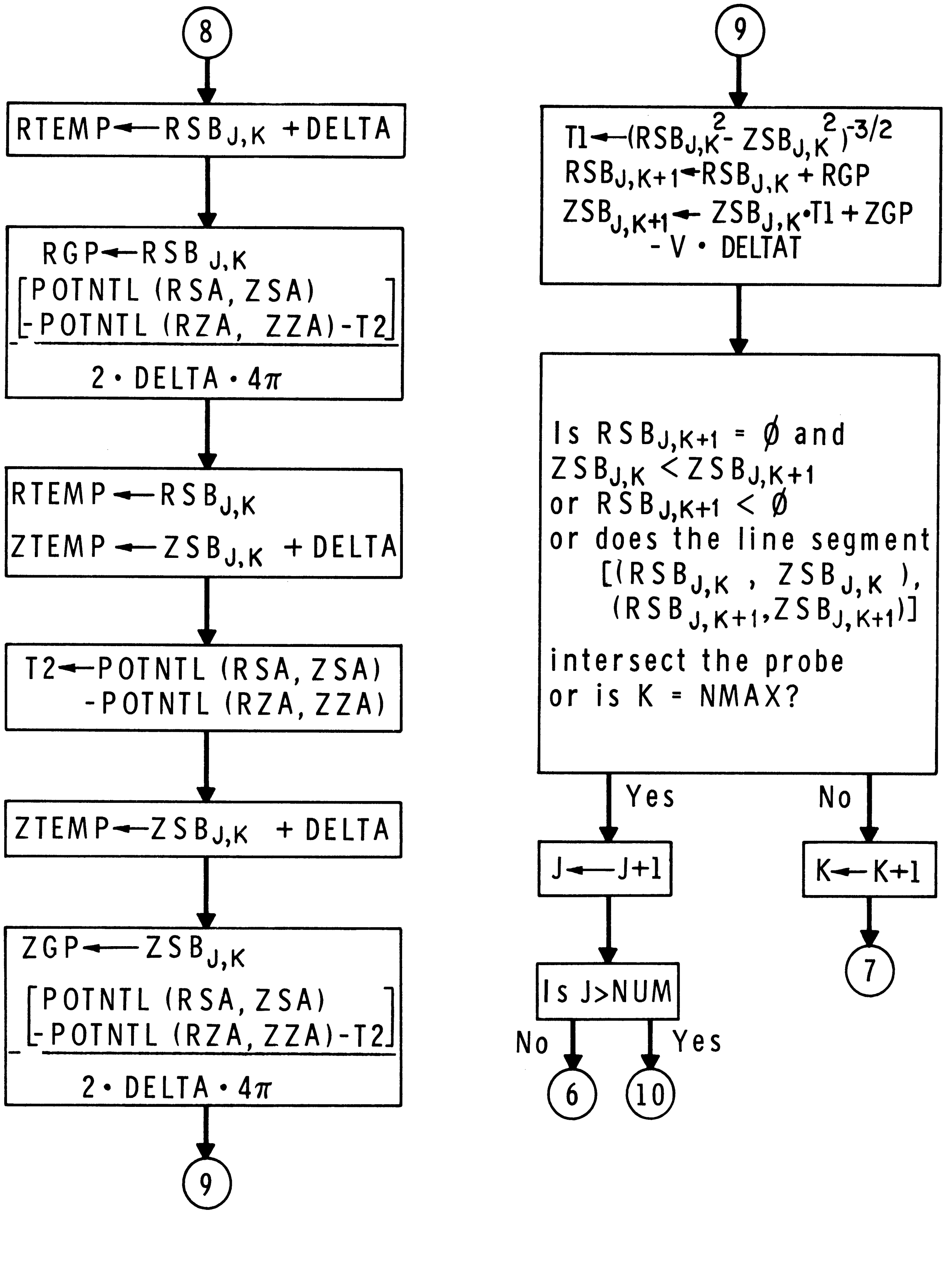
8
RTEMP ← RSB J,K + DELTA
RGP ← RSB J,K
[POTNTL (RSA, ZSA)
- POTNTL (RZA, ZZA) - T2]
2 · DELTA · 4π
RTEMP ← RSB J,K
ZTEMP ← ZSB J,K + DELTA
T2 ← POTNTL (RSA, ZSA)
- POTNTL (RZA, ZZA)
ZTEMP ← ZSB J,K + DELTA
ZGP ← ZSB J,K
[POTNTL (RSA, ZSA)
- POTNTL (RZA, ZZA) - T2]
2 · DELTA · 4π
9
9
T1 ← (RSB J,K 2 - ZSB J,K 2) -3/2
RSB J,K+1 ← RSB J,K + RGP
ZSB J,K+1 ← ZSB J,K · T1 + ZGP
- V · DELTAT
Is RSB J,K+1 = Ø and
ZSB J,K < ZSB J,K+1
or RSB J,K+1 < Ø
or does the line segment
[(RSB J,K , ZSB J,K),
(RSB J,K+1 , ZSB J,K+1)]
intersect the probe
or is K = NMAX?
Yes
No
J ← J+1
K ← K+1
7
Is J>NUM
No
Yes
6
10

(10)

Set $J \leftarrow 1$ and repeat the steps from (6) through the preceding step for RZB and ZZB using

$$RGP \leftarrow RZB_{J,K} + \frac{\left[\begin{array}{l}\text{POTNTL}(RSA, ZSA)\\ -\text{POTNTL}(RZA, ZZA) - T2\end{array}\right]}{2 \bullet DELTA \bullet 4\pi}$$

$$ZGP \leftarrow ZZB_{J,K} + \frac{\left[\begin{array}{l}\text{POTNTL}(RSA, ZSA)\\ -\text{POTNTL}(RZA, ZZA) - T2\end{array}\right]}{2 \bullet DELTA \bullet 4\pi}$$

$$RZB_{J,K+1} \leftarrow -RZB_{J,K} \bullet T1 + RGP$$

$$ZZB_{J,K+1} \leftarrow -ZZB_{J,K} \bullet T1 + ZGP - V \bullet DELTAT$$

(11)

(11)

For $J \leftarrow 1, 2, \ldots, NUM$ and $K \leftarrow 1, 2, \ldots, NMAX$

$RSA_{J,K} \leftarrow RSB_{J,K}$

$ZSA_{J,K} \leftarrow ZSB_{J,K}$

$RZA_{J,K} \leftarrow RZB_{J,K}$

$ZZA_{J,K} \leftarrow ZZB_{J,K}$

Print the new flow line iteration from the "A" matrices

(5)

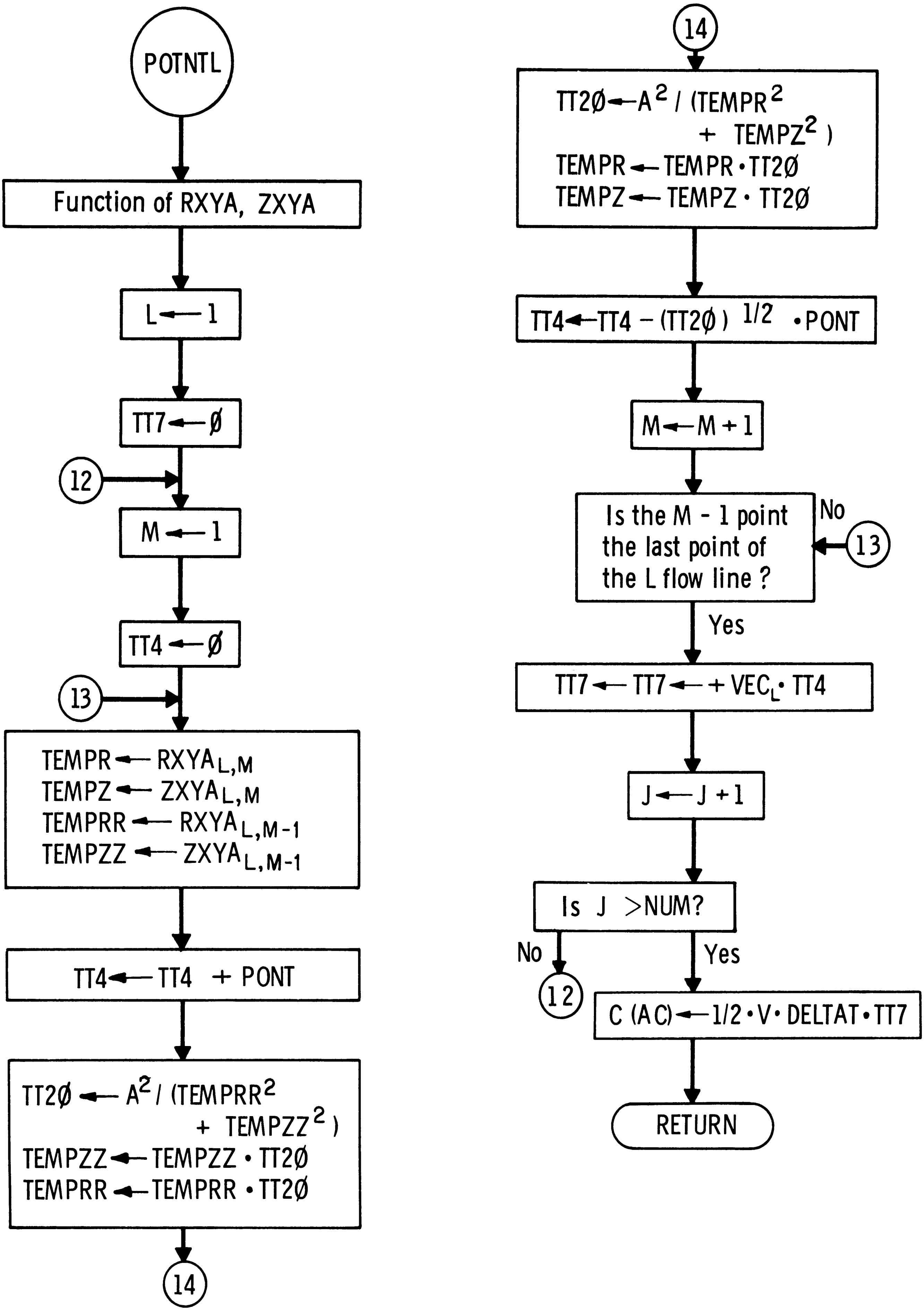
POTNTL
Function of RXYA, ZXYA
L ← 1
TT7 ← Ø
12
M ← 1
TT4 ← Ø
13
TEMPR ← RXYA L,M
TEMPZ ← ZXYA L,M
TEMPRR ← RXYA L,M-1
TEMPZZ ← ZXYA L,M-1
TT4 ← TT4 + PONT
TT2Ø ← A2 / (TEMPRR2 + TEMPZZ2)
TEMPZZ ← TEMPZZ · TT2Ø
TEMPRR ← TEMPRR · TT2Ø
14
14
TT2Ø ← A2 / (TEMPR2 + TEMPZ2)
TEMPR ← TEMPR · TT2Ø
TEMPZ ← TEMPZ · TT2Ø
TT4 ← TT4 − (TT2Ø) 1/2 · PONT
M ← M + 1
Is the M - 1 point the last point of the L flow line ?
No
13
Yes
TT7 ← TT7 ← + VECL · TT4
J ← J + 1
Is J >NUM?
No
12
Yes
C (AC) ← 1/2 · V · DELTAT · TT7
RETURN

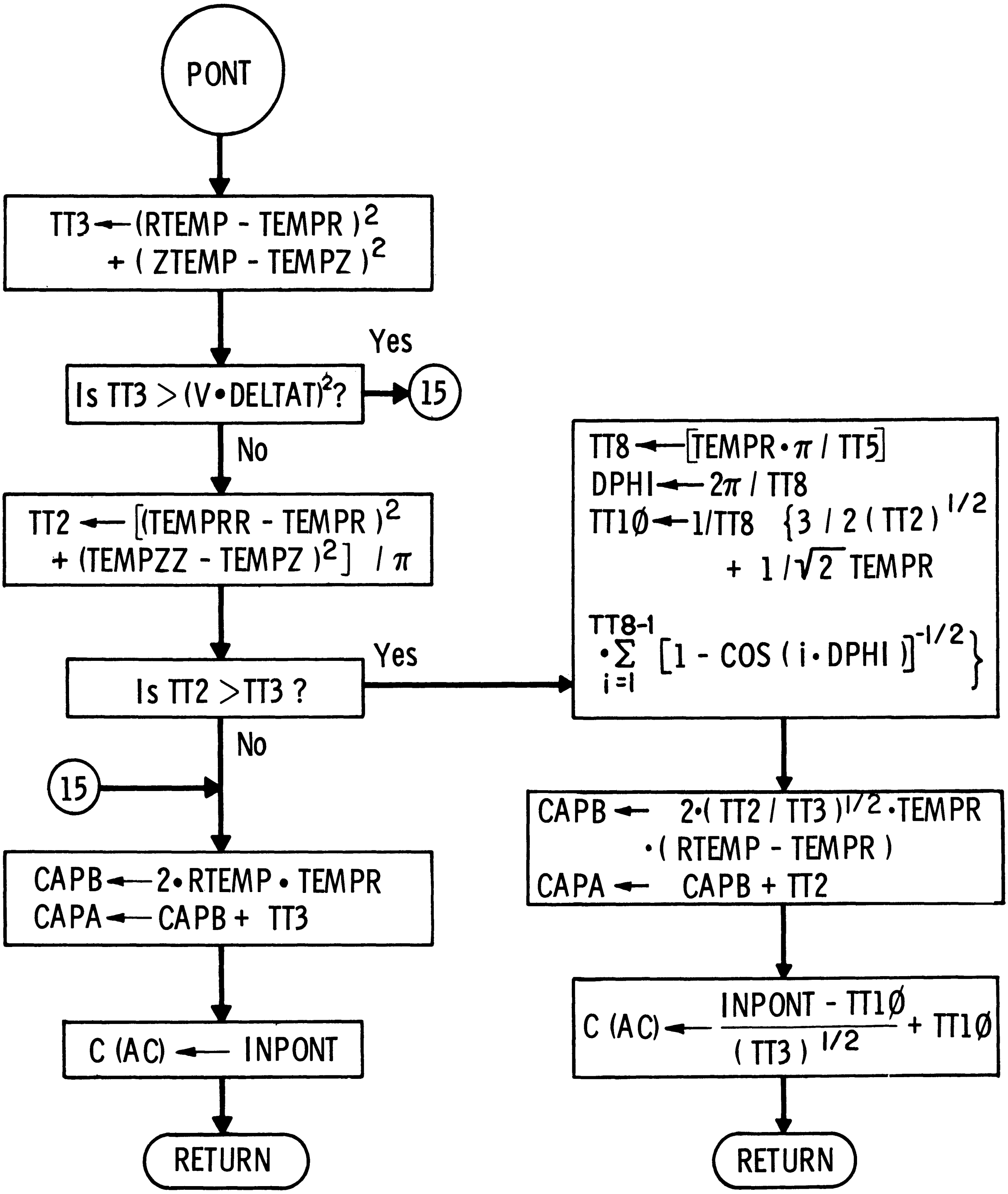
PONT
TT3 ← (RTEMP - TEMPR)2 + (ZTEMP - TEMPZ)2
Yes
Is TT3 > (V•DELTAT)2?
15
No
TT2 ← [(TEMPRR - TEMPR)2 + (TEMPZZ - TEMPZ)2] / π
Yes
Is TT2 > TT3 ?
No
15
CAPB ← 2•RTEMP • TEMPR
CAPA ← CAPB + TT3
C (AC) ← INPONT
RETURN
TT8 ← [TEMPR•π / TT5]
DPHI ← 2π / TT8
TT1Ø ← 1/TT8 {3 / 2 (TT2) 1/2
+ 1 / √2 TEMPR
•Σ i=1 TT8-1 [1 - COS (i•DPHI)]-1/2}
CAPB ← 2•(TT2 / TT3)1/2 •TEMPR •(RTEMP - TEMPR)
CAPA ← CAPB + TT2
C (AC) ← (INPONT - TT1Ø) / (TT3) 1/2 + TT1Ø
RETURN

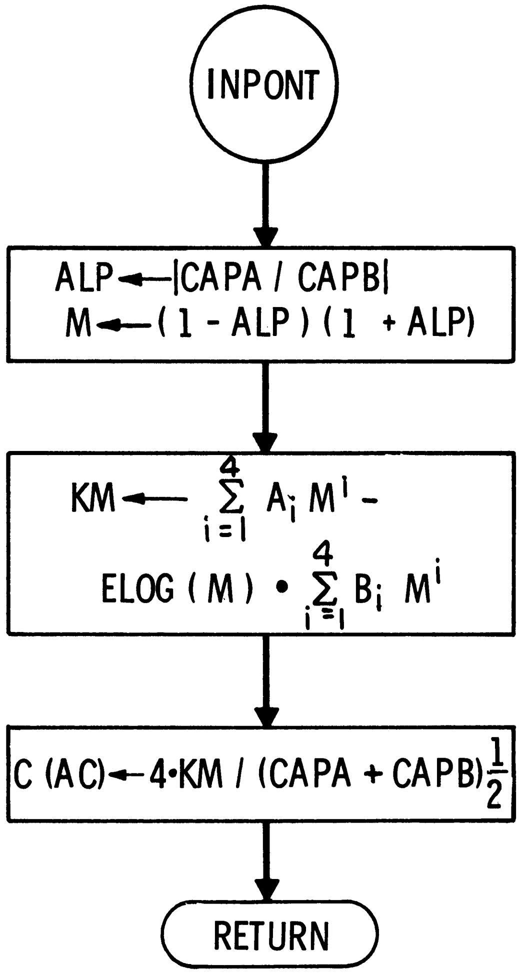

INPONT
ALP ← |CAPA / CAPB|
M ← (1 - ALP) (1 + ALP)
KM ← $\sum_{i=1}^{4} A_i M^i$ -
ELOG (M) • $\sum_{i=1}^{4} B_i M^i$
C (AC) ← 4•KM / (CAPA + CAPB)$\frac{1}{2}$
RETURN

```
PROGRAM LENGTH (CCTAL)  522C7        PRCGRAM COMMCN LENGTH    CCCCC        LOWEST ERASABLE DEFINED OCCOO
INITIAL TRANSFER VECTCR CCCCC        TRANSFER VECTCR LENGTH   CCO11        FIRST LOCATION EXECUTED 00011

EXTERNAL RCUTINES CALLED BY THIS PROGRAM
     CCCCC  622563254626     CC     SETECF
     CCCC1  33512521246C     CC     .READ
     CCCC2  33CCC1C3CCCC     CC     .C13CO
     CCC03  334751314563     CC     .PRINT
     CCCC4  24217C633144     CC     CAYTIM
     CCCC5  625C51636C6C     CC     SQRT
     CCCC6  23466260CC6C     CC     COS
     CCCC7  254346276C60     CO     ELCG
     CCC1C  25515146516C     CO     ERRCR

PROGRAM LISTING (NUMBERS IN CCTAL)
                                                  BRIEF   CN
                                                  PMC     CFF
     CCC11  0074 CC 4 CCCCC  C1C                  CALL    SETECF,END
     CCC13  0074 CC 4 CCC01  C1C          START   READ    FIN         READ PARAMETERS AND STARTING POINTS
     CCC15 -1 CCCCC 0 C267C  C1C                  ICP     V           VELCCITY
     CCC16 -1 OCCCC C C2671  C1C                  ICP     PHI         PRCBE POTENTIAL
     CCC17 -1 CCCCC C C2672  C1C                  IOP     DELTAT      TIME INCREMENT
     CCC20 -1 CCCCC C C2673  C1C                  IOP     A           PRCBE RADIUS
     CCC21  C56C CC C C2673  C1C                  LCQ     A
     CCC22  C26C CC C C2673  C1C                  FMP     A
     CCC23  0601 CC C C2674  C1C                  STO     A2
     CCC24  C56C CC C C267C  C1C                  LCQ     V
     CCC25  C260 CO C C2672  C1C                  FMP     DELTAT
     CCC26  0601 CC C C2676  C1C                  STO     VCT
     CCC27  C131 CC C CCCCC  CC                   XCA
     CCC30  C26C CC C C2676  C1C                  FMP     VCT
     CCC31  06C1 CC C C2675  C1C                  STO     V2
     CCC32  C560 CC C C2671  C1C                  LCQ     PHI
     CCC33  C260 CC C C2672  C1C                  FMP     CELTAT
     CCC34  0601 CC C C27CC  C1C                  STO     K
     OCC35 -1 CCCCC C C2701  C1C                  ICP     ZMIN        MINIMUM Z CCORCINATE
     CCC36 -1 CCCCC C C27C3  C1C                  ICP     H           FRACTICN OF TCP OF TRAJECTCRY SPACING FOR
                                                                      PCINTS FCR FINCING GRACIENTS
     CCC37 -1 CCCCC C C2717  C1C                  ICP     NUM         NUMBER CF TRAJECTORIES
     CCC4C -1 CCCCC C C272C  C1C                  ICP     NMAX        MAXIMUM NUMBER OF POINTS PER TRAJECTORY
     CCC41 -1 CCCCC C C2721  C1C                  IOP     NITER       NUMBER OF INTERATIONS TC BE MADE
     CCC42 -1 CCCCC C C2641  C1C                  ICP     PSW
     CCC43  05C0 CC 0 C272C  C10                  CLA     NMAX
     CCC44  04CC CC C 522C6  C1C                  ACD     =1
     CCC45  0601 CC C C272C  C10                  STO     NMAX
     CCC46  0534 CC 1 C272C  C1C                  LXA     NMAX,1      SET
     CCC47 -0634 CO 1 CC222  C1C                  SXC     S5,1        UP
     CCC5C -0634 CO 1 CC241  C1C                  SXD     S6,1        LCCP
     CCC51 -0634 CC 1 CC373  C1C                  SXD     S7,1        TERMINATICNS
     CCC52 -0634 CC 1 CC6C6  C1C                  SXC     S8,1        AND
     CCC53 -0634 CO 1 CC727  C1C                  SXD     S9,1        INCREMENTS
     CCC54 -0634 CC 1 CC744  C1C                  SXD     L2CAC,1
     CCC55 -0634 CC 1 C1513  C1C                  SXD     S31,1
     CCC56 -0634 CC 1 C1224  C1C                  SXD     S1C,1
     CCC57 -C634 CC 1 C2052  C10                  SXD     S11,1
```

```
CCC60 -0634 CC 1 CC072  C1C          SXD    S17,1
CCC61 -C634 CC 1 CCC75  C1C          SXD    S18,1
CCC62 -0634 CC 1 CCC71  C1C          SXD    S16,1
CCC63  1 77776 1 CCC64  C1C          TXI    *+1,1,-2
CCC64 -0634 CC 1 CC364  C1C          SXD    S12,1
CCC65 -0634 CC 1 C0577  C1C          SXD    S13,1
0CC66 -0634 CC 1 C1215  C1C          SXD    S14,1
CCC67 -0634 CC 1 C1504  C1C          SXD    S15,1
CCC70  1 CCCC2 1 CC071  C1C          TXI    *+1,1,2
CCC71  1 CCCCC 1 CC072  C1C   S16    TXI    *+1,1,**       **=NMAX
CCC72  1 CCCCC 1 CCC73  C10   S17    TXI    *+1,1,**       **=NMAX
CCC73 -0634 CC 1 C1242  C1C          SXD    S19,1
CCC74 -0634 CC 1 C1531  C1C          SXD    S2C,1
CCC75  1 CCCC0 1 CC076  C1C   S18    TXI    *+1,1,**       **=NMAX
CCC76 -C634 CC 1 CC613  C1C          SXD    S21,1
CCC77 -0634 CC 1 CC4CC  C1C          SXD    S22,1
CC1CC  0535 CC 1 C272C  C1C          LAC    NMAX,1         ACDRESS
0C1C1 -0634 CC 1 CC125  C1C          SXD    S23,1          MCDIFICATION
CC1C2 -0634 CC 1 CC142  C1C          SXD    S24,1
CC1C3  1 C7636 1 CC104  1C1C         TXI    *+1,1,RSA
CC1C4  0634 CC 1 C0437  C1C          SXA    S25,1
0C1C5  0634 CC 1 C1625  C1C          SXA    S27,1
CC1C6  0634 CC 1 C0733  C1C          SXA    L2CA,1
CC1C7  0634 CC 1 C0736  C1C          SXA    S29,1
CC11C  1 11612 1 C0111  C1C          TXI    *+1,1,RZA-RSA
CC111  C634 CC 1 CC652  C1C          SXA    S26,1
CC112  C634 CC 1 C1704  C1C          SXA    S28,1
CC113  1 73C73 1 CC114  C1C          TXI    *+1,1,ZSA-RZA
CC114  C634 CC 1 C044C  C1C          SXA    S25+1,1
0C115  0634 CC 1 C1626  C1C          SXA    S27+1,1
CC116  1 11612 1 CC117  C1C          TXI    *+1,1,ZZA-ZSA
CC117  0634 CC 1 CC653  C1C          SXA    S26+1,1
0C12C  0634 CC 1 017C5  C1C          SXA    S28+1,1
CC121  1 C47C5 1 CC122  C1C          TXI    *+1,1,RSB-ZZA
0C122  0634 CC 1 CC755  C1C          SXA    L2CC,1
CC123  1 1161C 1 CC124  C1C          TXI    *+1,1,RZB-RSB
0C124  0634 CC 1 C1246  C1C          SXA    L3CC,1
0C125  1 CCCCC 1 CC126  C1C   S23    TXI    *+1,1,**       **=-NMAX
CC126  1 42544 1 CC127  C1C          TXI    *+1,1,RSA-RZB
CC127  0634 CC 1 CC444  C1C          SXA    S25A,1
CC13C  0634 CC 1 C1632  C1C          SXA    S27A,1
CC131  1 11612 1 CC132  C1C          TXI    *+1,1,RZA-RSA
CC132  0634 CC 1 CC657  C1C          SXA    S26A,1
CC133  0634 CC 1 C1711  C1C          SXA    S28A,1
0C134  1 73C73 1 C0135  C1C          TXI    *+1,1,ZSA-RZA
CC135  C634 CC 1 CC445  C1C          SXA    S25A+1,1
CC136  C634 CC 1 C1633  C1C          SXA    S27A+1,1
CC137  1 11612 1 CC14C  C1C          TXI    *+1,1,ZZA-ZSA
CC14C  0634 CC 1 CC66C  C1C          SXA    S26A+1,1
CC141  0634 CC 1 C1712  C1C          SXA    S28A+1,1
CC142  1 CCCCC 1 CC143  C1C   S24    TXI    *+1,1,**       **=-NMAX
CC143  1 61261 1 CC144  C1C          TXI    *+1,1,RSA-ZZA
0C144  C634 CC 1 C0451  C1C          SXA    S25B,1
CC145  0634 CC 1 C1637  C1C          SXA    S27B,1
CC146  1 11612 1 CC147  C1C          TXI    *+1,1,RZA-RSA
CC147  0634 CC 1 CC664  C1C          SXA    S26B,1
0C15C  0634 CC 1 C1716  C1C          SXA    S28B,1
CC151  1 73C73 1 CC152  C1C          TXI    *+1,1,ZSA-RZA
```

```
0C152  C634 CC 1 CC452  C1C          SXA    S25B+1,1
0C153  0634 CC 1 C164C  C1C          SXA    S27B+1,1
CC154  1 11612 1 CC155  C1C          TXI    *+1,1,ZZA-ZSA
CC155  0634 C0 1 CC665  C1C          SXA    S26B+1,1
CC156  C634 CC 1 C1717  C1C          SXA    S28B+1,1
CC157  C5CC CC C C2717  C1C          CLA    NUM
CC16C  C621 CC C CC412  C1C          STA    L5A
CC161  C621 CC C CC625  C1C          STA    L15A
CC162  C621 CC C C1577  C1C          STA    L25A
CC163  C621 CC C C1656  C1C          STA    L35A
CC164  04CC CC C 522C5  C1C          ACD    =3               CCMPLTE
C0165  0131 CC C CCCCC  CC           XCA                     TCTAL
CC166 -C754 CC C CCCCC  CC           ZAC                     PAGES PER
CC167  0221 CC C 522C4  C1C          DVP    =4               TRAJECTCRY
CC17C -C6CC CC C C2725  C1C          STQ    TP               MATRIX
0C171 -0634 CC C CC371  C10          SXD    L3C,C
CC172 -C634 CC C CC6C4  C1C          SXD    L13C,C
CC173  0774 CC 1 C47C4  CC           AXT    SIZE,1           ZERC
CC174  06CC CC 1 C7636  C1C          STZ    RSA,1            CUT
0C175  C60C CC 1 14543  C1C          STZ    ZSA,1            TRAJECTCRY
CC176  06CC C0 1 2145C  C1C          STZ    RZA,1            MATRICES
CC177  C6CC CC 1 26355  C1C          STZ    ZZA,1
CC20C  06CC CC 1 33262  C1C          STZ    RSB,1
0C201  06CC C0 1 40166  C1C          STZ    ZSB,1
CC2C2  06C0 CC 1 45C72  C1C          STZ    RZB,1
CC2C3  06CC CC 1 51776  C1C          STZ    ZZB,1
CC2C4  2 CCCC1 1 CC174  C1C          TIX    *-8,1,1
0C2C5  C774 CC 2 CC0C1  C0           AXT    1,2
CC2C6  0534 CC 1 C2717  C1C          LXA    NUM,1            READ
CC2C7 -1 CCCCC 2 C7636  C1C     S4   IOP    RSA,2            AND
CC21C -1 CCCCC 2 14543  C1C          IOP    ZSA,2            SET
0C211  C5CC CC 2 07636  C1C          CLA    RSA,2            UP
CC212  C6C1 CC 2 2145C  C1C          STO    RZA,2            INITIAL
CC213  06C1 CC 2 C7637  C1C          STO    RSA+1,2
0C214  06C1 CC 2 21451  C1C          STO    RZA+1,2
CC215  C5CC CC 2 14543  C1C          CLA    ZSA,2            TRAJECTCRY
CC216  C6C1 CC 2 26355  C1C          STO    ZZA,2            PCINTS
CC217  C3CC CC C C2676  C1C          FAD    VCT
0C220  06C1 CC 2 14544  C1C          STO    ZSA+1,2
0C221  06C1 CC 2 26356  C1C          STO    ZZA+1,2
CC222  1 CCCCC 2 CC223  C1C     S5   TXI    *+1,2,**         **=NMAX
CC223  2 CCCC1 1 CC207  C1C          TIX    S4,1,1
CC224 -1 CCCCC C CCOCC  CC           ENDIO
CC225  2 CCCC1 2 CC226  C1C          TIX    *+1,2,1
CC226 -C634 CC 2 CC374  C1C          SXD    L4,2             C(IR2)=NMAX*NUM
CC227 -0634 CC 2 CC457  C1C          SXD    L8,2             MCRE
CC230 -0634 CC 2 CC6C7  C1C          SXD    L14,2            LCCP
0C231 -C634 CC 2 CC672  C1C          SXD    L18,2            SET
CC232 -C634 CC 2 C1226  C1C          SXD    L24A,2           UP
CC233 -0634 CC 2 C1547  C1C          SXD    L24E,2
0C234 -0634 CC 2 C1645  C1C          SXD    L28,2
CC235 -0634 CC 2 C1515  C1C          SXD    L34A,2
CC236 -C634 CC 2 C1563  C1C          SXD    L34E,2
CC237 -0634 CC 2 C1724  C1C          SXD    L38,2
CC24C -C634 CC 2 C2C6C  C1C          SXD    LL17,2
0C241  2 CCCCC 2 CC242  C1C     S6   TIX    *+1,2,**         **=NMAX
CC242 -0634 CC 2 CC745  C1C          SXD    L2CAE,2          C(IR2)=NMAX*(NUM-1)
CC243 -0634 CC 2 C1225  C1C          SXD    L24,2            LCCP
```

```
CC244 -C634 CC 2 C1514  C1C          SXD   L34,2          SET UP
CC245  C774 CC 2 CCCO1  CC           AXT   1,2
CC246  C754 CC 2 CCCCC  CC      L1   PXA   ,2             CCMPUTE
CC247  C734 CC 1 CCCCC  CC           PAX   ,1             INITIAL
CC25C  C774 CC 4 CCCC1  CC           AXT   1,4            APPRCXIMATICNS
CC251  C634 CC 4 CC36C  C1C          SXA   L2C,4          FCR
OC252  C634 CC 4 CC37C  C1C          SXA   L3B,4          SIGMA
OC253  C560 CC 1 C7636  C1C     L2   LDQ   RSA,1          TRAJECTCRIES
CC254  C26C CC 1 C7636  C1C          FMP   RSA,1
CC255  06C1 CC C C2642  C1C          STO   T1
CC256  056C CC 1 14543  C1C          LDQ   ZSA,1
CC257  C26C CC 1 14543  C1C          FMP   ZSA,1
CC26C  03CC CC C C2642  C1C          FAD   T1
CC261  C5CC CC C 522C3  C1C          LDQ   =-1.5
CC262  CC74 CC 4 CCCC2  C1C          CALL  .C13CC         EXPCNENTATICN SUBRCUTINE
CC263  C131 CC C CCCCC  CC           XCA
CC264  0260 CC C C27CC  C1C          FMP   K
OC265  06C1 CC C C2642  C1C          STO   T1
OC266  05CC CC C 522C2  C1C          CLA   =1.
CC267  C3CC CC C C2642  C1C          FAD   T1
CC27C  C6C1 CC C C2642  C1C          STO   T1
CC271  0131 CC C CCCCC  CC           XCA
CC272  C260 CC 1 C7636  C1C          FMP   RSA,1
CC273  C6C1 CC 1 C7635  C1C          STO   RSA-1,1
CC274 -C12C CC C CC367  C1C          TMI   L3A
CC275  C56C CC C C2642  C1C          LDQ   T1             PARTICULAR
OC276  C260 CC 1 14543  C1C          FMP   ZSA,1          TRAJECTCRY
CC277  03C2 CC C C2676  C1C          FSB   VDT            WILL BE
CC3CC  06C1 CC 1 14542  C1C          STO   ZSA-1,1        TERMINATED
CC3C1  04C2 CC C C2701  C1C          SUB   ZMIN           IF R VALUE
CC3C2 -C12C CC C CC366  C1C          TMI   L3             NEGATIVE
CC3C3  C5CC CC 1 C7636  C1C          CLA   RSA,1
CC3C4 -C1CC CC C CC31C  C1C          TNZ   *+4
CC3C5  C5CC CC 1 14542  C1C          CLA   ZSA-1,1
CC3C6  C3C2 CC 1 14543  C1C          FSB   ZSA,1
CC3C7  012C CC C CC366  C1C          TPL   L3
CC31C  0560 CC 1 C7635  C1C          LDQ   RSA-1,1
CC311  C260 CC 1 C7635  C1C          FMP   RSA-1,1
OC312  C6C1 CC C C2711  C1C          STO   TEMP
CC313  C560 CC 1 14542  C1C          LDQ   ZSA-1,1
CC314  C26C CC 1 14542  C1C          FMP   ZSA-1,1
CC315  C3CC CC C C2711  C1C          FAD   TEMP
CC316  C4C2 CC C C2674  C1C          SUB   A2
CC317 -C120 CC C CC366  C1C          TMI   L3
CC32C  C5CC CC 1 14543  C1C          CLA   ZSA,1
CC321  C3C2 CO 1 14542  C1C          FSB   ZSA-1,1
CC322  C6C1 CC C C2711  C1C          STO   TEMP
CC323  05CC CC 1 C7636  C1C          CLA   RSA,1
CC324  03C2 CC 1 C7635  C1C          FSB   RSA-1,1
CC325  C241 CC C C2711  C1C          FDP   TEMP
CC326 -C6CC CC C C2726  C1C          STQ   B
CC327  C260 CC C C2726  C1C          FMP   B
CC33C  C6C1 CC C C2727  C1C          STO   B2
CC331  C56C CC 1 14543  C1C          LDQ   ZSA,1
CC332  C260 CC C C2726  C1C          FMP   B
CC333  03C2 CC 1 C7636  C1C          FSB   RSA,1
CC334  06C1 CC C C273C  C1C          STO   B1
CC335  0131 CC C CCCCC  CC           XCA
```

```
CC336  C26C CC C C2730  C1C        FMP    B1
CC337  06C1 CC C C2731  C1C        STO    B12
CC34C  C3C2 CC C C2674  C1C        FSB    A2
CC341  0241 CC C C2731  C1C        FDP    B12
CC342 -06CC CC C C2711  C1C        STQ    TEMP
CC343  05CC CC C 522C2  C1C        CLA    =1.
CC344  0241 CC C C2727  C1C        FDP    B2
CC345  0131 CC C CCCCC  CC         XCA
CC346  03CC CC C 522C2  C1C        FAD    =1.
CC347  0131 CC C CCCCC  CC         XCA
CC35C  C26C CC C C2711  C1C        FMP    TEMP
CC351  04C2 CC C 522C2  C1C        SUB    =1.
CC352  C1CC CC C CC366  C1C        TZE    L3
CC353  C12C CC C CC357  C1C        TPL    L2B
CC354  C560 CC 1 14543  C1C        LDQ    ZSA,1
CC355  026C CC 1 14542  C1C        FMP    ZSA-1,1
CC356 -C12C CC C CC366  C1C        TMI    L3
0C357   1 CCCC1 1 CC36C C1C   L2B  TXI    *+1,1,1
CC36C  C774 CC 4 CCCCC  CC    L2C  AXT    **,4         **=INTERMEDIATE IMAXSA
CC361   1 CCCC1 4 CC362 C1C        TXI    *+1,4,1
CC362  C634 CC 4 C036C  C1C        SXA    L2C,4
CC363  C634 CO 4 CC37C  C1C        SXA    L3B,4
CC364 -3 CCCCC 4 CC253  C1C   S12  TXL    L2,4,**      **=NMAX-1
CC365  0C2C CC C CC371  C1C        TRA    L3C
CC366  C6CC CC 1 14542  C1C   L3   STZ    ZSA-1,1
CC367  C6C0 CC 1 07635  C1C   L3A  STZ    RSA-1,1
CC37C  C774 CC 4 CCCCC  CC    L3B  AXT    **,4         **=INTERMEDIATE IMAXSA
CC371 -3 CCCCC 4 CC373  C1C   L3C  TXL    *+2,4,**     **=IMAXSA
CC372 -0634 CO 4 CC371  C1C        SXD    L3C,4
CC373   1 CCCCC 2 CC374 C1C   S7   TXI    *+1,2,**     **=NMAX
CC374 -3 CCCCC 2 CC246  C1C   L4   TXL    L1,2,**      **=NMAX*NUM
CC375 -0534 CC 4 CC371  C1C        LXD    L3C,4
0C376  0634 CC 4 CC4C6  C1C        SXA    L5,4
CC377 -0535 CO 4 CC371  C1C        LDC    L3C,4
0C4CC   1 CCCCC 4 CC4C1 C1C   S22  TXI    *+1,4,**     **=4*NMAX
CC4C1 -0634 CC 4 CC456  C1C        SXD    L7,4
CC4C2  05CC CC 0 52204  C1C        CLA    =4
CC4C3  0601 CC C C2723  C1C        STO    VAR          FORMAT VARIABLE
CC4C4  0774 CC 2 CCCC1  CC         AXT    1,2
CC4C5  C6CC CC C C2724  C1C        STZ    P
C04C6  C774 CC 1 CCCCC  CC    L5   AXT    **,1         **=IMAXSA
CC4C7  05C0 CC C C2724  C1C        CLA    P            PAGE NUMBER
CC41C  04CC CC C 522C6  C1C        ADD    =1
CC411  06C1 CC C C2724  C1C        STO    P
00412  C774 CO 4 CCOCC  CC    L5A  AXT    **,4         **=SIGMA TRAJECTORIES STILL TO BE PRINTED
CC413   2 CCCC4 4 CC415 C1C        TIX    *+2,4,4
CC414  C634 CC 4 C2723  C1C        SXA    VAR,4
C0415  C634 CC 4 C0412  C1C        SXA    L5A,4
00416  CC74 CO 4 CCCC3  C1C        PRINT  FVAR,...,FCLT1,P,TP,V,PHI,CELTAT,A,H,ZMIN
CC43C  C5CC CC C C2723  C1C        CLA    VAR
0C431  01CC CC C CC453  C1C        TZE    L7-3
0C432 -1 CCCCC 2 07636  C1C   L6   ICP    RSA,2        PRINT INITIAL
CC433 -1 CCCCC 2 14543  C1C        ICP    ZSA,2        SIGMA TRAJECTCRIES
CC434  C5CC CC C C2723  C1C        CLA    VAR
CC435  04C2 CC C 522C6  C1C        SUB    =1
CC436  01CC CC C C0453  C1C        TZE    L7-3
CC437 -1 CCCCC 2 CCOCC  CC    S25  ICP    **,2         **=RSA-NMAX
CC44C -1 CCCCC 2 CCCCC  CO         ICP    **,2         **=ZSA-NMAX
```

```
0C441   05CC CC C C2723  C1C         CLA    VAR
CC442   04C2 CC C 522C1  C1C         SUB    =2
CC443   01CC CC C CC453  C1C         TZE    L7-3
CC444 -1 CCCCC 2 CCOCC  CC    S25A   ICP    **,2           **=RSA-2*NMAX
CC445 -1 CCCCO 2 CCCCC  CC           ICP    **,2           **=ZSA-2*NMAX
CC446   05C0 CC C C2723  C1C         CLA    VAR
CC447   04C2 CC C 522C5  C1C         SUB    =3
CC45C   C1CC CC C C0453  C1C         TZE    L7-3
00451 -1 CCCCC 2 CCCCC  CC    S25B   IGP    **,2           **=RSA-3*NMAX
CC452 -1 CCCCC 2 CCCCC  CC           IGP    **,2           **=ZSA-3*NMAX
CC453   1 CCCC1 2 CC454  C1C         TXI    *+1,2,1
0C454   2 CCCC1 1 C0432  C1C         TIX    L6,1,1
CC455 -1 CCCCC C CCCCC  CC           ENDIO
CC456   1 CCCCC 2 CC457  C1C   L7    TXI    *+1,2,**       **=4*NMAX-IMAXSA
CC457 -3 CCCCC 2 CC406  C1C   L8    TXL    L5,2,**        **=NMAX*NUM
CC46C   0774 CC 2 CC001  CC          AXT    1,2
CC461   0754 CC 2 CCCCC  CC    L11   PXA    ,2
CC462   C734 CC 1 CCCCC  CC          PAX    ,1             COMPLTE
CC463   0774 CC 4 CC001  CC          AXT    1,4            INITIAL
0C464   0634 C0 4 C0573  C1C         SXA    L12C,4         ZETA TRAJECTCRIES
CC465   C634 CC 4 CC6C3  C1C         SXA    L13B,4
CC466   C56C CC 1 2145C  C1C   L12   LCQ    RZA,1
CC467   C26C CC 1 2145C  C1C         FMP    RZA,1
0C470   06C1 CC C C2642  C1C         STO    T1
CC471   C560 CC 1 26355  C1C         LCQ    ZZA,1
CC472   C26C CC 1 26355  C1C         FMP    ZZA,1
CC473   C3CC CC C C2642  C1C         FAD    T1
0C474   C560 CC 0 522C3  C1C         LCQ    =-1.5
CC475   CC74 CC 4 CC0C2  C1C         CALL   .C13CC
CC476   0131 CC C CCOCC  CC          XCA
CC477   C26C CC C C27CC  C1C         FMP    K
0C5CC   06C1 CC C C2642  C1C         STO    T1
0C5C1   05C0 CC C 522C2  C1C         CLA    =1.
CC5C2   03C2 CC C C2642  C1C         FSB    T1
0C5C3   06C1 CC C C2642  C1C         STO    T1
0C5C4   0131 CC C CCOCC  CC          XCA
0C5C5   C26C CC 1 2145C  C1C         FMP    RZA,1
CC5C6   06C1 CC 1 21447  C1C         STO    RZA-1,1
0C5C7 -012C CC 0 CC602  C1C         TMI    L13A
0C51C   056C CC C C2642  C1C         LCQ    T1
0C511   026C CC 1 26355  C1C         FMP    ZZA,1
CC512   03C2 CC C C2676  C1C         FSB    VCT
0C513   06C1 CC 1 26354  C1C         STO    ZZA-1,1
0C514   C4C2 CC C C27C1  C1C         SUB    ZMIN
CC515 -C12C CC C CC6C1  C1C         TMI    L13
CC516   05CC CC 1 2145C  C1C         CLA    RZA,1
0C517 -C1CC CC C C0523  C1C         TNZ    *+4
0C520   C5CC CC 1 26354  C1C         CLA    ZZA-1,1
0C521   03C2 CC 1 26355  C1C         FSB    ZZA,1
CC522   012C CC C CC6C1  C1C         TPL    L13
CC523   C56C CC 1 21447  C1C         LDQ    RZA-1,1
0C524   C26C CC 1 21447  C1C         FMP    RZA-1,1
CC525   06C1 CC C C2711  C1C         STO    TEMP
0C526   C56C CC 1 26354  C1C         LCQ    ZZA-1,1
0C527   C26C CC 1 26354  C1C         FMP    ZZA-1,1
0C53C   C3CC CC C C2711  C1C         FAD    TEMP
CC531   04C2 CC C C2674  C1C         SUB    A2
CC532 -C12C CC C CC6C1  C1C         TMI    L13
```

```
00533  0500 00 1 26355  010        CLA   ZZA,1
00534  0302 00 1 26354  010        FSB   ZZA-1,1
00535  0601 00 0 02711  010        STO   TEMP
00536  0500 00 1 21450  010        CLA   RZA,1
00537  0302 00 1 21447  010        FSB   RZA-1,1
00540  0241 00 0 02711  010        FDP   TEMP
00541 -0600 00 0 02726  010        STQ   B
00542  0260 00 0 02726  010        FMP   B
00543  0601 00 0 02727  010        STO   B2
00544  0560 00 1 26355  010        LDQ   ZZA,1
00545  0260 00 0 02726  010        FMP   B
00546  0302 00 1 21450  010        FSB   RZA,1
00547  0601 00 0 02730  010        STO   B1
00550  0131 00 0 00000  00         XCA
00551  0260 00 0 02730  010        FMP   B1
00552  0601 00 0 02731  010        STO   B12
00553  0302 00 0 02674  010        FSB   A2
00554  0241 00 0 02731  010        FDP   B12
00555 -0600 00 0 02711  010        STQ   TEMP
00556  0500 00 0 52202  010        CLA   =1.
00557  0241 00 0 02727  010        FDP   B2
00560  0131 00 0 00000  00         XCA
00561  0300 00 0 52202  010        FAD   =1.
00562  0131 00 0 00000  00         XCA
00563  0260 00 0 02711  010        FMP   TEMP
00564  0402 00 0 52202  010        SUB   =1.
00565  0100 00 0 00601  010        TZE   L13
00566  0120 00 0 00572  010        TPL   L12B
00567  0560 00 1 26355  010        LDQ   ZZA,1
00570  0260 00 1 26354  010        FMP   ZZA-1,1
00571 -0120 00 0 00601  010        TMI   L13
00572  1 00001 1 00573  010  L12B  TXI   *+1,1,1
00573  0774 00 4 00000  00   L12C  AXT   **,4           **=INTERMEDIATE IMAXZA
00574  1 00001 4 00575  010        TXI   *+1,4,1
00575  0634 00 4 00573  010        SXA   L12C,4
00576  0634 00 4 00603  010        SXA   L13B,4
00577 -3 00000 4 00466  010  S13   TXL   L12,4,**       **=NMAX-1
00600  0020 00 0 00604  010        TRA   L13C
00601  0600 00 1 21447  010  L13   STZ   RZA-1,1
00602  0600 00 1 26354  010  L13A  STZ   ZZA-1,1
00603  0774 00 4 00000  00   L13B  AXT   **,4           **=INTERMEDIATE IMAXZA
00604 -3 00000 4 00606  010  L13C  TXL   *+2,4,**       **=IMAXZA
00605 -0634 00 4 00604  010        SXD   L13C,4
00606  1 00000 2 00607  010  S8    TXI   *+1,2,**       **=NMAX
00607 -3 00000 2 00461  010  L14   TXL   L11,2,**       **=NMAX*NUM
00610 -0534 00 4 00604  010        LXD   L13C,4
00611  0634 00 4 00621  010        SXA   L15,4
00612 -0535 00 4 00604  010        LDC   L13C,4
00613  1 00000 4 00614  010  S21   TXI   *+1,4,**       **=4*NMAX
00614 -0634 00 4 00671  010        SXD   L17,4
00615  0500 00 0 52204  010        CLA   =4
00616  0601 00 0 02723  010        STO   VAR
00617  0774 00 2 00001  00         AXT   1,2
00620  0600 00 0 02724  010        STZ   P
00621  0774 00 1 00000  00   L15   AXT   **,1           **=IMAXZA
00622  0500 00 0 02724  010        CLA   P
00623  0400 00 0 52206  010        ADD   =1
00624  0601 00 0 02724  010        STO   P
```

```
00625  0774 00 4 00000  00   L15A  AXT   **,4               **=ZETA TRAJECTCRIES STILL TO BE PRINTED
00626  2 00004 4 00630  010         TIX   *+2,4,4
00627  0634 00 4 02723  010         SXA   VAR,4
00630  0634 00 4 00625  010         SXA   L15A,4
00631  0074 00 4 00003  010         PRINT FVAR,...,FCUT2,F,TP,V,PHI,CELTAT,A,H,ZMIN
00643  0500 00 0 02723  010         CLA   VAR
00644  0100 00 0 00666  010         TZE   L17-3
00645 -1 00000 2 21450  010   L16   IOP   RZA,2
00646 -1 00000 2 26355  010         IOP   ZZA,2
00647  0500 00 0 02723  010         CLA   VAR
00650  0402 00 0 52206  010         SUB   =1
00651  0100 00 0 00666  010         TZE   L17-3
00652 -1 00000 2 00000  00    S26   IOP   **,2               **=RZA-NMAX
00653 -1 00000 2 00000  00          IOP   **,2               **=ZZA-NMAX
00654  0500 00 0 02723  010         CLA   VAR
00655  0402 00 0 52201  010         SUB   =2
00656  0100 00 0 00666  010         TZE   L17-3
00657 -1 00000 2 00000  00    S26A  IOP   **,2               **=RZA-2*NMAX
00660 -1 00000 2 00000  00          IOP   **,2               **=ZZA-2*NMAX
00661  0500 00 0 02723  010         CLA   VAR
00662  0402 00 0 52205  010         SUB   =3
00663  0100 00 0 00666  010         TZE   L17-3
00664 -1 00000 2 00000  00    S26B  IOP   **,2               **=RZA-3*NMAX
00665 -1 00000 2 00000  00          IOP   **,2               **=ZZA-3*NMAX
00666  1 00001 2 00667  010         TXI   *+1,2,1
00667  2 00001 1 00645  010         TIX   L16,1,1
00670 -1 00000 0 00000  00          ENDIO
00671  1 00000 2 00672  010   L17   TXI   *+1,2,**           **=4*MAX-IMAXZA
00672 -3 00000 2 00621  010   L18   TXL   L15,2,**           **=MAX*NUM
00673  0600 00 0 02714  010         STZ   CCUNT
00674 -0534 00 4 00371  010         LXD   L3C,4
00675 -0634 00 4 01231  010         SXD   L24AA,4
00676 -0534 00 4 00604  010         LXD   L13C,4
00677 -0634 00 4 01520  010         SXD   L34AA,4
00700  0500 00 0 02714  010   L20   CLA   CCUNT
00701  0402 00 0 02721  010         SUB   NITER
00702  0100 00 0 00013  010         TZE   START
00703 -0634 00 0 01222  010         SXD   L23C,0
00704 -0634 00 0 01511  010         SXD   L33C,0
00705  0774 00 2 00001  00          AXT   1,2
00706  0534 00 1 02717  010         LXA   NUM,1
00707  0500 00 2 07636  010   S8.5  CLA   RSA,2
00710  0601 00 2 33262  010         STO   RSB,2              PCINTS
00711  0500 00 2 14543  010         CLA   ZSA,2              FCR NEXT
00712  0601 00 2 40166  010         STO   ZSB,2              APPRCXIMATICN
00713  0500 00 2 21450  010         CLA   RZA,2              TC TRAJECTCRIES
00714  0601 00 2 45072  010         STO   RZB,2
00715  0500 00 2 26355  010         CLA   ZZA,2
00716  0601 00 2 51776  010         STO   ZZB,2
00717  0500 00 2 07637  010         CLA   RSA+1,2
00720  0601 00 2 33263  010         STO   RSB+1,2
00721  0500 00 2 14544  010         CLA   ZSA+1,2
00722  0601 00 2 40167  010         STO   ZSB+1,2
00723  0500 00 2 21451  010         CLA   RZA+1,2
00724  0601 00 2 45073  010         STO   RZB+1,2
00725  0500 00 2 26356  010         CLA   ZZA+1,2
00726  0601 00 2 51777  010         STO   ZZB+1,2
00727  1 00000 2 00730  010   S9    TXI   *+1,2,**           **=NMAX
```

```
CC73C  2 CCCC1 1 CC7C7  C1C          TIX    S8.9,1,1
CC731  0774 CC 1 CCCC1  CC           AXT    1,1
CC732  0774 CC 2 CCCC1  CC           AXT    1,2
CC733  C5CC CC 2 CCCCC  CO    L2CA   CLA    **,2          **=RSA-NMAX
CC734  C3C2 CC 2 C7636  C1C          FSB    RSA,2
CC735  C601 CC C C27C4  C1C          STO    DA
CC736  C5CO CC 2 CCCCC  CC    S29    CLA    **,2          **=RSA-NMAX
CC737  C3CC CC 2 C7636  C1C          FAD    RSA,2
CC74C  C131 CC C CCCCC  CC           XCA
CC741  C26C CC C C27C4  C1C          FMP    DA
CC742  06C1 CC 1 52166  C1C          STO    VEC,1
CC743  1 CCCC1 1 C0744  C1C          TXI    **1,1,1
CC744  1 CCCCC 2 CC745  C1C   L2CAC  TXI    **1,2,**      **=NMAX
CC745 -3 CCCCC 2 CC733  C1C   L2CAE  TXL    L2CA,2,**     **=NMAX*(NUM-1)
CC746  05CO CC 2 C7636  C1C          CLA    RSA,2
CC747  04CC CC C 522CC  C1C          ACD    =K1K9
OC75C  C3CC CC C C2704  C1C          FAD    DA
CC751  0131 CC C CCCCC  CC           XCA
CC752  C26C CC C C2704  C1C          FMP    DA
CC753  06C1 CC 1 52166  C1C          STO    VEC,1
CC754  0774 CC 2 CC0C1  CC           AXT    1,2
CC755  05CC CC 2 CCCCC  CC    L2CC   CLA    **,2          **=RSB-NMAX
CC756  03C2 CC 2 33262  C1C          FSB    RSB,2         COMPLTE
OC757  0131 CC C CCCCC  CC           XCA                  NEXT
CC76C  C26C CC C C27C3  C1C          FMP    H             APPROXIMATIONS
CC761  06C1 CC C C2677  C1C          STO    DELTA         TC TRAJECTORIES
OC762  0754 CC 2 CC0CC  CC    L21    PXA    ,2
OC763  C734 CC 1 CCCCC  CC           PAX    ,1
CC764  C774 CC 4 CCCC1  CC           AXT    1,4
CC765  0634 CC 4 C1211  C1C          SXA    L22C,4
OC766  0634 CC 4 C1221  C1C          SXA    L23B,4
OC767 -C520 CC C C2641  C1C   L22    NZT    PSW
CC77C  CC2C CC C C1CC1  C1C          TRA    L22.1
OC771  CC74 CC 4 CC004  C1C          CALL   DAYTIM
CC772  C6C1 CC C C264C  C1C          STO    X2
CC773  CC74 CO 4 CCCC3  C1C          PRINT  F1
CC775 -1 CCCCC 1 33262  C1C          ICP    RSB,1
CC776 -1 CCCCC 1 4C166  C1C          ICP    ZSB,1
CC777 -1 CCCCC C C264C  C1C          IOP    X2
O1CCC -1 CCCCC C CCCCC  CO           ENDIO
O1CC1  C5CC CC 1 33262  C1C   L22.1  CLA    RSB,1
C1CC2  01CC CC C C1C40  C1C          TZE    L22.2
C1CC3  C3C2 CC C C2677  C1C          FSB    DELTA
O1CC4  0EC2 CC C C2660  C1C          SLW    RTEMP
O1CC5  C5CC CC 1 4C166  C1C          CLA    ZSB,1
C1CC6  OEC1 CC C C2661  C1C          STC    ZTEMP
O1CC7  CC74 CC 4 C1726  C1C          TSX    PCINTL,4
O1C1C  3 CCCCC C 2145C  C1C          PAR    RZA
C1C11  3 CCCCC C 26355  C1C          PAR    ZZA
O1C12  06C1 CC C C2642  C1C          STC    T1
O1C13  CC74 CC 4 C1726  C1C          TSX    PCINTL,4
O1C14  3 CCCCC C C7636  C1C          PAR    RSA
C1C15  3 CCCCC C 14543  C1C          PAR    ZSA
C1C16  C3C2 CC C C2642  C1C          FSB    T1
O1C17  C6C1 CC C C2643  C1C          STO    T2
C1C2C  C5CC CC 1 33262  C1C          CLA    RSB,1
C1C21  03CC CC C C2677  C1C          FAD    DELTA
O1C22  06C1 CC C C266C  C1C          STO    RTEMP
```

```
C1C23  CC74 CC 4 C1726  C1C          TSX    PCTNTL,4
C1C24  3 CCCCC C 2145C  C1C          PAR    RZA
01C25  3 CCCCC C 26355  C1C          PAR    ZZA
C1C26  06C1 CC C C2642  C1C          STO    T1
01C27  CC74 CC 4 C1726  C1C          TSX    PCTNTL,4
C1C30  3 CCCCC C C7636  C1C          PAR    RSA
01C31  3 CCCCC C 14543  C1C          PAR    ZSA
C1C32  03C2 CC C C2642  C1C          FSB    T1
C1C33  C3C2 CC C C2643  C1C          FSB    T2
01C34  0241 CC C C2677  C1C          FDP    DELTA
01C35  026C CC C 52177  C1C          FMP    =.C397EE7      =.5/(4*PI)
01C36  C76C CC C CCCC2  CC           CHS
01C37  03CC CC 1 33262  C1C          FAD    RSB,1
C1040  06C1 CC C C2666  C1C   L22.2  STO    RGP
01041  05CC CC 1 33262  C1C          CLA    RSB,1
01C42  06C1 CC C C266C  C1C          STO    RTEMP
01C43  05C0 CC 1 4C166  C1C          CLA    ZSB,1
01044  C3C2 CC C C2677  C1C          FSB    DELTA
01C45  06C1 CC C C2661  C1C          STO    ZTEMP
C1C46  0C74 CC 4 C1726  C1C          TSX    PCTNTL,4
C1C47  3 0CCCC C 2145C  C1C          PAR    RZA
C1C5C  3 CCCCC C 26355  C1C          PAR    ZZA
01C51  C6C1 CC 0 C2642  C1C          STO    T1
01C52  CC74 CC 4 C1726  C1C          TSX    PCTNTL,4
01C53  3 CCCCC C C7636  C1C          PAR    RSA
01054  3 CCCCC C 14543  C1C          PAR    ZSA
01C55  03C2 CC 0 C2642  C1C          FSB    T1
01C56  06C1 CC C C2643  C1C          STO    T2
C1C57  05C0 CC 1 4C166  C1C          CLA    ZSB,1
01C60  03CC CC C C2677  C1C          FAD    DELTA
01C61  06C1 CC C C2661  C1C          STO    ZTEMP
01C62  0C74 CC 4 C1726  C1C          TSX    PCTNTL,4
01C63  3 CCCCC C 2145C  C1C          PAR    RZA
01C64  3 CCCCC C 26355  C1C          PAR    ZZA
01C65  C6C1 CC C C2642  C1C          STO    T1
01C66  0C74 CC 4 C1726  C1C          TSX    PCTNTL,4
C1C67  3 CCCCC C C7636  C1C          PAR    RSA
C107C  3 CCCCC C 14543  C1C          PAR    ZSA
01071  03C2 CC C C2642  C1C          FSB    T1
01C72  03C2 CC C C2643  C1C          FSB    T2
C1C73  0241 CC C C2677  C1C          FDP    DELTA
C1C74  C26C CC C 52177  C1C          FMP    =.C397EE7
01C75  C76C CC C CC0C2  CC           CHS
C1C76  03C0 CC 1 4C166  C1C          FAD    ZSB,1
C1C77  06C1 CC C C2667  C1C          STO    ZGP
011CC  056C CC 1 33262  C1C          LDQ    RSB,1
011C1  C260 CC 1 33262  C1C          FMP    RSB,1
011C2  0601 CC C C2642  C1C          STO    T1
011C3  0560 CC 1 4C166  C1C          LDQ    ZSB,1
011C4  C260 CC 1 40166  C1C          FMP    ZSB,1
011C5  03CC CC C C2642  C1C          FAD    T1
C11C6  C6C1 CC C C2642  C1C          STO    T1
C11C7  0131 CC C CCCCC  CC           XCA
C111C  C26C CC C C2642  C1C          FMP    T1
C1111  06C1 CC C C2643  C1C          STO    T2
C1112  0C74 CC 4 CCCC5  C1C          CALL   SQRT,T1
C1114  C241 CC C C2643  C1C          FDP    T2
01115  C26C CC C C27CC  C1C          FMP    K
```

```
01116   06C1 CC C C2642  C1C        STO    T1
01117   0131 CC C CC0CC  CC         XCA
0112C   C26C CC 1 33262  C1C        FMP    RSB,1
01121   03C0 CC C C2666  C1C        FAD    RGP
01122   06C1 CC 1 33261  C1C        STO    RSB-1,1
01123   C1CC CC C C1125  C1C        TZE    *+2
01124  -0120 CC C C122C  C1C        TMI    L23A
01125   0560 CC C C2642  C1C        LDQ    T1
01126   C26C CC 1 40166  C1C        FMP    ZSB,1
01127   C3CC CC C C2667  C1C        FAD    ZGP
0113C   03C2 CC C C2676  C1C        FSB    VCT
01131   06C1 CC 1 4C165  C1C        STO    ZSB-1,1
01132   C4C2 CC C C2701  C1C        SUB    ZMIN
C1133  -012C CC 0 C1217  C1C        TMI    L23
01134   05CC CC 1 33262  C1C        CLA    RSB,1
C1135  -C1CC CC C C1141  C1C        TNZ    *+4
01136   05CC CC 1 4C165  C1C        CLA    ZSB-1,1
01137   C3C2 CC 1 4C166  C1C        FSB    ZSB,1
C114C   012C CC C C1217  C1C        TPL    L23
C1141   0560 CC 1 33261  C1C        LDQ    RSB-1,1
01142   0260 CC 1 33261  C1C        FMP    RSB-1,1
01143   C601 CC C C2711  C1C        STO    TEMP
C1144   C560 CC 1 4C165  C1C        LDQ    ZSB-1,1
C1145   0260 CC 1 40165  C1C        FMP    ZSB-1,1
01146   03CC CC C C2711  C1C        FAD    TEMP
C1147   C4C2 CC C C2674  C1C        SUB    A2
01150  -0120 CC C C1217  C1C        TMI    L23
01151   05C0 CC 1 4C166  C1C        CLA    ZSB,1
01152   03C2 CC 1 4C165  C1C        FSB    ZSB-1,1
01153   06C1 CC C C2711  C1C        STO    TEMP
01154   05CC CC 1 33262  C1C        CLA    RSB,1
01155   03C2 CC 1 33261  C1C        FSB    RSB-1,1
01156   0241 CC C C2711  C1C        FCP    TEMP
01157  -C600 CC C C2726  C1C        STQ    B
0116C   0260 CC C C2726  C1C        FMP    B
C1161   06C1 CC C C2727  C1C        STO    B2
C1162   0560 CC 1 4C166  C1C        LDQ    ZSB,1
01163   C260 CC C C2726  C1C        FMP    B
C1164   03C2 CC 1 33262  C1C        FSB    RSB,1
C1165   06C1 CC C C2730  C1C        STO    B1
01166   0131 CC C CC0CC  C0         XCA
01167   C260 CC C C273C  C1C        FMP    B1
C117C   06C1 CC C C2731  C1C        STO    B12
C1171   03C2 CC C C2674  C1C        FSB    A2
01172   0241 CC C C2731  C1C        FCP    B12
01173  -C6C0 CC C C2711  C1C        STQ    TEMP
C1174   C5C0 CC C 522C2  C1C        CLA    =1.
01175   C241 CC C C2727  C1C        FCP    B2
01176   0131 CC C CC0CC  CC         XCA
C1177   03C0 CC C 522C2  C1C        FAD    =1.
012CC   0131 CC C CC0CC  CC         XCA
012C1   C26C CC C C2711  C1C        FMP    TEMP
012C2   04C2 CC 0 522C2  C1C        SUB    =1.
012C3   C1CC CC C C1217  C1C        TZE    L23
012C4   0120 CC C C121C  C1C        TPL    L22B
C12C5   056C CC 1 4C166  C1C        LDQ    ZSB,1
012C6   C26C CC 1 4C165  C1C        FMP    ZSB-1,1
012C7  -C12C CC C C1217  C1C        TMI    L23
```

```
0121C  1 CCCC1 1 C1211  C1C  L22B   TXI    *+1,1,1
01211  0774 CC 4 CCCCC  CC   L22C   AXT    **,4          **=INTERMEDIATE IMAXSB
C1212  1 CCCC1 4 C1213  C1C         TXI    *+1,4,1
C1213  0634 CC 4 C1211  C1C         SXA    L22C,4
01214  C634 CC 4 C1221  C1C         SXA    L23B,4
C1215 -3 CCCCC 4 CC767  C1C  S14    TXL    L22,4,**      **=NMAX-1
C1216  CC2C CC C C1222  C1C         TRA    L23C
01217  C6CC CC 1 40165  C1C  L23    STZ    ZSB-1,1
C122C  C6CC CC 1 33261  C1C  L23A   STZ    RSB-1,1
C1221  C774 CC 4 CCCCC  CC   L23B   AXT    **,4          **=INTERMEDIATE IMAXSB
C1222 -3 CCCCC 4 C1224  C1C  L23C   TXL    *+2,4,**      **=IMAXSB
01223 -0634 CO 4 C1222  C1C         SXD    L23C,4
01224  1 CCCCC 2 C1225  C1O  S1C    TXI    *+1,2,**      **=NMAX
01225 -3 CCCCC 2 CC755  C1C  L24    TXL    L2CC,2,**     **=NMAX*(NUM-1)
C1226 -3 CCCCC 2 CC762  C1C  L24A   TXL    L21,2,**      **=NMAX*NUM
01227 -C534 CC 2 C1222  C1C         LXD    L23C,2
C123C -0534 CC 4 C1222  C1C         LXD    L23C,4
C1231  3 CCCCO 4 C1233  C1C  L24AA  TXH    *+2,4,**      **=PREVICUS IMAXSB
C1232 -0534 CC 4 C1231  C1C         LXD    L24AA,4
01233  0634 CC 4 C1535  C1C         SXA    L24B,4
01234  C634 CO 4 C1573  C1C         SXA    L25,4
                                    MICCLE
C1235  0754 CC 4 CCOCC  CC          PXA    ,4
01236 -C76C CC C CCOC3  CC          SSM
C1237  C4CO CC C C272C  C1C         ACD    NMAX
O124C  0734 CC 4 CCCCC  CC          PAX    ,4
C1241 -0634 CO 4 C1546  C1C         SXD    L24D,4
01242  1 CCCCO 4 C1243  C1C  S19    TXI    *+1,4,**      **=3*NMAX
C1243 -U634 CC 4 C1644  C1C         SXD    L27,4
C1244 -0634 CC 2 C1231  C1C         SXD    L24AA,2
C1245  C774 CC 2 CCOO1  CC          AXT    1,2
01246  05CC CO 2 CCOCO  CC   L3CC   CLA    **,2          **=RZB-NMAX
C1247  03C2 CC 2 45C72  C1C         FSB    RZB,2
C125C  C131 CC C CCCCC  CC          XCA
01251  026C CC C C27C3  C1C         FMP    H
01252  06C1 CC C C2677  C1C         STO    DELTA
01253  0754 CC 2 CCCCC  CO   L31    PXA    ,2
01254  0734 CC 1 CCCCO  CC          PAX    ,1
01255  C774 CC 4 CCCO1  CC          AXT    1,4
01256  C634 CO 4 C15CC  C1C         SXA    L32C,4
01257  C634 CC 4 C151C  C1C         SXA    L33B,4
C126C -052C CC C C2641  C1C  L32    NZT    PSW
C1261  CC74 CC 4 CCOO4  C1C         CALL   DAYTIM
C1262  C6C1 CC C C264C  C1C         STC    X2
01263  CC74 CC 4 CCCC3  C1C         PRINT  F1
C1265 -1 CCCCC 1 45C72  C1C         ICP    RZB,1
C1266 -1 CCCCC 1 51776  C1C         ICP    ZZB,1
C1267 -1 CCCCC C C2640  C1C         ICP    X2
0127C -1 CCCCC C CCCCC  CC          ENDIO
C1271  O5CC CC 1 45C72  C1C  L32.1  CLA    RZB,1
C1272  C1CC CC C C1327  C1C         TZE    L32.2
C1273  C3C2 CC C C2677  C1C         FSB    DELTA
C1274  O6C2 CC C C266C  C1C         SLW    RTEMP
C1275  O5CO CC 1 51776  C1C         CLA    ZZB,1
C1276  O6C1 CC C C2661  C1C         STO    ZTEMP
O1277  CC74 CO 4 C1726  C1C         TSX    PCTNTL,4
C13CC  3 CCCCC C 2145C  C1C         PAR    RZA
C13C1  3 CCCCC C 26355  C1C         PAR    ZZA
```

```
C13C2  06C1 CC C C2642  C1C          STO    T1
C13C3  0C74 CC 4 C1726  C1C          TSX    PCTNTL,4
C13C4  3 CCCCC C C7636  C1C          PAR    RSA
C13C5  3 CCCCC C 14543  C1C          PAR    ZSA
013C6  03C2 CC C C2642  C1C          FSB    T1
C13C7  C6C1 CC C C2643  C1C          STO    T2
0131C  C5CC CC 1 45C72  C1C          CLA    RZB,1
C1311  C3CC CC C C2677  C1C          FAD    DELTA
01312  06C1 CC C C2660  C1C          STO    RTEMP
C1313  CC74 CC 4 C1726  C1C          TSX    PCTNTL,4
01314  3 CCCCC 0 2145C  C1C          PAR    RZA
01315  3 CCCCC C 26355  C1C          PAR    ZZA
01316  06C1 CC C C2642  C1C          STO    T1
01317  CC74 CC 4 C1726  C1C          TSX    PCTNTL,4
0132C  3 CCCCC C C7636  C1C          PAR    RSA
01321  3 CCCCC C 14543  C1C          PAR    ZSA
C1322  03C2 CC C C2642  C1C          FSB    T1
01323  03C2 CC C C2643  C1C          FSB    T2
01324  C241 CC C C2677  C1C          FDP    DELTA
C1325  0260 CC C 52177  C1C          FMP    =.C397EE7
C1326  C3CC CC 1 45C72  C1C          FAD    RZB,1
01327  06C1 CC C C2666  C1C   L32.2  STO    RGP
C1330  05CC CC 1 45C72  C1C          CLA    RZB,1
01331  C6C1 CC C C266C  C1C          STO    RTEMP
C1332  05C0 CC 1 51776  C1C          CLA    ZZB,1
01333  C3C2 CC C C2677  C1C          FSB    DELTA
C1334  06C1 CC C C2661  C1C          STO    ZTEMP
01335  0C74 CC 4 C1726  C1C          TSX    PCTNTL,4
C1336  3 CCCCC C 2145C  C1C          PAR    RZA
01337  3 CCCCC C 26355  C1C          PAR    ZZA
C1340  C6C1 CC C C2642  C1C          STO    T1
C1341  CC74 CC 4 C1726  C1C          TSX    PCTNTL,4
C1342  3 CCCCC C C7636  C1C          PAR    RSA
C1343  3 CCCCC C 14543  C1C          PAR    ZSA
01344  03C2 CO C C2642  C1C          FSB    T1
C1345  06C1 CC C C2643  C1C          STO    T2
C1346  05C0 CC 1 51776  C1C          CLA    ZZB,1
C1347  03CC CC C C2677  C1C          FAD    DELTA
0135C  06C1 CC C C2661  C1C          STO    ZTEMP
C1351  0C74 CC 4 C1726  C1C          TSX    PCTNTL,4
C1352  3 CCCCC C 2145C  C1C          PAR    RZA
C1353  3 CCCCC C 26355  C1C          PAR    ZZA
01354  C6C1 CC C C2642  C1C          STO    T1
01355  CC74 CC 4 C1726  C1C          TSX    PCTNTL,4
C1356  3 CCCCC C C7636  C1C          PAR    RSA
01357  3 CCCCC C 14543  C1C          PAR    ZSA
0136C  03C2 CC C C2642  C1C          FSB    T1
C1361  03C2 CC C C2643  C1C          FSB    T2
C1362  0241 CC C C2677  C1C          FDP    DELTA
01363  0260 CC 0 52177  C1C          FMP    =.C397EE7
C1364  03CC CC 1 51776  C1C          FAD    ZZB,1
C1365  C6C1 CC C C2667  C1C          STO    ZGP
C1366  0560 CC 1 45C72  C1C          LDQ    RZB,1
C1367  026C CC 1 45C72  C1C          FMP    RZB,1
C1370  C601 CC C C2642  C1C          STO    T1
C1371  0560 CC 1 51776  C1C          LDQ    ZZB,1
C1372  026C CC 1 51776  C1C          FMP    ZZB,1
C1373  03CC CC C C2642  C1C          FAD    T1
```

```
01374  06C1 CC C C2642  C1C      STO   T1
C1375  C131 CC C CCCCC  CC       XCA
01376  026C CC C C2642  C1C      FMP   T1
C1377  06C1 CC C C2643  C1C      STO   T2
014CC  0C74 CC 4 CCCC5  C1C      CALL  SQRT,T1
014C2  0241 CC C C2643  C1C      FDP   T2
014C3  C26C CC C C27CC  C1C      FMP   K
C14C4  0601 CC C C2642  C1C      STO   T1
014C5  0131 CC C CCCC0  CC       XCA
C14C6  0260 CC 1 45C72  C1C      FMP   RZB,1
014C7  C76C CC C CCCC2  CC       CHS
C141C  03CC CC C C2666  C1C      FAD   RGP
C1411  06C1 CC 1 45C71  C1C      STO   RZB-1,1
01412 -C12C CC C C15C7  C1C      TMI   L33A
C1413  0560 CC C C2642  C1C      LDQ   T1
C1414  026C CC 1 51776  C1C      FMP   ZZB,1
C1415  076C CC C CC0C2  CC       CHS
01416  C3CC CC C C2667  C1C      FAD   ZGP
C1417  03C2 CC C C2676  C1C      FSB   VCT
C142C  0601 CC 1 51775  C1C      STO   ZZB-1,1
C1421  04C2 CC C C2701  C1C      SUB   ZMIN
01422 -C12C CC C C15C6  C1C      TMI   L33
C1423  05C0 CC 1 45C72  C1C      CLA   RZB,1
C1424 -01CC CC C C1430  C1C      TNZ   *+4
01425  05CC CC 1 51775  C1C      CLA   ZZB-1,1
01426  03C2 CC 1 51776  C1C      FSB   ZZB,1
C1427  012C CC C C15C6  C1C      TPL   L33
C143C  0560 CC 1 45C71  C1C      LDQ   RZB-1,1
01431  C260 CC 1 45C71  C1C      FMP   RZB-1,1
01432  06C1 CC C C2711  C10      STO   TEMP
C1433  0560 CC 1 51775  C1C      LDQ   ZZB-1,1
C1434  0260 CC 1 51775  C1C      FMP   ZZB-1,1
01435  C3CC CC C C2711  C1C      FAD   TEMP
01436  04C2 CC C C2674  C1C      SUB   A2
C1437 -C12C CC C C15C6  C1C      TMI   L33
C144C  05CC CC 1 51776  C1C      CLA   ZZB,1
C1441  03C2 CC 1 51775  C1C      FSB   ZZB-1,1
C1442  0601 CC C C2711  C1C      STO   TEMP
C1443  05C0 CC 1 45C72  C1C      CLA   RZB,1
C1444  03C2 CC 1 45C71  C1C      FSB   RZB-1,1
01445  0241 CC C C2711  C1C      FDP   TEMP
01446 -C6CC CC C C2726  C1C      STQ   B
C1447  C260 CC C C2726  C1C      FMP   B
C1450  06C1 CC C C2727  C1C      STO   B2
C1451  C560 CC 1 51776  C1C      LDQ   ZZB,1
01452  C260 CC C C2726  C1C      FMP   B
01453  03C2 CC 1 45C72  C1C      FSB   RZB,1
01454  C6C1 CC C C2730  C1C      STO   B1
01455  0131 CC C CC0C0  CC       XCA
C1456  C260 CC C C273C  C1C      FMP   B1
01457  06C1 CC C C2731  C1C      STO   B12
01460  03C2 CC C C2674  C1C      FSB   A2
C1461  C241 CC C C2731  C1C      FDP   B12
01462 -C6C0 CC C C2711  C1C      STQ   TEMP
C1463  C5C0 CC C 522C2  C1C      CLA   =1.
C1464  C241 CC C C2727  C1C      FDP   B2
C1465  0131 CC C CCCCC  CC       XCA
01466  C3C0 CC C 522C2  C1C      FAD   =1.
```

```
01467  C131 CC C CCCCC  CC           XCA
C147C  0260 CC C C2711  C1C          FMP    TEMP
C1471  04C2 CC C 522C2  C1C          SUB    =1.
01472  01CC CC C C1506  C1C          TZE    L33
01473  C120 CC C C1477  C1C          TPL    L32B
01474  C560 CC 1 51776  C1C          LDQ    ZZB,1
C1475  C260 CC 1 51775  C1C          FMP    ZZB-1,1
01476 -C12C CC 0 C15C6  C1C          TMI    L33
01477  1 CCCC1 1 C15CC  C1C   L32B   TXI    *+1,1,1
015CC  0774 CC 4 CCCCC  CO    L32C   AXT    **,4          **=INTERMEDIATE IMAXZB
C15C1  1 CCCC1 4 C15C2  C1C          TXI    *+1,4,1
015C2  C634 CC 4 015C0  C1C          SXA    L32C,4
015C3  0634 CO 4 C151C  C1C          SXA    L33B,4
C15C4 -3 CCCCC 4 C1260  C1C   S15    TXL    L32,4,**      **=NMAX-1
C15C5  0C2C CC C C1511  C1C          TRA    L33C
01506  06CC CC 1 51775  C1C   L33    STZ    ZZB-1,1
015C7  C6CC CC 1 45C71  C1C   L33A   STZ    RZB-1,1
0151C  0774 CO 4 CCCCC  CO    L33B   AXT    **,4          **=INTERMEDIATE IMAXZB
C1511 -3 CCCC0 4 C1513  C1C   L33C   TXL    *+2,4,**      **=IMAXZB
01512 -C634 CO 4 C1511  C1C          SXD    L33C,4
01513  1 CCCCO 2 C1514  C1C   S31    TXI    *+1,2,**      **=NMAX
01514 -3 CCCCO 2 C1246  C1C   L34    TXL    L3CC,2,**     **=NMAX*(NUM-1)
C1515 -3 CCCCC 2 01253  C1C   L34A   TXL    L31,2,**      **=NMAX*NUM
01516 -0534 CO 2 C1511  C1C          LXD    L33C,2
01517 -C534 CO 4 C1511  C1C          LXD    L33C,4
0152C  3 CCCCO 4 C1522  C1C   L34AA  TXH    *+2,4,**      **=PREVICUS IMAXZB
C1521 -0534 CC 4 C152C  C1C          LXD    L34AA,4
01522  0634 CO 4 01551  C1C          SXA    L34B,4
01523  0634 CO 4 C1652  C1C          SXA    L35,4
01524  0754 CC 4 CCCCO  CC           PXA    ,4
C1525 -C760 CC C CCOC3  CC           SSM
01526  04CC CC C C2720  C1C          ACD    NMAX
01527  0734 CO 4 CCCCC  CO           PAX    ,4
0153C -C634 CC 4 C1562  C1C          SXD    L34C,4
01531  1 CCCCO 4 C1532  C1C   S2C    TXI    *+1,4,**      **=3*NMAX
01532 -0634 CC 4 C1723  C1C          SXD    L37,4
C1533 -0634 CC 2 C152C  C1C          SXD    L34AA,2
01534  C774 CC 2 CC001  CC           AXT    1,2
01535  C774 CC 1 CCOCC  CC    L24B   AXT    **,1          **=MAXIMUM IMAXSB
01536  05CC CC 2 33262  C1C   L24C   CLA    RSB,2         SHIFT NEW
01537  06C1 CC 2 C7636  C1C          STO    RSA,2         SIGMA
C1540  0600 CC 2 33262  C1C          STZ    RSB,2         TRAJECTCRIES
C1541  05CO CC 2 40166  C1C          CLA    ZSB,2         TC A
01542  06C1 CC 2 14543  C1C          STO    ZSA,2         MATRICES
01543  06CO CC 2 4C166  C1C          STZ    ZSB,2
C1544  1 CCCC1 2 C1545  C1C          TXI    *+1,2,1
01545  2 CCCC1 1 C1536  C1C          TIX    L24C,1,1
01546  1 CCCCO 2 C1547  C1C   L24C   TXI    *+1,2,**      **=NMAX-(MAXUMUM IMAXSB)
01547 -3 CCCCC 2 C1535  C1C   L24E   TXL    L24B,2,**     **=NMAX*NUM
0155C  0774 CC 2 CCCO1  CC           AXT    1,2
01551  0774 CC 1 CCOCO  CC    L34B   AXT    **,1          **=MAXIMUM IMAXZB
01552  05CO CC 2 45C72  C1C   L34C   CLA    RZB,2
01553  06C1 CC 2 21450  C1C          STO    RZA,2
01554  06CC CC 2 45C72  C1C          STZ    RZB,2
01555  05CO CC 2 51776  C1C          CLA    ZZB,2
01556  C6C1 CC 2 26355  C1C          STO    ZZA,2
01557  C6CO CC 2 51776  C1C          STZ    ZZB,2
0156C  1 CCCC1 2 C1561  C1C          TXI    *+1,2,1
```

```
01561  2 CCCC1 1 C1552  C1C         TIX    L34C,1,1
C1562  1 CCCCC 2 C1563  C1C   L34C  TXI    **+1,2,**      **=NMAX-(MAXIMUM IMAXZB)
01563 -3 CCCC0 2 C1551  C1C   L34E  TXL    L34B,2,**      **=NMAX*NUM
01564  05C0 CC C C2714  C1C         CLA    CCUNT
C1565  04CC CC C 52206  C1C         ACD    =1
C1566  06C1 CC C 02714  C1C         STO    CCUNT
01567  05C0 CC 0 52204  C1C         CLA    =4
0157C  06C1 CC C C2723  C1C         STC    VAR
01571  0774 CC 2 CCC01  CC          AXT    1,2
C1572  C6CC CC C 02724  C1C         STZ    P
01573  0774 CC 1 CCOCC  CO    L25   AXT    **,1           **=MAXIMUM IMAXSB
01574  C5C0 CC C C2724  C1C         CLA    P
01575  04CC CC C 52206  C1C         ACD    =1
01576  06C1 CC C C2724  C1C         STO    P
01577  0774 CO 4 CCCCC  CC    L25A  AXT    **,4           **=SIGMA TRAJECTORIES STILL TC BE PRINTED
C16CC  2 CCCC4 4 C1602  C1C         TIX    *+2,4,4
016C1  0634 CC 4 C2723  C1C         SXA    VAR,4
01602  0634 CC 4 C1577  C1C         SXA    L25A,4
01603  CC74 CO 4 CC003  C1C         PRINT  FVAR,...,FCLT3,CCUNT,P,TP,V,PHI,DELTAT,A,H,ZMIN
01616  05C0 CC 0 C2723  C1C         CLA    VAR
01617  01C0 CC C C1641  C1C         TZE    L27-3
01620 -1 CCCCC 2 07636  C1C   L26   IOP    RSA,2
C1621 -1 CCCC0 2 14543  C1C         ICP    ZSA,2
01622  05C0 CC C C2723  C1C         CLA    VAR
C1623  04C2 CC 0 52206  C1C         SUB    =1
01624  01CC CC C C1641  C1C         TZE    L27-3
01625 -1 CCCC0 2 CC000  CO    S27   ICP    **,2           **=RSA-NMAX
01626 -1 CCCCC 2 CCC00  CO          IOP    **,2           **=ZSA-NMAX
C1627  05CC CC C C2723  C1C         CLA    VAR
C1630  04C2 CC C 52201  C1C         SUB    =2
01631  01CC CC 0 C1641  C1C         TZE    L27-3
01632 -1 CCCCC 2 CCCCC  CC    S27A  IOP    **,2           $*=RZA-2*NMAX
C1633 -1 CCCCC 2 CCCCC  CC          ICP    **,2           **=ZSA-2*NMAX
01634  C5C0 CC C C2723  C1C         CLA    VAR
01635  04C2 CC C 522C5  C1C         SUB    =3
C1636  01CC CC C C1641  C1C         TZE    L27-3
C1637 -1 CCCCC 2 CCCCC  CC    S27B  ICP    **,2           **=RSA-3*NMAX
01640 -1 CCCCC 2 CCCC0  CC          ICP    **,2           **=ZSA-3*NMAX
01641  1 CCCC1 2 C1642  C1C         TXI    *+1,2,1
C1642  2 CCCC1 1 C162C  C1C         TIX    L26,1,1
C1643 -1 CCCCC C CCOCC  CC          ENDIO
01644  1 CCCCC 2 01645  C1C   L27   TXI    **+1,2,**      **=4*NMAX-(MAXIMUM IMAXSB)
01645 -3 CCCCC 2 C1573  C1C   L28   TXL    L25,2,**       **=NMAX*NUM
C1646  05CC CC C 52204  C1C         CLA    =4
C1647  0601 CC C C2723  C1C         STO    VAR
0165C  0774 CC 2 CC001  CC          AXT    1,2
01651  06CC CC C C2724  C1C         STZ    P
01652  0774 CC 1 CCCCC  CC    L35   AXT    **,1           **=MAXIMUM IMAXZB
01653  05CC CC C C2724  C1C         CLA    P
01654  04CC CC 0 522C6  C1C         ACD    =1
01655  06C1 CC C C2724  C1C         STO    P
01656  0774 CC 4 CCCC0  CO    L35A  AXT    **,4           **=ZETA TRAJECTCRIES STILL TC BE PRINTED
C1657  2 CCCC4 4 C1661  C1C         TIX    *+2,4,4
0166C  C634 CO 4 C2723  C1C         SXA    VAR,4
01661  C634 CC 4 C1656  C1C         SXA    L35A,4
C1662  CC74 CC 4 CCCC3  C1C         PRINT  FVAR,...,FCLT4,CCUNT,P,TP,V,PHI,DELTAT,A,H,ZMIN
C1675  05CC CC C C2723  C1C         CLA    VAR
01676  C1CC CC O C172C  C1C         TZE    L37-3
```

```
C1677 -1 CCCCC 2 2145C  C1C   L36     ICP      RZA,2
C17CC -1 CCCCC 2 26355  C1C           ICP      ZZA,2
C17C1   C5CC CC C C2723  C1C           CLA      VAR
C17C2   04C2 CC C 52206  C1C           SUB      =1
C17C3   C1CC CC C C1720  C1C           TZE      L37-3
017C4 -1 CCCCC 2 CCCCC  CC    S28     ICP      **,2
017C5 -1 CCCCC 2 CCCCC  CC            IOP      **,2
C17C6   05CC CC C C2723  C1C           CLA      VAR
017C7   04C2 CC 0 52201  C1C           SUB      =2
0171C   C1CC CC 0 CJ720  C1C           TZE      L37-3
C1711 -1 CCCCC 2 CCCC0  CO    S28A    IOP      **,2
C1712 -1 CCCCC 2 CCCC0  CC            ICP      **,2
C1713   05C0 CC C C2723  C1C           CLA      VAR
C1714   04C2 CC 0 522C5  C1C           SUB      =3
C1715   C1C0 CC C C172C  C1C           TZE      L37-3
C1716 -1 CCCCC 2 CC0CC  CC    S28B    ICP      **,2
01717 -1 CCCCC 2 CC000  CO            ICP      **,2
0172C   1 CCCC1 2 C1721  C1C           TXI      *+1,2,1
C1721   2 CCCC1 1 C1677  C1C           TIX      L36,1,1
C1722 -1 CCCCC C CC00C  CC            ENDIO
C1723   1 CCCCC 2 C1724  C1C   L37     TXI      *+1,2,**       **=4*NMAX-(MAXIMUM IMAXZB)
C1724 -3 CCCC0 2 C1652  C1C   L38     TXL      L35,2,**       **=NMAX*NUM
C1725   0C20 CC C CC7C0  C1C           TRA      L2C
C1726   0634 CC 4 C2064  C1C   PCTNTL  SXA      LL18,4         SAVE
C1727   0634 C0 1 C2065  C1C           SXA      LL19,1         INDEX
C173C   0634 CC 2 C2066  C1C           SXA      LL2C,2         REGISTERS
C1731   05C0 CC 4 CC0C1  CC            CLA      1,4            TRANSFER
C1732   0621 CC C C1754  C1C           STA      LL6            ARGUMENTS
01733   0621 CC C C2045  C1C           STA      LL14
01734   05C0 C0 4 CC0C2  C0            CLA      2,4
C1735   0621 CC C C1756  C1C           STA      LL7
C1736   0621 CC C C2047  C1C           STA      LL15
C1737   0774 CC 2 CC0C1  C0            AXT      1,2
0174C   0634 CC 2 C1747  C1C           SXA      LL2,2
C1741   0634 CC 2 C2C51  C1C           SXA      LL16,2
C1742   C6CC CC C C2652  C1C           STZ      TT7
01743   0754 C0 2 CC0CC  C0    LL1     PXA      ,2
01744   0734 C0 1 CCCCC  C0            PAX      ,1
C1745   06CC CC C C2647  C1C           STZ      TT4
C1746   C6CC CC 0 C2715  C1C           STZ      CCUNT2
01747   0774 CC 2 CC0CC  C0    LL2     AXT      **,2           **=1ST VEC SUBSCRIPT CN CURRENT TRAJECTORY
0175C   05C0 CC 2 52166  C1C   LL4     CLA      VEC,2
C1751   C6C1 CC C C2644  C1C           STO      TT1
C1752   1 CCCC1 2 C1753  C1C           TXI      *+1,2,1
01753   0634 CC 2 C1747  C1C           SXA      LL2,2
01754   05CC CC 1 CCCCC  CC    LL6     CLA      **,1
C1755   06C1 CC C C2662  C1C           STO      TEMPR
01756   05CC CC 1 CC0CC  CC    LL7     CLA      **,1
01757   C6C1 CC 0 C2663  C1C           STO      TEMPZ
0176C   1 77777 1 C1761  C1C           TXI      *+1,1,-1
01761   0522 CC C C1754  C1C           XEC      LL6
01762   C6C1 CC C C2664  C1C           STO      TEMPRR
C1763   0522 CC C C1756  C1C           XEC      LL7
01764   0601 CC C C2665  C1C           STC      TEMPZZ
C1765   CC74 C0 4 C2C7C  C1C           TSX      PCNT,4
C1766   03CC CC C C2647  C1C           FAD      TT4
C1767   C6C1 CC 0 C2647  C1C           STO      TT4
0177C   C56C CC C C2664  C1C           LDQ      TEMPRR
```

```
01771  0260 00 0 02664  010          FMP    TEMPRR
01772  0601 00 0 02656  010          STO    TT20
01773  0560 00 0 02665  010          LDQ    TEMPZZ
01774  0260 00 0 02665  010          FMP    TEMPZZ
01775  0300 00 0 02656  010          FAD    TT20
01776  0601 00 0 02656  010          STO    TT20
01777  0500 00 0 02674  010          CLA    A2
02000  0241 00 0 02656  010          FDP    TT20
02001 -0600 00 0 02656  010          STQ    TT20
02002  0260 00 0 02665  010          FMP    TEMPZZ
02003  0601 00 0 02665  010          STO    TEMPZZ
02004  0560 00 0 02656  010          LDQ    TT20
02005  0260 00 0 02664  010          FMP    TEMPRR
02006  0601 00 0 02664  010          STO    TEMPRR
02007  0560 00 0 02662  010    S32   LDQ    TEMPR
02010  0260 00 0 02662  010          FMP    TEMPR
02011  0601 00 0 02656  010          STO    TT20
02012  0560 00 0 02663  010          LDQ    TEMPZ
02013  0260 00 0 02663  010          FMP    TEMPZ
02014  0300 00 0 02656  010          FAD    TT20
02015  0601 00 0 02656  010          STO    TT20
02016  0500 00 0 02674  010          CLA    A2
02017  0241 00 0 02656  010          FDP    TT20
02020 -0600 00 0 02656  010          STQ    TT20
02021  0260 00 0 02662  010          FMP    TEMPR
02022  0601 00 0 02662  010          STO    TEMPR
02023  0560 00 0 02656  010          LDQ    TT20
02024  0260 00 0 02663  010          FMP    TEMPZ
02025  0601 00 0 02663  010          STO    TEMPZ
02026  0074 00 4 00005  010          CALL   SQRT,TT20
02030  0601 00 0 02656  010          STO    TT20
02031  0074 00 4 02070  010          TSX    PCNT,4
02032  0760 00 0 00002  00           CHS
02033  0131 00 0 00000  00           XCA
02034  0260 00 0 02656  010          FMP    TT20
02035  0300 00 0 02647  010          FAD    TT4
02036  0601 00 0 02647  010          STO    TT4
02037  0500 00 0 02715  010    S33   CLA    COUNT2
02040  0400 00 0 52206  010          ADD    =1
02041  0601 00 0 02715  010          STO    COUNT2
02042  0402 00 0 02720  010          SUB    NMAX
02043  0100 00 0 02051  010          TZE    LL16
02044  1 00002 1 02045  010          TXI    *+1,1,2
02045  0500 00 1 00000  00     LL14  CLA    **,1             **=RMTRX
02046 -0100 00 0 01754  010          TNZ    LL6
02047  0500 00 1 00000  00     LL15  CLA    **,1             **=ZMTRX
02050 -0100 00 0 01754  010          TNZ    LL6
02051  0774 00 2 00000  00     LL16  AXT    **,2             **=1ST MTRX SUBSCRIPT ON CURRENT TRAJECTORY
02052  1 00000 2 02053  010    S11   TXI    *+1,2,**         **=NMAX
02053  0634 00 2 02051  010          SXA    LL16,2
02054  0560 00 0 02644  010          LDQ    TT1
02055  0260 00 0 02647  010          FMP    TT4
02056  0300 00 0 02652  010          FAD    TT7
02057  0601 00 0 02652  010          STO    TT7
02060 -3 00000 2 01743  010    LL17  TXL    LL1,2,**         **=MAX*NUM
02061  0500 00 0 02652  010          CLA    TT7
02062  0241 00 0 52176  010          FDP    =2.
02063  0260 00 0 02676  010          FMP    VDT
```

```
02C64  0774 CC 4 CCCCC  CC   LL18   AXT   **,4          **=ACCRESS CCMPLEMENT FOR TSX TO POTNTL
C2C65  C774 CC 1 CC000  CC   LL19   AXT   **,1          **=CCNTENTS CF XR1 BEFORE TSX TO POTNTL
02066  C774 CC 2 CC00C  CO   LL20   AXT   **,2          **=CCNTENTS CF XR2 BEFCRE TSX TO POTNTL
02C67  CC20 CO 4 CCCC3  CO          TRA   3,4
02C7C  0634 CC 4 C2260  C1C  PCNT   SXA   RET,4
02071  05C0 CC C C2660  C1C         CLA   RTEMP
02C72  0302 CC 0 C2662  C1C         FSB   TEMPR
02C73  06C1 CC 0 C2646  C10         STO   TT3
02C74  0131 CC C CCC0C  CC          XCA
02C75  0260 CC C C2646  C1C         FMP   TT3
02C76  0601 CO C C2646  C1C         STO   TT3
02C77  05C0 CC C C2661  C1C         CLA   ZTEMP
021CC  03C2 CC C C2663  C1C         FSB   TEMPZ
021C1  06C1 CC C C2645  C1C         STO   TT2
021C2  0131 CC C CC000  CO          XCA
021C3  0260 CC C C2645  C1C         FMP   TT2
C21C4  03CC CC C C2646  C1C         FAD   TT3
02105  0601 CC C 02646  C1C         STO   TT3
02106  04C2 CC 0 C2675  C1C         SUB   V2
021C7  C120 CC C C2131  C1C         TPL   LL2CA
0211C  05C0 CC C C2664  C1C         CLA   TEMPRR
02111  03C2 CC C C2662  C1C         FSB   TEMPR
02112  06C1 CC C 02645  C10         STO   TT2
02113  0131 CC C CCCCC  CO          XCA
C2114  0260 CC C C2645  C1C         FMP   TT2
02115  0601 CC C C2645  C1C         STO   TT2
02116  05CC CC C 02665  C1C         CLA   TEMPZZ
02117  03C2 CO C C2663  C1C         FSB   TEMPZ
C2120  0601 CC C C27C2  C1C         STO   ALP
02121  0131 CC C CC0CC  CC          XCA
02122  0260 CC C C27C2  C1C         FMP   ALP
02123  03C0 CC C C2645  C1C         FAD   TT2
02124  0241 CC C 52175  C1C         FDP   =3.1415927
02125  0131 CC C CC00C  CO          XCA
02126  0601 CC C C2645  C1C         STO   TT2
02127  04C2 CC C C2646  C1C         SUB   TT3
C213C  0120 CC C C2141  C1C         TPL   LL12
02131  05CC CC C 02660  C1C  LL2CA  CLA   RTEMP         NCRMAL
02132  0241 CC 0 52174  C10         FCP   =.5           PCTENTIAL
02133  0260 CC 0 C2662  C1C         FMP   TEMPR         CALCULATICN
02134  0601 CC C C2713  C1C         STO   CAPB
02135  03CC CC 0 C2646  C10         FAD   TT3
02136  0601 CC C C2712  C10         STO   CAPA
02137  C074 CC 4 C2262  C1C         TSX   INPCNT,4
C214C  CC20 CC C C2260  C1C         TRA   RET
02141  0C74 CO 4 CC005  C10  LL12   CALL  SQRT,TT2      CALCLLATICN
02143  06C1 CC 0 C265C  C1C         STO   TT5           FCR PCINTS
C2144  C600 CC C C2655  C1C         STZ   TT1C
02145  05CC CC C C2662  C1C         CLA   TEMPR
02146  0241 CC 0 C265C  C1C         FCP   TT5
02147  0260 CC C 52175  C1C         FMP   =3.1415927    SPHERE CF
0215C -C3C0 CC C 52173  C1C         UFA   =K233K9       EXCLUSICN
C2151  06C1 CC C C2653  C1C         STO   TT8
02152  0322 CC 0 52173  C1C         ERA   =K233K9
02153  04C2 CC 0 522C6  C10         SUB   =1
02154  034C CC C 522C6  C1C         CAS   =1
C2155  0C20 CC C C2162  C1C         TRA   *+5
02156  CC20 CC 0 C2157  C1C         TRA   *+1
```

```
02157  05C0 CC 0 52202  C1C         CLA   =1.
J2160  06C1 CC 0 02653  C10         STO   TT8
02161  0C20 C0 C C2223  C1C         TRA   SS2+4
C2162  06C1 CC C C2654  C1C         STO   TT9
02163  05C0 CC 0 C2653  C1C         CLA   TT8
02164  C300 CC 0 52173  C10         FAD   =K233K9
02165  0601 CC C C2653  C1C         STO   TT8
02166  05C0 CC 0 52172  C1C         CLA   =6.2831853
02167  0241 CC C C2653  C1C         FDP   TT8
C2170 -06C0 C0 C C2706  C10         STQ   DPHI
02171  0131 CC C CC000  C0          XCA
02172  0601 CC C C2705  C1C   SS3   STO   PHIN
02173  0C74 CC 4 CC006  C1C         CALL  COS,PHIN
02175  0760 CC C CC002  C0          CHS
02176  03C0 CC C 52202  C10         FAD   =1.
02177  0601 CC C C2657  C1C         STO   TT4C
C22CC  0074 CC 4 CC005  C10         CALL  SQRT,TT40
02202  0601 CC C C2657  C1C         STO   TT4C
022C3  05C0 CC C 522C2  C10         CLA   =1.
022C4  0241 CC C C2657  C1C         FDP   TT40
022C5  0131 C0 0 C00C0  C0          XCA
022C6  C3CC CC 0 C2655  C10         FAD   TT1C
022C7  0601 CC 0 C2655  C10         STO   TT1C
0221C  05C0 CC C C2654  C10         CLA   TT9
02211  04C2 CC 0 52206  C10         SUB   =1
02212  01C0 CC C C2217  C10         TZE   SS2
02213  0601 CC C C2654  C10         STO   TT9
C2214  05C0 CC C C2705  C1C         CLA   PHIN
02215  C3CC C0 0 C2706  C10         FAD   DPHI
02216  0C20 CC C C2172  C10         TRA   SS3
02217  0500 CC C C2655  C10   SS2   CLA   TT1C
0222C  0241 CC C C2662  C1C         FDP   TEMPR
02221  0260 CC 0 52171  C10         FMP   =.70711
02222  0601 CC C C2655  C10         STO   TT1C
02223  05C0 CC C 52170  C10         CLA   =1.5
02224  0241 CC 0 C2650  C1C         FDP   TT5
02225  0131 C0 0 CC000  C0          XCA
02226  0300 CC C C2655  C1C         FAD   TT1C
02227  0131 CC C CCCCC  CC          XCA
02230  0241 CC C C2653  C1C         FDP   TT8
02231  0260 CC 0 52167  C10         FMP   =6.2831853072
02232  0601 CC 0 C2655  C10         STO   TT1C
C2233  0074 CC 4 CC005  C1C         CALL  SQRT,TT3
02235  06C1 CC 0 C2646  C1C         STO   TT3
02236  C5C0 CC 0 C265C  C1C         CLA   TT5
C2237  0241 CC C C2646  C1C         FDP   TT3
0224C -06CC CC C C2646  C1C         STQ   TT3
02241  05CC CC C C2660  C1C         CLA   RTEMP
02242  03C2 CC 0 C2662  C10         FSB   TEMPR
02243  0131 CC C CCCCC  C0          XCA
02244  0260 CC C C2646  C1C         FMP   TT3
02245  0300 CC C C2662  C1C         FAD   TEMPR
02246  0241 CC 0 52174  C10         FDP   =.5
02247  C260 CC C C2662  C1C         FMP   TEMPR
0225C  0601 CC C C2713  C1C         STO   CAPB
02251  03CC CC C C2645  C1C         FAD   TT2
02252  0601 CC 0 C2712  C1C         STO   CAPA
02253  0C74 CC 4 C2262  C1C         TSX   INPCNT,4
```

```
02254  03C2 CC 0 C2655  C1C          FSB    TT1C
02255  0241 CC C C2646  C1C          FDP    TT3
02256  0131 CC C CCOCC  CC           XCA
02257  03CC CC 0 C2655  C1C          FAD    TT1C
0226C  0774 CC 4 CCCCC  CO    RET    AXT    **,4
C2261  CC20 CO 4 CCCC1  CO           TRA    1,4
02262  0634 CC 4 C2347  C1C   INPCNT SXA    LL29,4
02263  05CC CC C C2713  C1C          CLA    CAPB
02264  0241 CC C C2712  C10          FDP    CAPA
02265  0131 CC C CCOCO  CO           XCA
02266  06C2 CC C 027C2  C1C          SLW    ALP
                              NEST   MACRO  X
                                     LDQ    X+4
                                     FMP    M
                                     FAD    X+3
                                     XCA
                                     FMP    M
                                     FAD    X+2
                                     XCA
                                     FMP    M
                                     FAD    X+1
                                     XCA
                                     FMP    M
                                     FAD    X
                              NEST   END
02267  05CC CC C 52202  C1C          CLA    =1.
02270  03CC CC C C27C2  C1C          FAD    ALP
02271  C6C1 CO 0 C2711  C1C          STO    TEMP
02272  05C0 CC C 522C2  C1C          CLA    =1.
02273  03C2 CC C C27C2  C1C          FSB    ALP
C2274  0241 CC C C2711  C1C          FDP    TEMP
02275 -06CC CC C C27C7  C1C          STQ    M
02276  CC74 CC 4 CCC07  C1C          CALL   ELCG,M
C23C0  0601 CC C C2711  C1C          STO    TEMP
C23C1                                NEST   BB
02315  0131 CC 0 CCOCC  CO           XCA
02316  026C CC C C2711  C1C          FMP    TEMP
C2317  06C1 CC C C2711  C1C          STO    TEMP
02320                                NEST   AA
02334  03C2 CC 0 C2711  C1C          FSB    TEMP
02335  06C1 CC C C271C  C1C          STO    KM
C2336  05CC CC C C2712  C1C          CLA    CAPA
02337  03CC CC C C2713  C1C          FAD    CAPB
C2340  06C1 CC C 02711  C1C          STO    TEMP
02341  C074 CC 4 CCCC5  C1C          CALL   SQRT,TEMP
C2343  06C1 CC C C2711  C1C          STO    TEMP
C2344  05CC CC C C2710  C1C          CLA    KM
02345  0241 CC C C2711  C1C          FDP    TEMP
C2346  0260 CC C 52166  C1C          FMP    =4.
C2347  0774 CC 4 CC000  CC    LL29   AXT    **,4
0235C  0C2C CC 4 CC001  CC           TRA    1,4
02351  0C74 CC 4 CCC03  C1C   ENC    PRINT  FMT,C
C2354  0C74 CC 4 CCC1C  C1C          CALL   ERRCR
C2355  6521516C6C6C     CC           BCI    1,VAR           FCRMAT VARIABLE
02356  0 CCCCC 1 C2723  C1C          PZE    VAR,1           SYMBCL
02357  0 CCCCC C CCCC2  CC    FVAR   PZE    2               TABLE
C2360  02C53CC1633C     CO    FMT    BCI    *,25H1THE BEGINNING CF THE END*
C2365  C626C1CC73C4     CO    FIN    BCI    *,6F1C,4I5/(2F1C)*
```

```
     C2370  3C2CC1623127      CO    FCUT1  BCI     *,H+1SIGMA FLCW LINES - INITIAL APPRCXIMATICN+S59,5HPAGE
     C2401  6031C273043C      CO           ETC     I2,4H CF I2/1H-/S1C,3HV =F7.2,S10,5HPHI =F7.2,S10,9HDELTA
     02412  254363216C63      CO           ETC      T =F7.4,S1C,3HA =F7.4,S10,3HH =F7.4,S10,6HZMIN =F7.2/1H-
     02424  4C62C4731465      CO           ETC     S4,'VAR'(S9,1HRS12,1HZS8)//'VAR'(S8,WF10.4,S3,WF10.4)*
     02436  3C2CC16C7125      CO    FCUT2  BCI     *,H+1 ZETA FLCW LINES - INITIAL APPRCXIMATICN+S59,5HPAGE
     C2447  6031C273C430      CO           ETC     I2,4H CF I2/1H-/S1C,3HV =F7.2,S10,5HPHI =F7.2,S10,9HDELTA
     0246C  254363216C63      CO           ETC      T =F7.4,S10,3HA =F7.4,S10,3HH =F7.4,S10,6HZMIN =F7.2/1H-
     02472  4C62C4731465      CO           ETC     S4,'VAR'(S9,1HRS12,1HZS8)//'VAR'(S8,WF10.4,S3,WF10.4)*
     025C4  302CC1623127      CO    FCUT3  BCI     *,H+1SIGMA FLCW LINES - ITERATICN +I2,S83,KHPAGE I2,4H OF
     02515  266031C261C1      CO           ETC      I2/1H-/S1C,3HV =F7.2,S10,5HPHI =F7.2,S10,9HDELTA T =F7.4
     02526  260733047362      CO           ETC     ,S1C,3HA =F7.4,S1C,3H =F7.4,S10,6HZMIN =F7.2/1H-S4,'VAR'(
     0254C  74621C736626      CO           ETC     S8,WF1C.4,S3,WF10.4)*
     02544  302CC16C7125      CO    FCUT4  BCI     *,H+1 ZETA FLCW LINES - ITERATICN +I2,S83,KHPAGE I2,4H OF
     02555  266031C261C1      CO           ETC      I2/1H-/S10,3HV =F7.2,S10,5HPHI =F7.2,S10,9HDELTA T =F7.4
     02566  260733047362      CO           ETC     ,S1C,3HA =F7.4,S1C,3H =F7.4,S10,6HZMIN =F7.2/1H-S4,'VAR'(
     026CC  74621C736626      CO           ETC     S8,WF1C.4,S3,WF1C.4)*
     02604  02053C4C2225      CO    F1     BCI     *,25H-BEGINNING WCRK CN   R = F10.4,S3,4HZ = F10.4,S5,50
     C2615  30633C256C63      CO           BCI     *,FTHE TIME IS (IN 1/60THS CF A SECOND PAST MIDNIGHT)I9*
     02626 +2C154271C277      CC    AA     DEC     1.38629436112,.C9666344259,.03590092383,.03742563713
     02632 +172733415505      CO           DEC     .C145119212
     02633 +2004CCCCCCCC      CO    BB     DEC     .5,.12498593597,.06880248576,.03328355346,.C0441787012
     02640                                 ASSIGN  X2,PSW                                                    *
     02642                                 ASSIGN  T1,T2,TT1,TT2,TT3,TT4,TT5,TT6,TT7,TT8,TT9,TT10,TT20,TT40
     0266C                                 ASSIGN  RTEMP,ZTEMP,TEMPR,TEMPZ,TEMPRR,TEMPZZ,RGP,ZGP
     C2670                                 ASSIGN  V,PHI,DELTAT,A,A2,V2,VCT,DELTA,K,ZMIN,ALP,H,DA,PHIN,DPHI
     02707                                 ASSIGN  M,KM,TEMP,CAPA,CAPB
     02714                                 ASSIGN  COUNT,CCUNT2,NA,NUM,NMAX,NITER,ISW,VAR,P,TP
     C2726                                 ASSIGN  B,B2,B1,B12
                            C4704     SIZE   SYN     25CC
     C7636                                 BES     SIZE
     07636  0 CCCCC 0 CCCCC   CO    RSA    PZE
     14543                                 BES     SIZE
     14543  0 CCCCC C CCCC0   CC    ZSA    PZE
     2145C                                 BES     SIZE
     2145C  0 CCCCC C CCOCC   CC    RZA    PZE
     26355                                 BES     SIZE
     26355  0 CCCCC C CCCCC   CC    ZZA    PZE
     33262                          RSB    BES     SIZE
     40166                          ZSB    BES     SIZE
     45C72                          RZB    BES     SIZE
     51776                          ZZB    BES     SIZE
     52166                          VEC    BES     120
                                           BRIEF   OFF
                                           END

PROGRAM LITERALS
     52166  2C34CCCCCCC0      CC
     52167  203622C77325      CC
     5217C  2016CCCCCCCC      CC
     52171  2CC552024511      CC
     52172  203622077324      CC
     52173  233CCCCCCCCC      CC
     52174  2CC4CCCCCCCC      CC
     52175  2C2622077326      CC
     52176  2024CCCCCCC0      CC
     52177  1745C5745716      CC
     522CC  001CCCCCCCCC      CC
     52201  CCCCCCCCCCC2      CC
```

```
     52202  2C14CCCCCCCC      CC
     52203  6016CCCCCCCC      CC
     52204  CCCCCCCCCCC4      CC
     52205  CCCCCCCCCCC3      C0
     52206  0CCCCCCCCCC1      C0

**** 52207 IS THE FIRST LOCATION NOT USED BY THIS PROGRAM.
```